ASSESSMENT OF THE EFFECT OF URBANISATION AND GLOBAL WARMING NEXUS ON THE THERMAL ENVIRONMENT OF TAHOUA AND ZINDER CITIES, NIGER REPUBLIC

BY

DOULAY SEYDOU, Kadiza

PhD/SPS/FT/2021/13005

WEST AFRICAN SCIENCE SERVICE CENTRE ON CLIMATE CHANGE AND ADAPTED LAND USE, CLIMATE CHANGE AND HUMAN HABITAT

(WASCAL - CC&HH)

FEDERAL UNIVERSITY OF TECHNOLOGY MINNA

APRIL, 2025

ASSESSMENT OF THE EFFECT OF URBANISATION AND GLOBAL WARMING NEXUS ON THE THERMAL ENVIRONMENT OF TAHOUA AND ZINDER CITIES, NIGER REPUBLIC

BY

DOULAY SEYDOU, Kadiza

PhD/SPS/FT/2021/13005

A THESIS SUBMITTED TO THE POSTGRADUATE SCHOOL, FEDERAL UNIVERSITY OF TECHNOLOGY, MINNA, NIGERIA IN PARTIAL FULFILMENT OF THE REQUIREMENTS FOR THE AWARD OF THE DEGREE OF DOCTOR OF PHILOSOPHY (PhD) IN CLIMATE CHANGE AND HUMAN HABITAT

APRIL, 2025

DECLARATION

I hereby declare that this thesis titled: "**Assessment of the Effect of Urbanisation and Global Warming Nexus on the Thermal Environment of Tahoua and Zinder Cities, Niger Republic**" is a collection of my original research work and has not been presented for any other qualification anywhere. Information from other sources (published or unpublished) has been duly acknowledged.

DOULAY SEYDOU, Kadiza
PhD/SPS/FT/2021/13005
FEDERAL UNIVERSITY OF TECHNOLOGY
MINNA, NIGER STATE

SIGNATURE/DATE

CERTIFICATION

The thesis titled: "**Assessment of the Effect of Urbanisation and Global Warming Nexus on the Thermal Environment of Tahoua and Zinder Cities, Niger Republic**" by: DOULAY SEYDOU, Kadiza (Registration number: PhD/SPS/FT/2021/130005) meets the regulations governing the award of the degree of PhD of the Federal University of Technology, Minna and it is approved for its contribution to scientific knowledge and library presentation.

Prof. O. O. Morenikeji ----------------------
Major Supervisor Signature & Date

Dr. A. Diouf --------13/08/2025---
Co-Supervisor Signature & Date

Prof. R. Loewner -------13/08/2025-
Co-Supervisor Signature & Date

Prof. A. A. Okhimamhe ------------------------
Director of WASCAL, Doctoral Research Programme in Climate Change and Human Habitat Signature & Date

Prof. A. N. Saidu -------------------------
Dean of Postgraduate School Signature & Date

DEDICATION

This thesis is dedicated to my loving husband, Dan Rani Chitou, whose unwavering support, patience, and encouragement have been a constant source of strength throughout this journey. It is also dedicated to my dear son, Yashim Chitou, whose resilience and quiet inspiration have played a vital role in successfully completing this programme.

ACKNOWLEDGEMENTS

I am profoundly grateful to my Heavenly Father, whose strength, grace, and gift of good health sustained me throughout this academic journey. I sincerely thank the West African Science Service Centre on Climate Change and Adapted Land Use (WASCAL) for their generous financial support, without which this research would not have been possible.

My deepest appreciation goes to my major supervisor, Prof. Oluwale Morenikeji, and my co-supervisors, Dr. Abdoulaye Diouf and Prof. Ralf Lowner, for their invaluable expertise, insightful guidance, and unwavering encouragement. Their mentorship not only shaped the direction of this research but also inspired me to exceed my own expectations. I am also immensely grateful to Dr. Erdanaev Elbek for his thoughtful feedback and valuable contributions, which greatly enhanced the quality of this work. Special thanks to Prof. J.J. Dukiya, my internal examiner, for his critical evaluation and constructive input. I appreciate Dr. G. I. Kuta, the Postgraduate Representative, for his meticulous attention to detail and commitment to ensuring this thesis met the required academic standards of FUT Minna.

I would like to express my heartfelt gratitude to the entire WASCAL CC&HH team: Prof. Appollonia A. Okhimamhe (Director), Dr. Emmanuel Tanko Umaru (Deputy Director), Dr. (Mrs.) Saratu Ibrahim (former Deputy Director), Mrs. Lucy Peter, Dr. (Mrs.) Mary Odekunle, Dr. Anita Adamu, Mallam Yahaya Abdulrahman, Engr. Raphael Agboola, Dr. Julia Eichie, Dr. Isaiah Sule, Madam Sidikatu Aliyu, Mr. Yamma Wakili, Mrs. Florence Adams, and Mr. Ayuba Noma. Your support and dedication were instrumental throughout my time at WASCAL.

My deepest gratitude goes to my beloved parents, Doulaye Seydou and Adama Oudou, as well as my siblings, for their prayers, belief in my potential, and unwavering support. Your love and faith in me have been instrumental in bringing this journey to a successful end. Thank you for standing by me every step of the way.

I would also like to extend my heartfelt appreciation to Musa and Regina Yashim, whose steadfast support, shared joy in every success, and willingness to carry my burdens alongside me meant more than words can express. Your prayers, encouragement, and unwavering presence carried me through every challenge and made my stay in Minna memorable and truly rewarding.

I am especially thankful to my in-laws, Dan Rani Guéro and Banaou for their prayers, encouragement, and support. To my wonderful Batch 5 colleagues: Olivier Enagnon Ahouandjinou, Aliou Gadiaga, Kagou Dicko, Deborah Ishaku, Kofi Alex Joel, Emmanuel Aweda, Mariama Cissé, Youssoufa Doulla Nouhou, Rotimi Obateru, and Adjowa Yewa Toussoukpe, thank you for your camaraderie, encouragement, and collaboration. Your presence made this academic journey not only possible but truly memorable.

ABSTRACT

Understanding the combined effects of urbanisation and global warming in medium-sized cities is crucial for addressing environmental challenges, fostering sustainable development, protecting public health, and building climate-resilient urban environments. This study examines the impact of urbanisation and global warming on the thermal environment of Tahoua and Zinder, two rapidly expanding cities in Niger Republic. Using remote sensing (RS), geographic information system (GIS) techniques, and urban growth models, this research characterises and quantifies the landscapes of Tahoua and Zinder from 1988 to 2022. Landsat satellite time series were used to classify land use and land cover (LULC) into "vegetation," "built-up," "water," and "agriculture land" through a machine learning (ML) random forest algorithm. The relationship between LULC indices and land surface temperature (LST) was then evaluated using both Ordinary Least Squares (OLS) and Geographically Weighted Regression (GWR). Additionally, extreme temperature trends were analysed using Climpact2, integrated into R software, to assess the trend of heat indices over time. A heat vulnerability assessment was also conducted based on the IPCC Fourth Assessment Report (AR4) framework, mapping vulnerable areas to extreme heat. Lastly, future urban growth was projected using machine learning-based cellular automata models, including Logistic Regression (CA-LR) and Artificial Neural Network (CA-ANN), and future LST, offering insights into potential future environmental challenges. The findings reveal a significant increase in built-up areas, with growth of +10% in Tahoua and +11.5% in Zinder, primarily at the expense of vegetation (-13.14% in Tahoua and -3.5% in Zinder) and agricultural class (-3.13% in Tahoua and -7.79% in Zinder) between 1988 and 2022. Contrary to expectations, the correlation between urban expansion and population dynamics was statistically non-significant ($r(1) = 0.29$, $p > 0.5$ in Zinder; $r(1) = 0.67$, $p > 0.5$ in Tahoua). Moreover, while many studies have observed a positive correlation between the Normalised Difference Vegetation Index (NDVI) and LST, this research highlights an unstable relationship due to the vegetation characteristics. Over the past three decades, heat-related risks have increased substantially, as evidenced by a marked rise in heatwave frequency (HWF) and duration (HWD), with respective annual slopes of 0.41 and 0.08 in Tahoua and 0.43 and 0.08 in Zinder, increasing the exposure of local populations to heat stress. Future projections under a business-as-usual scenario suggest that the vegetation cover in Tahoua will decrease from 17.90% in 1988 to just 4.17% in 2042 and Zinder from 7.74% in 1988 to 0.27% in 2043. On the other hand, the mean LST during the hot period is projected to reach 42.96°C in 2032 and 43.23°C in 2042 in Zinder. In Tahoua, it is projected to be 37.78°C in 2032 to 38.68°C in 2042. This will exacerbate environmental, climatic, and socio-economic challenges. This research calls for managing artificial land expansion and safeguarding natural landscapes to balance human development and environmental preservation. It highlights the urgent necessity for urban planning policies that integrate climate adaptation and mitigation strategies. The study contributes to the growing body of knowledge on the intersection of urbanisation, climate change, and sustainable development, with implications for cities across the Sahel region

TABLE OF CONTENTS

Contents **Page**

LIST OF TABLES

LIST OF FIGURES

LIST OF APPENDICES

LIST OF ABBREVIATIONS

AFOLU: Agriculture, Forestry, and Other Land Use (AFOLU)

CA-ANN: Cellular Automata Artificial Neural Network

CA-LR: Cellular Automata Logistic Regression

DEM: Digital Elevation Model

DHS: Demographic and Health Surveys

DMN: Direction de la Météorologie National (National Direction of Meteorology)

EHE: Extreme Heat Events

ETCCDI: Expert Team on Sector-specific Climate Indices

GIS: Geographic Information System

GWR: Geographically Weighted Regression

GWR: Geographically Weighted Regression

INS: Institut National de la Statistique (National Institute of Statistics)

IPCC: The Intergovernmental Panel on Climate Change

IRD: Institut de Recherche pour le Développement (Research Institution of development)

LEI: Landscape Expansion Index

LST: Land Surface Temperatures

LULC: Land use and land cover

MEDD: Ministère de l'Environnement et de Développement Durable

MICS: Multiple Indicator Cluster Surveys

ML: Machine Learning

OLS: Ordinary Least Squares

OLS: Ordinary Least Squares Regression

PA: Producer Accuracy

RS: Remote Sensing

SONARA: Société Nigérienne de Commercialisation de l'Arachide et du Niébé (Nigerien Society Groundnuts and Cowpea Marketing)

SRTM: Shuttle Radar Topography Mission

UA: User Accuracy

UD: Urban Density Index

UEII: Urban Environmental Impact Index

UHI: Urban Heat Island

CHAPTER ONE

1.0 INTRODUCTION

1.1 Background to the Study

Cities are irrefutably becoming centres of attraction worldwide due to their benefits, including access to better health and educational facilities, greater economic possibilities, and other advantages. Before 2007, the global rural population outnumbered the urban population, but this trend shifted, and by 2018, 55% of the world's population resided in urban areas. By 2050, this proportion is projected to rise to 68%, with approximately 90% of the increase occurring in Africa and Asia (United Nations, 2018). Migration from rural to urban areas is the primary driver of this substantial urban population growth in African nations (Ibn *et al*., 2017; Selod and Shilpi, 2021). This phenomenon accounts for 40 to 60% of annual urban population growth (Manu *et al*., 2015) and, in rare instances, can reach 75% (Ibn *et al*., 2017). As urban populations rapidly increase, cities expand to accommodate people and their socio-economic activities. While urbanisation is fuelled by population growth, urban areas in some regions are expanding even faster than the population (Rossi and Dobigny, 2019).

Rapid urbanisation alters land use and land cover (LULC) and ecosystem services, presenting a global environmental challenge. This challenge is further exacerbated by global climate change, which involves long-term increases in average temperatures and alterations in weather patterns. The intersection of these challenges has led to coordinated global efforts through frameworks like the United Nations Framework Convention on Climate Change (UNFCCC) and the annual Conference of the Parties (COPs). These platforms emphasise mitigation and adaptation strategies, culminating in key agreements such as the Paris Agreement, which aims to limit global temperature rise to well below

2°C while pursuing efforts to keep it within 1.5°C (UNFCC, 2018). Central to these efforts are Nationally Determined Contributions (NDCs), which encourage countries to define their climate goals, and National Adaptation Plans (NAPs), providing a roadmap for integrating climate adaptation into national development planning. Together, these frameworks highlight the need for climate resilience in cities.

Urban expansion is recognized as a primary driver of LULC change, often leading to the loss of green spaces and agricultural land while substantially influencing climatic variations and human life (Hussain *et al*., 2022). This trend is expected to continue with the projected growth of urban populations and urban areas. Unfortunately, the combined effects of urbanisation and global climate change are seriously affecting the environmental process, the ecological equilibrium and the social stability of the world (Ramachandra *et al*., 2014). For instance, urbanisation impacts urban areas' temperature by making them experience higher temperatures than rural areas. This phenomenon is known as the Urban Heat Island (UHI) effect (Reis *et al*., 2022).

The rapid expansion of cities and climate change have become one of the most challenging concerns for urban planners in the current century (Lin *et al*., 2020; Guo *et al*., 2022). The Intergovernmental Panel on Climate Change (IPCC) experts projected that an increase of 1.5°Cin global temperatures will cause longer warm seasons, shorter cold seasons, and extreme heat events (EHEs) in different regions worldwide (IPCC, 2021). This change will not only affect temperatures but also affect the water cycle, causing a change in rainfall pattern and intensity, flooding and drought in other regions (Arias *et al*., 2021). Studies have shown that in the future warmer climates, EHEs will become more frequent, longer-lasting and more intense, and cities are expected to experience this more frequently due to the UHI effect (He *et al*., 2021).

Urban heat island effect is one of the most noticeable effects of urbanisation in cities. It is caused by the change of a natural surface to a manmade surface (Buo *et al*., 2021). For example, a study conducted by (Hu and Li, 2022) in Liaoning province, China, suggested that urbanisation affects the heat experienced in this province. The correlation was mainly observed with nighttime temperatures, as the heat trapped by buildings and other infrastructures is released when the ambient temperatures reduce. The findings showed that the key spatial elements linked to urbanisation that influenced severe temperatures were the size and fragmentation of the metropolitan landscape.

In many other parts of the world, such as India (Vinayak *et al*., 2022), Australia (Deilami *et al*., 2016), Ethiopia (Debele and Beketie, 2024) and Nigeria (Adeyeri *et al*., 2017; Alademomi *et al*., 2022) evidence has shown a correlation between LULC change due to urbanisation and increased heat. Based on this fact, Vinayak *et al.* (2022) projected future temperatures in Mumbai. The study found that an average minimum increase of 1.41˚C is expected by 2050, following the same pattern of urbanisation in the locality. However, although urbanisation causes rising temperatures in cities, Deilami *et al.* (2016) pointed out that temperature changes are not only attached explicitly to urbanisation (urban expansion) but also due to the population growth in an area and urban form (Liang *et al*., 2020).

Extreme heat due to global climate change coupled with UHI in cities adversely impact human life, health and the economy (Watson *et al*., 2020). In Europe, up to 70,000 fatalities were recorded due to heatwaves in 2003 and up to 20,000 fatalities in Moscow in 2010. In Australia, heatwaves cause death more than any other natural hazard (Guigma *et al*., 2020). Likewise, economic projections highlighted that rising temperature will likely reduce labour capacity during peak months of heat to 80% by 2050 and a reduction of 23% of the mean global income may be observed by 2100 (Kunz-Plapp *et al*., 2016). All these impacts call for a better urbanisation plan to minimise their negative (-) effects on humans and their habitats.

In Niger Republic, less attention is given to urban planning and environmental management in cities, although this is very crucial for sustainable development; instead, most attention is given to infrastructural development. Cities are expanding without any serious planning (Illiassou *et al*., 2015). This makes them not only vulnerable to extreme heat but also has an adverse impact on biodiversity and ecosystem services due to LULC change (Mahamane and Mahamane, 2005). Understanding the dynamics of our cities is critical to understanding the urbanisation effect of LULC change and making informed decisions towards sustainable urban expansion. This study focuses on two medium cities of the Niger Republic. Generally, medium cities are overlooked when evaluating the impact of urbanisation on urban landscapes. Much attention is given to megacities and metropolitan areas. However, these medium cities contribute to environmental changes, mainly due to the shift from a rural setting to an urban environment. Additionally, they provide important opportunities for understanding balanced urban growth by preventing the over-concentration of resources and tackling urban difficulties on a manageable scale before they reach challenging levels. This will allow the design of more resilient, sustainable, and inclusive urban systems.

1.2 Statement of the Research Problem

Urbanisation is a characteristic of human development, driving economic growth and modernisation through urban area expansion, infrastructure development, and population increase (Guo *et al*., 2021). United Nations reported that developing countries will account for 96% of future urban growth, making them more economically sustainable, and this will contribute to the global effort for sustainable development. When properly managed, urbanisation has the potential to enhance social, environmental, and economic well-being and tackle challenges such as unemployment, poverty, social inequality, and climate change (UN-Habitat, 2020). However, rapid urbanisation, when not carefully managed, also brings complex environmental, inequalities, and health challenges.

Urbanisation affects temperatures by altering the urban canopy energy budget through changes to the physical and thermal properties of the urban surface (Hu and Li, 2022). The replacement of natural landscapes with impervious surfaces like concrete and asphalt lowers albedo (the reflectivity of surfaces), causing urban areas to absorb more solar radiation (Vujovic *et al*., 2021). This absorption increases surface and air temperatures, mainly as these materials release stored heat slowly during the night (Lee and Lim, 2022). Reducing vegetation limits Latent Heat Fluxes (LHF), the cooling effect from evapotranspiration, shifting the balance toward Sensible Heat Fluxes, which release heat directly into the air. Additionally, dense building structures and limited ventilation trap heat within urban spaces, increasing the UHI effect by modifying airflow and concentrating heat near the surface (Liang *et al*., 2020) . These changes in energy fluxes contribute to persistent warming in urban environments.

The impact of urbanisation on urban temperatures is further intensified by climate change, which increases the experience of more frequent and extended heat periods, thereby accentuating the Urban Heat Island (UHI) effect (Guo *et al*., 2022). As global and regional temperatures rise, urban areas in countries like Niger experience even more pronounced warming (Russo *et al*., 2016), leading to a cascade of challenges. Increased temperatures strain urban infrastructure by driving up energy demand for cooling, which can be difficult to sustain in developing regions with limited energy resources. On the other hand, the increased energy demand for cooling, also compounds urban heat challenges (Jaiye, 2020). The heightened demand often leads to more fossil fuel combustion, which in turn releases more greenhouse gases (GHGs) and air pollutants, further intensifying the urban heat island (UHI) effect (Hertel *et al*., 2012). Additionally, cooling systems expel heat back into the urban environment as a byproduct, raising the ambient temperature in densely populated and built-up areas. The heightened heat exposure exacerbates health risks, particularly for vulnerable populations such as the elderly, children, and marginalized groups, who may lack adequate shelter and access to cooling resources.

In Niger, 17% of the population lives in urban centres, and the number will increase by 4.02% per annum (Ayeni, 2018). Though modest compared to global rates, this remains a challenge because of the limited capacity to deal with risk and the limited safety nets. Unplanned urban growth is a reality in Niger which is accompanied by many adverse effects including LULC changes (Abdoulaye, 2019; Illiassou *et al*., 2015) and heat exposure with extremely high temperatures, particularly during dry periods (DMN, 2023). The country has elaborated a strategic urban planning document to address the challenges posed by urbanisation (MEDD, 2011). However, the document primarily emphasises the economic aspect of urbanisation, issues of land management and urban poverty with no reference to urban heat, despite it being a significant issue in Niger. This omission may be due to a lack of documented studies on urban heat in Niger, a gap that this research aims to help bridge.

This study focuses on two medium cities, Tahoua and Zinder. These cities, located in the Sahel, face increased urban growth with high vulnerability to extreme heat. Zinder, for instance, is projected to be Africa's second fastest-growing city, with a projected growth rate of 118% from 2020 to 2030 (Kamer, 2022). Contributing factors include increased migration due to regional instability, such as the Boko Haram conflict, leading to rapid, often unplanned urban expansion (Leslie, 2015). Since 2002, Zinder's population growth has surpassed that of Niamey. On the other hand, Tahoua's recent infrastructure growth and strategic location also position it as a hub which accelerates its urban expansion (PDC, 2019). It is important to note that the two regions are classified as high-risk areas of extreme heat hazard (World Bank, 2007). Additionally, they present high vulnerability to health and environmental risks, as exemplified by their classification regarding measles incidence. Tahoua is ranked among the highest-risk regions, with over 1000 reported cases, while Zinder follows closely, with between 500 and 1000 cases (Lamine, 2023). This health vulnerability underscores the necessity of examining these areas' exposure to additional climate-related stressors, such as extreme heat, which further endangers public health.

Despite the increasing attention to urbanisation patterns and their relation to urban temperatures globally, medium-sized cities in developing regions, particularly within the Sahel, remain underrepresented in scholarly research. Zinder and Tahoua exemplify this gap. There is a lack of comprehensive analysis of how urban expansion manifests in such settings. Meanwhile understanding the dynamics of medium cities is particularly important as they have greater flexibility to adapt their development pathways, unlike megacities, which have often established entrenched growth patterns that are challenging to reverse. This study seeks to fill this knowledge gap by thoroughly examining Zinder's and Tahoua's urban expansion and its relationship with urban temperatures.

1.3 Research Questions

i. How have LULC changes, urban growth dynamics, and expansion patterns in Tahoua and Zinder evolved from 1988 to 2022?

ii. How do spatiotemporal variations in LST correlate to changes in LULC indices in Tahoua and Zinder over time?

iii. What are the historical trends of heat indices in Tahoua and Zinder, and how have these indices changed over time in response to global climate change?

iv. Which areas in Tahoua and Zinder are most vulnerable to extreme heat, and what are the best practices for heat coping and adaptation strategies?

v. How will future urban growth in Tahoua and Zinder evolve under a business-as-usual scenario, and what are the implications for future LST?

1.4 Aim and Objectives of the Study

This study aimed to provide empirical evidence of the impact of urbanisation and global warming on LST in order to guide policy formulation on sustainable urban planning in Tahoua and Zinder.

The specific objectives of this study are to:

i. Examine LULC dynamics in Tahoua and Zinder from 1988 to 2022;

ii. Analyze the spatiotemporal patterns of LST and its relationship with LULC indices in Tahoua and Zinder;

iii. Investigate the historical patterns of heat indices in Tahoua and Zinder in relation to global climate change;

iv. Analyse and map the levels of heat vulnerability of Tahoua and Zinder, and identify the population’s heat coping and adaptation strategies;

v. Simulate future urban growth and LST in Tahoua and Zinder under a business-as-usual scenario.

1.5 Justification for the Study

Policy improvement: The information about the rate and extent of Tahoua and Zinder cities’ growth and the impact of this expansion on the natural environment challenges policymakers to evolve appropriate policies and provide useful adaptation plans for sustainable cities due to the fact that the growth of cities in Africa is an inevitable situation. Understanding the driving factors of urbanisation in Tahoua and Zinder is very useful as this information could be integrated into planning urban expansion. Hence an important contribution to achieving sustainable development goal (SDG) 11 is to make cities and human settlements inclusive, safe, resilient and sustainable, and SDG 3 ensure good health and well-being of humans by reducing health challenges related to heat.

Performance improvement: This study is useful to the Ministry of Urban Planning, Housing, and the Public Domain to support urban development planning and sustainable growth. It particularly supports decisions while elaborating the national strategy of urban development document. The study is also helpful for the local district leaders in knowing how important it is to integrate urban expansion into their developmental strategic document.

Further research: The detailed visual presentation of LULC dynamics is useful for future environmental monitoring studies under the supervision of the Ministry of the Environment and Sustainable Development. The study might also stimulate researchers’ interest in conducting similar impact studies in other parts of Niger and Africa to understand how the urbanisation process interacts with the human environment on medium scale cities which are often neglected.

Body of knowledge: Finally, this study provides valuable insights into the present and future urban growth patterns and the associated heat challenges faced by urban areas in developing countries, specifically Niger. While heat vulnerability and risk studies have been conducted globally, they were often carried out at a large scale, using cities or districts as units of analysis (Inostroza *et al*., 2016; Voelkel *et al*., 2018; Jagarnath *et al*., 2020). However, no such studies have been conducted in Niger. Furthermore, regional or multicity-level studies, while useful for broad comparisons, often lack the resolution needed for targeted interventions.

This study addresses this gap by providing a framework for assessing heat vulnerability at a fine scale, specifically focusing on localized, community-level analyses within urban areas. By utilizing primary data, this approach captures variations in heat exposure, sensitivity, and adaptive capacity at a level that is detailed enough to identify the most vulnerable neighbourhoods or communities. This fine-scale assessment enables the development of precise and actionable adaptation and mitigation strategies tailored to the unique needs of specific areas within cities.

Likewise, although studies on urban dynamics have gained traction in urban geography, less attention has been given to medium size cities globally and the subject matter in Niger; hence there is less documented information about the evolution of cities in this area. The only notable studies include the study of Djibo (2019) who evaluated, Zinder city expansion using Google Earth image but focusing only on the historical aspect of governance. Additionally, Illiassou *et al*. (2015) examined the dynamics of Niamey and Maradi, linking their growth to population increases and highlighting the ecological problems caused by urbanisation. However, these studies did not include future projections, leaving a gap in understanding the long-term implications of urbanisation. Although heat is a frequent challenge faced by Niger's population, especially in summer when the daily maximum temperature could easily surpass 40°C, as measured at the city's weather stations (DMN, 2023) yet no documented study was carried out in Niger's cities despite the adverse effect of heat on human population and their environment. It is thus important to understand how urbanisation contributes to the heat experience in Tahoua and Zinder cities. Understanding this interaction will be useful for planning urbanisation.

1.6 Description of the Study Area

1.6.1 Geographical location of the study area

This study is conducted in two cities in the Niger Republic (Tahoua and Zinder) (Figure 1.1). These cities were selected for this study due to their unique urban growth patterns and the environmental challenges they face. Locally known as Damagaram, Zinder is the second largest city in Niger after the capital city Niamey. It is located within latitude 13° 44' N and 13° 54' N and longitude 8° 54' E and 9° 40' E, and was Niger's first capital city. The city has grown significantly, having experienced a population increase from just 12 466 in 1950 to 600 961 in 2024 (World Population Review, 2024). As the capital of the region, it has recently experienced extreme population growth and migration, mainly due to Boko Haram conflicts (Leslie, 2015).

Tahoua, on the other hand, is located between latitude 14° 50' N and 14° 57' N and longitude 5° 10' E and 5° 20' E. It is the fourth largest city in Niger. The population of the city was 117,826 inhabitants in 2012 (City population, 2018). The city is an important hub for trade and agriculture, and it is the administrative capital city of the Tahoua region. Except for Niamey, there is no official cities boundary in Niger. They are dynamic features located in the communes. For the purpose of this study, 2km buffer zone boundaries were created from the last building identified to constitute the study area.

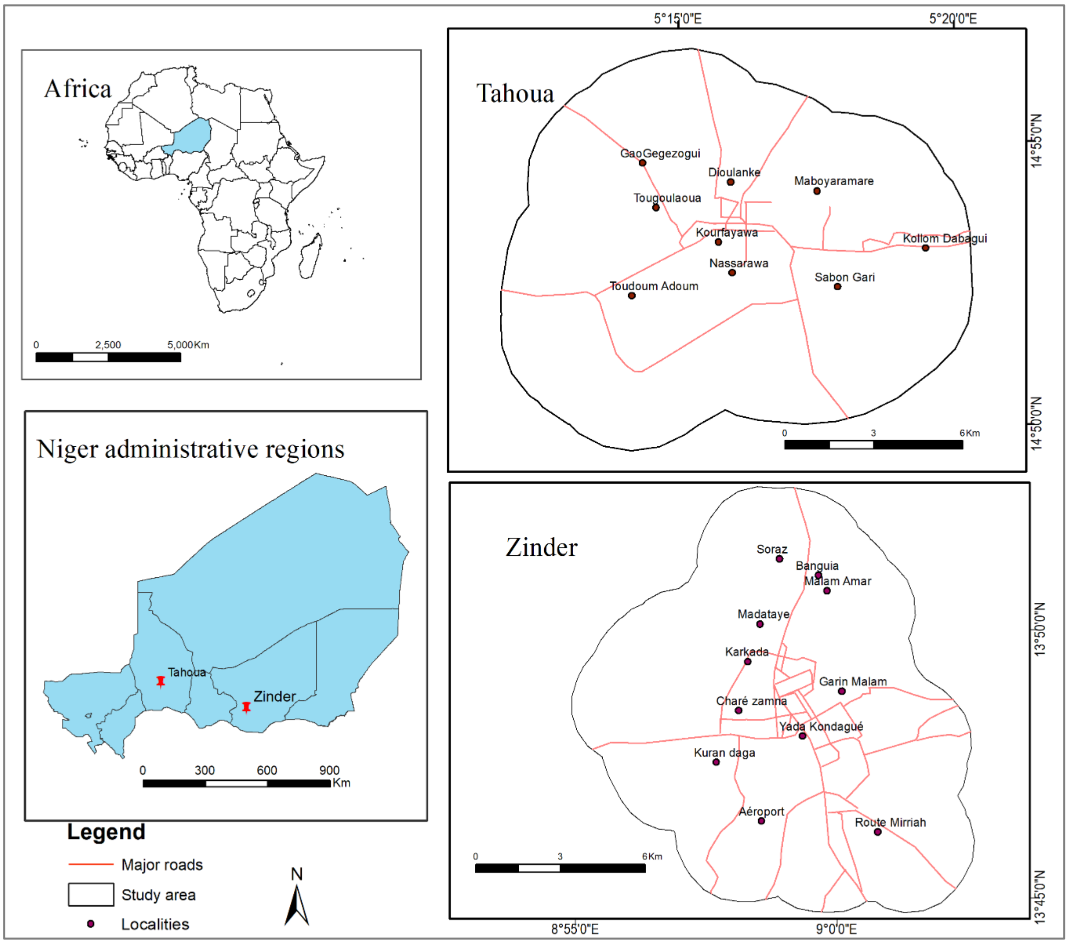

Figure 1.1 Location of the Study Area

1.6.2 Climate of the study area

The rainy season in the study area generally lasts for only 3 to 4 months, typically from June to September. However, this pattern has changed in recent decades, with the rainy season now often starting in July. The remaining months of the year are characterised by a long dry season. Both cities experience a semi-arid climate, where the displacement of the intertropical front governs the succession of seasons. Annual rainfall in Tahoua ranges between 200 mm and 500 mm, while in Zinder, it is from 235 mm to 531 mm (DMN, 2023). August is the wettest month and an average humidity of 72% in Tahoua and 76% in Zinder. Temperatures during August are often oppressive. In contrast, March temperatures are generally more bearable.

The average monthly temperatures in Tahoua from 1991 to 2020 range as follows: the minimum temperature is 15.92°C in January, while the maximum temperature reaches 41.14°C in April (DMN, 2023). Interannual temperature variations rarely exceed 2°C, while the annual thermal amplitude exceeds 15°C. In Zinder, the warmest month is May, with an average high temperature of 42.8°C, while January records the lowest average high temperature at 9°C (Figure 2.2).

Both cities are influenced by trade winds, similar to the rest of Niger Republic. Two main winds alternate depending on the season. The Harmattan, a dry continental trade wind originating from the northeast to northwest, typically blows from October to February. It carries fine dust particles from the Sahara Desert, resulting in dry and hazy conditions, lower humidity, and cooler nighttime temperatures. The Harmattan is a steady and very dry wind. In contrast, the Monsoon is characteristic of the rainy season. It originates from the southwest and often reaches the southern part of the region from March to April.

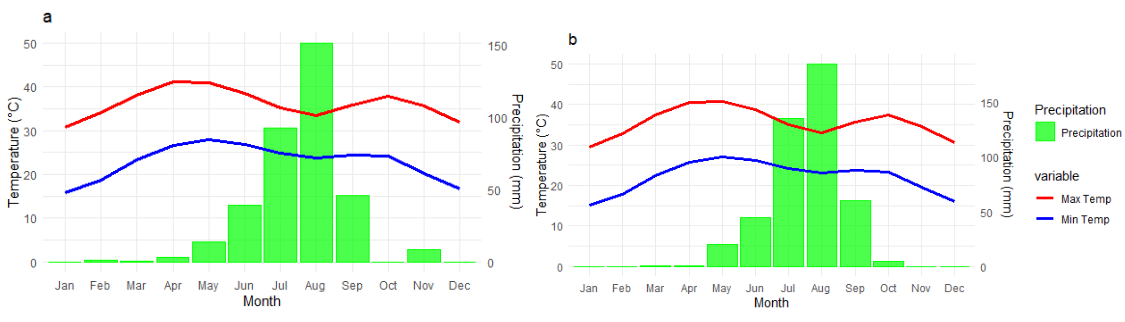

Figure 1.2 Average Monthly Temperature and Rainfall (1991-2022) in Tahoua (a) and Zinder (b) (data source: DMN, 2023)

1.6.3 Soil, vegetation and hydrology

Tahoua region is located in the zone called *Ader Doutchi maggia*, a vast plateau gashed with valleys. This plateau was covered with vegetation which is disappearing due to recurrent drought and land use change. The soil is lateritious which makes infiltration difficult. This made the population focus on the valleys, where the deposits of thin alluviums make the soils fertile (Moussa *et al*., 2016). The vegetation is sparse in Tahoua region, the most common woody species found in the study area are *Guiera senegalensis* J.F.Gmel*, Combretum glutinosum* Combretum glutinosum Guill. And Perr*, Acacia macrostachya* Reichenb.*, Senegalia ataxacantha* Kyal. And Boatwr.*, Combretummicranthum* G. Don*, Boscia senegalensis* (Pers.) Lam.*, Acacia tortilis* (Forssk.) Hayne, *Acacia nilotica* (L.) Willd.*, Boscia angustifolia* A. Rich.*, Balanites aegyptiaca* (L.) Del.*, Ziziphus mauritiana* Lam.*, Pilostigma reticulatum* (DC.) Hochst.*, Bauhinia rufescents* Lam.*, Faidherbia albida* (Del.) Chev.The most common herbaceous species are *Andropogon gayanus* Kunth*, Andropogon pseudapricus* Stapf*, Cassia tora* Linn*, Pennisetum pedicellatum* Trin.*, Zornia glochidiata* Reichb.*, Schizachyrium exile* Hochst.*, Andropogon pseudapricus* Stapf.,(Baggnnian *et al*., 2021). There are several ponds in the region (permanent and semi-permanent) some of which are used for market gardening.

In Zinder region, the soil type is mainly ferruginous and Acacia and Prosopis dominate the vegetation. Among others, we can find *Faidherbia albida* (Del.) Chev.*, Acacia nilotica* (L.) Willd*, Acacia séya* Del.*, Acacia radiana* Savi*, Balanites aegyptiaca* (L.) Del and *Adansonia digitata* (Sina *et al*., 2021). There is no river in the region, however, there are ponds even in the city, which are pressured by increasing urbanisation and cause flooding (Malam *et al*., 2021).

Although Tahoua and Zinder present limited water bodies, their potential cooling effects cannot be overlooked. Water bodies can regulate local temperatures through evaporative cooling and heat storage, creating microclimates that reduce surrounding temperatures (Albdour and Baranyai, 2019). This effect is particularly significant during the daytime in arid and semi-arid environments, where the thermal contrast between water bodies and surrounding land is pronounced.

1.6.4 Socio-economic activities of the population

The socioeconomic activities in Tahoua and Zinder are very similar. It is mainly centred on agriculture and livestock to which we can add handicrafts and trade. Tahoua is a commercial hub between the Maghreb and coastal countries. The region is dedicated to pastoralism, and the north is mainly populated by nomadic communities. It benefits from commercial opportunities to coastal (such as Benin, Togo and Cote d'Ivoire) and Maghreb states as well as to Nigeria. Taking advantage of its large valleys, ponds and groundwater resources, the Tahoua region has invested heavily in irrigated agriculture (Hanana *et al*., 2021). On the other hand, Zinder economy particularity is based on the presence of four recognized industries: Tannery Malam Yaro (leather tanning), Gidan Alkaki (cake production), and Sahara Sahel Foods, and SORAZ (petrol refinery the first and only petrol refinery in Niger (Heasahel, 2016).

1.7 Scope and Limitations of the Study

1.7.1 Scope of the Study

Time boundary: The temporal range of this study is 1988-2022 which was selected because the year 1990s marked an important shift of population from rural areas to urban. In this study, the absence of quality images from 1990 motivated the use of 1988 as base date. This shift of population was due to recurrent drought before this period but also the failure of the structural adjustment programme which was set up by the World Bank to enable developing countries to emerge from their economic crisis. It promoted access to credit for a reduction in state expenditure, privatization, including certain public services, and the opening up of markets. The programme rather raised the informal sector and raised the poverty level and social tension (Some, 2013). Another factor that affected rural areas negatively in Niger was the fall of Seyni Koutche's regime. While alive, he gave particular attention to rural areas promoting agriculture by valorising agricultural products. There were agricultural product transformation refineries like SONARA which were located in rural areas and gave working opportunities to the rural population. There was also an important engagement of youth for local development. For example, there was a vast movement typical of Niger, born in the villages called Samaria which brings together all young people. It is based on mutual aid and solidarity, Samaria played an active role in the village by maintaining the unity of its inhabitants, the safety of the village and promoting its well-being. They also campaign to promote certain neglected agricultural products. All these assets and organizations were neglected after general Seyni Koutche's regime (Klotchkoff, 2012). The above factors encouraged youth people in villages to migrate to urban areas in search of better living conditions. The prediction scope (2023-2053) is chosen to be in the same scope of the information we have about the increase in world urban population (68% by 2050) given by United Nation (2018).

Space Boundary: This study is limited to the urban areas within the cities of Zinder and Tahoua, which serve as the capitals of their respective regions. Tahoua consists of two urban districts, while Zinder comprises four. Although each district includes numerous villages and towns outside the main urban centre, this study focuses exclusively on the urban portions. The rural areas within these districts are excluded, as the urban centres of Zinder and Tahoua are more directly impacted by the challenges addressed in this research, including rapid urbanisation, environmental changes, and heightened vulnerability to extreme temperatures.

Content Boundary: This study covers an assessment of LULC changes, trends in extreme temperatures, LST patterns, and urban heat vulnerability in Tahoua and Zinder. It uses satellite data from sources like Landsat for LULC analysis and MODIS for LST analysis. The study tracks LULC changes and evaluates LST and temperature extreme trends over time. It explores the relationship between LULC indices such as NDVI and NDBI and LST over different seasons to understand the effects of urban growth on heat distribution. It also investigates urban heat vulnerability, pinpointing areas at risk, and examines coping and adaptation strategies related to extreme heat conditions.

1.7.2 Limitations of the study

The non-availability of sufficient in situ temperature data was a limitation of this study. With only one weather station available per city, the spatial coverage for analysing temperature trends and urban heat was limited. To address this challenge, MODIS 8-day LST data were utilised to analyse the spatiotemporal variation of urban temperatures across the study area. These products provide surface temperature and emissivity data with a spatial resolution of 1 km, offering a practical alternative to compensate for the lack of in situ measurements.

Another limitation was the unavailability of official neighbourhood boundary data for Tahoua. Due to security reasons, attempts to obtain this data from the National Urban Planning Agency and its local representatives were unsuccessful. Without such data, artificial neighbourhood divisions were created based on the neighbourhood names, and the location of interviewed individuals collected through the field survey and logical spatial divisions, which considered major roads.

Additionally, the absence of heat-related mortality and morbidity data at the neighbourhood level posed a challenge for directly validating the vulnerability mapping with observed health outcomes. This limitation is not unique to this study, as similar studies (Oh *et al*., 2017; Verdonck *et al*., 2018) also faced challenges in performing such validations due to data unavailability. To address this, the study employed two distinct formulas for vulnerability mapping, which enabled the identification of highly vulnerable areas by focusing on zones consistently highlighted by both approaches.

Despite these limitations, the study provides valuable insights into urban heat dynamics and vulnerability in Zinder and Tahoua.

CHAPTER TWO

2.0 LITERATURE REVIEW

2.1 Conceptual Framework

2.1.1 Urbanisation

In the scientific community, there are three main definitions of urbanisation. First, it is defined as an increase in population size; second, it is defined as an increase in urban population and urban areas due to the conversion of rural areas to urban; and finally, it is defined as the adoption of an urban lifestyle and behaviour (ideology), also known as urbanism (Chaolin, 2020).

Urbanisation is an important driver of economic growth and modernisation, and it becomes unavoidable for the development of every human society. The term synchro-urbanisation is used to describe the process by which urbanisation leads to socio-economic development (Guo *et al*., 2021). In opposition, hyper-urbanisation refers to an important increase in urban population and urban landscape transformation without significant economic increase. They attach this issue to a lack of planning. The concept of hyper-urbanisation is used by some scholars to qualify the urbanisation pattern of Africa, Asia and Latin America. In this case, urbanisation is not viewed as a positive asset. However, many urbanisations' contemporary literature rejects this concept. They argue that the same pattern of urbanisation observed in these continents was also observed during the industrialization period in developed countries therefore there is nothing wrong with their urbanisation pattern (Chaolin, 2020). In this study, the concept of urbanisation will refer to the increase of the urban population and the physical changes in the urban landscape. The economic aspect of urbanisation will not be considered in this study.

There is no universal definition of urban areas in the literature. The compilation of urban demographic information through world urbanisation prospects faced the same challenge in defining an urban area. They do not use their definition of urban areas but they follow that of each country (United Nations, 2012). For instance, a city is described as an inhabited place of larger size, population, or importance than a town or village in the Merriam-Webster dictionary. Such definition is ambiguous and therefore, definitions vary from one country to another depending on their economic development and their cultural background. Some researchers have attempted to standardize urban areas. The definition thresholds are based on minimum population density and size and the maximum travel by road. However, the definition is universally inapplicable (United Nations, 2012). Some common criteria used to designate cities are population size, population density, economy, and administrative function. In China, a city is described as an area where the non-agricultural population is more than 100,000 inhabitants with a revenue of more than 4000 million renminbi (about 596 million US dollars). In the United Kingdom, the monarch has the right to designate a community and assign the status of the city. In this case, the number of people or the economy is not a factor of choice. In Nigeria, a city is an agglomeration with a population of more than 20,000 inhabitants while in Mali the characteristic population of cities is 30,000 or more (Williams, 2012). In Niger, an urban district has more than 10,000 inhabitants (Loi 2001-2, article 6) and we can find many urban districts in a city. For example, the city of Niamey has 5 districts. In this study, Niger's definition of a city will be considered as the study will be conducted in Niger.

Urbanisation is a complex system. It affects social life, health, environment, agglomeration and values. Urbanisation goes together with the anthropogenic transformation of the natural environment which affects the landscape structure and function through deforestation, pollution, land use change etc. In ecology, a landscape refers to the physical, and structural complexity of the components on the earth's surface. Since the first United Nations conference on the human environment in Stockholm in 1972, it has been established that humans contribute to the degradation of their environment through diverse activities (United Nations, 1973).

2.1.2 Global warming and climate change

Global warming and climate change are pressing global challenges driven primarily by the increase in greenhouse gas emissions from human activities. According to IPCC, (2021) Global greenhouse gas emissions are primarily categorized into four major sectors. The energy sector is the largest contributor, accounting for 73.2% of emissions, driven by fossil fuel combustion for electricity, heat, transportation, and industrial energy use. The agriculture, forestry, and other land use (AFOLU) sector contributes 18.4%, primarily from deforestation, land-use changes, livestock emissions, and fertilizer use. The industry sector accounts for 5.2%, arising from non-energy industrial processes such as cement and chemical production. Finally, the waste sector contributes 3.2%, mainly through methane emissions from landfills and wastewater.

The high concentration of greenhouse gases in the atmosphere significantly alters the earth's climate system. Land-climate interactions play a vital role in these processes (Figure 2.1). These interactions can have positive outcomes, such as carbon sequestration through afforestation, or negative impacts, such as increasing greenhouse gas concentrations through deforestation and fossil fuel consumption.

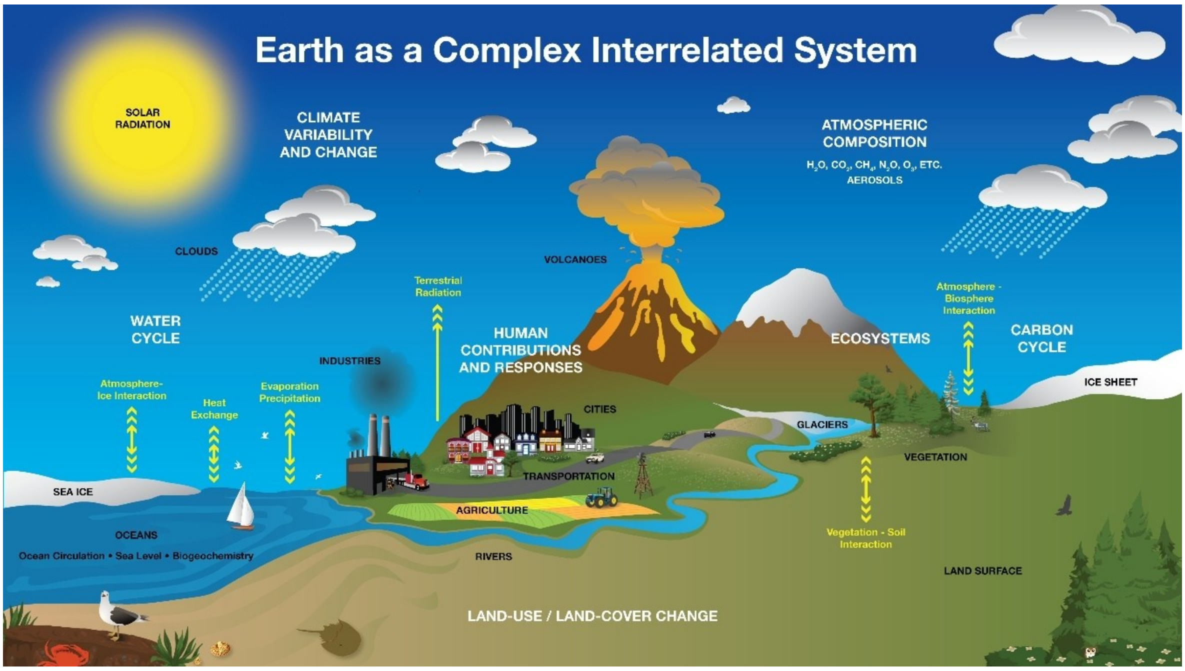

Figure 2.1 Interaction Between Earth and the Climate System (Kevin, 2018)

The greenhouse effect refers to the ability of the atmosphere to act as transparent glass. It traps heat by allowing the incoming solar (longwave) radiation to reach the earth's surface and preventing the outgoing terrestrial (shortwave) radiation from passing through it due to the greenhouse gases in the atmosphere (Figure 2.2). The high concentration of greenhouse gases from anthropogenic activities and the destruction of vegetation, which has the ability for carbon sequestration, change the surface emissivity and increase the heat-trapping capacity of the atmosphere. These factors are responsible for global warming.

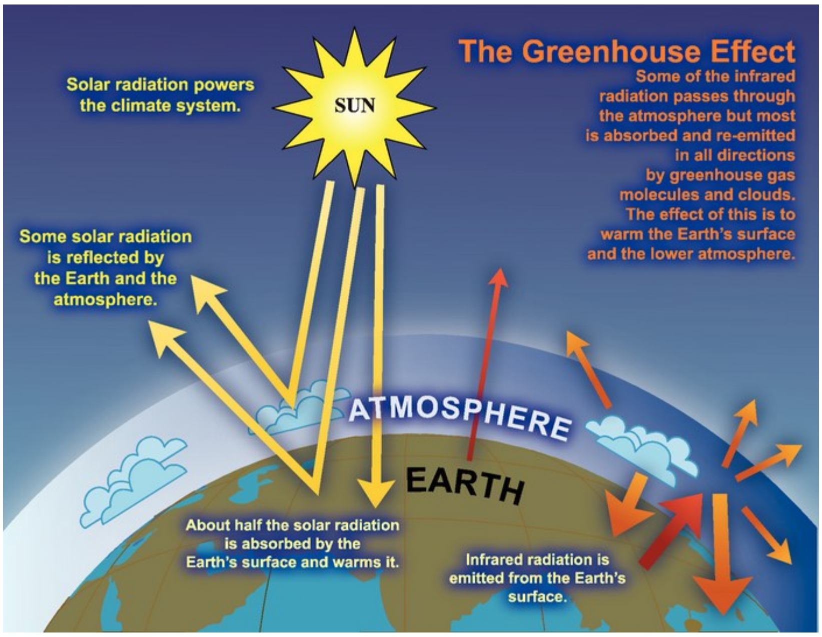

Figure 2.2 Greenhouse Effect Illustration (IPCC, 2007)

It is important to differentiate between global warming and climate change. Global warming is one aspect of climate change although it is sometimes used interchangeably. The two phenomena resulted from anthropogenic activities. According to Article 1 of the UNFCC, climate change is defined as "a change of climate that is attributed directly or indirectly to human activity that alters the composition of the global atmosphere and is in addition to natural climate variability observed over comparable time periods". In other words, global warming takes temperatures as a parameter, while climate change looks into all the weather elements, including temperature, rainfall, wind, and humidity. Along with IPCC reports, many scientific types of research related the extreme weather events experienced these decades to climate change. Some of these impacts include: drought, flooding, and extreme heat events also called heatwaves. In this work, we will only consider the impact related to extreme temperatures.

2.1.3 Urban Heat: Drivers and Implications

The combined effect of climate change and urban heat island is expected to worsen city dwellers' exposure to heat in the future (Azhdari *et al.*, 2018). The urban heat island effect is a trending concept which states that urban areas experience higher temperatures than the surrounding rural areas. It is influenced by many factors including population density and size, regional weather, ecosystem type in which the city resides, building material, building type and architecture, and vegetation type and density (Azhdari *et al*., 2018; Liang *et al*., 2020). Extreme heat negatively affects human health by causing thermal stress, hyperthermia and an increase in mortality and morbidity rates, especially for people with health issues, infants, and children (Malmquist *et al*., 2022). Understanding and quantifying how urbanisation and global warming induce heat in cities is one step towards implementing climate action in cities. Figure 2.3 summarises the conceptual framework of factors influencing extreme heat in cities.

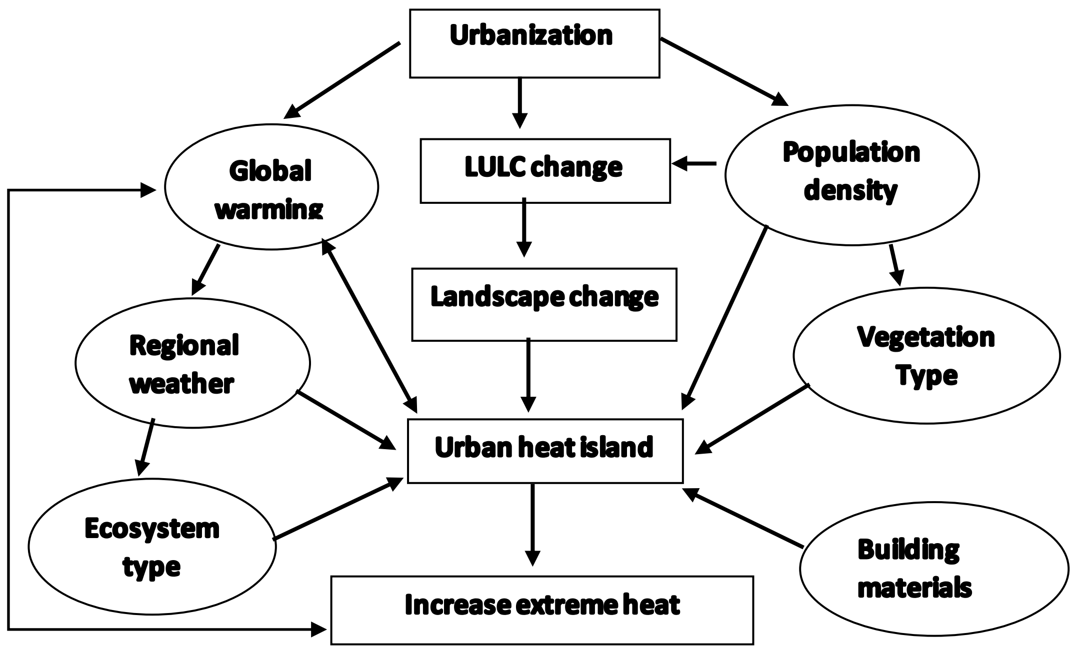

Figure 2.3 Factors Influencing Extreme Heat in Cities

2.2 Theoretical Framework

2.2.1 Urban land use theories

There are three key theories of settlement formation and its land use

Concentric Zone theory came from the observations of urban development by Park *et al*. (1925) (Figure 2.4). The example of Chicago city was used, and it was understood that cities developed around a core in the centre. As the city expanded, the central business district (CBD), which is the core, became surrounded by concentric development zones, much like the rings surrounding a tree. The concentration of buildings and land use developed in concentric zones. The zones are commercial centre, zone of transition, low-Class residence or zone of independent workers, medium and higher-class residence, also called zone of better residence, and commuter's zone. Taking this representation of urban areas, the CBD will be subjected to the highest UHI because of the concentration of the buildings.

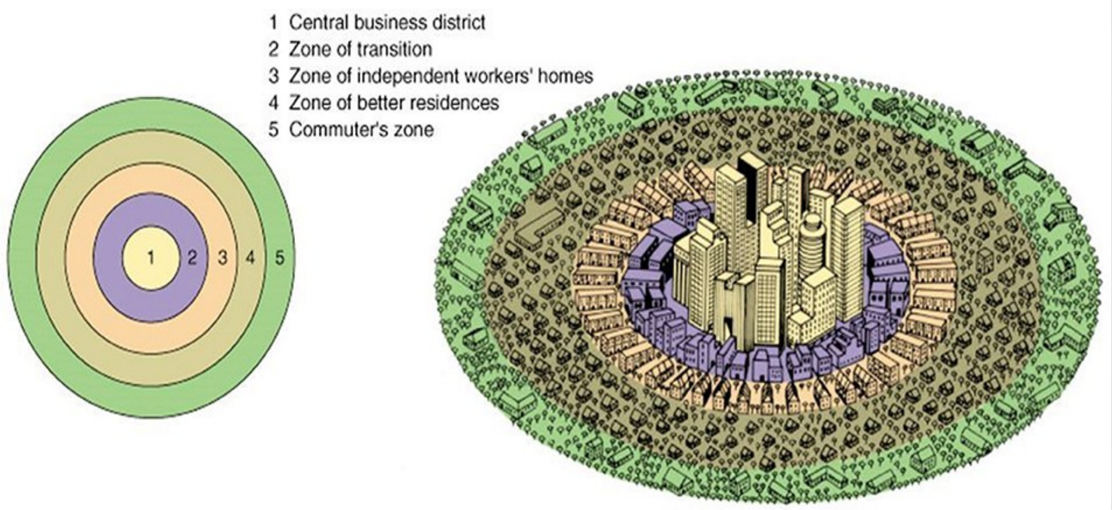

Figure 2.4 Concentric Zone Model (Source : Mandich, 2019)

Sector model, developed by C.D. Harris and Homer Hoyt was based on 34 American cities development. It stated that cities develop out from the CBD along transportation lines, making land use form into different sectors (Figure 2.5). According to this model, urban expansion happens along transportation lines (Burgess, 2015). Among other reason, the new development along the roads happens because of the easy access to the CBD.

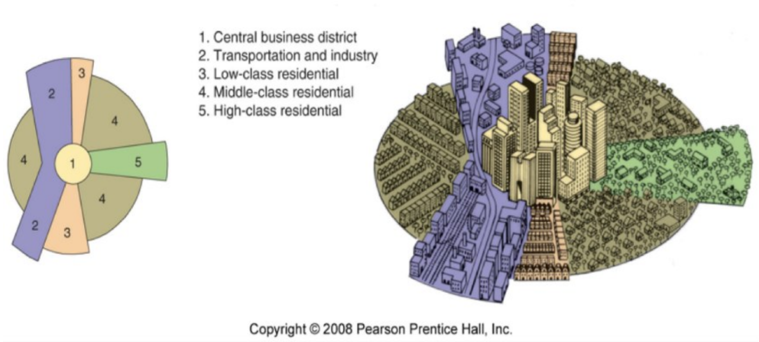

Figure 2.5 Sector Model (Source: Burgess, 2015)

Multiple nuclei by Harris and Ullmanstated that cities expand and centre their development around a variety of distinct business hubs or nuclei. Unlike the two previous theories, many CBDs can be found in a city (Figure 2.6). Even though a city might have started with a CBD, it predicts that other, smaller CBDs will sprout up on the city's outskirts. Each nucleus experiences outward growth until they all converge into a single huge urban area (Harris and Ullman, 1945).

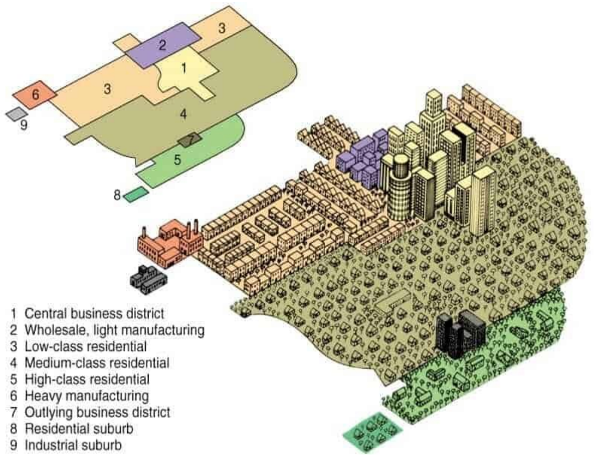

Figure 2.6 Multiple Nuclei Model (Source: Hassed, 2017)

These three theories are based on multiple assumptions which faced a lot of criticism. They have developed conceptual ties over time and are widely regarded as "the classic model of urban land use" in that they have shown to be catalysts for research on cities in both developed and developing nations and have withstood the test of time (Schwirian, 2007). They are still relevant for analysing urban development forms in cities. Hence, they will be used to assess the development type of our study area.

2.2.2 Urban Growth Model

Urban growth models are mathematical models which provide a framework for analysing the processes involved in urban LULC change. They are also used to make projections for future growth patterns and feedback on urban systems based on economics, geography, statistics and sociology. These models are excellent tools used in LULC change assessment to support policy decisions about the causes and consequences of LULC dynamics (Ustaoglu and Aydinoglu, 2019).

Many models have been developed to study the urban system. However, because of the complexity of the system, one single model could not accurately and comprehensively integrate all the content of the system. Therefore, a variety of urban growth models have been developed and applied based on the existing urban theories to meet diverse purposes. Cellular automaton (CA) models (Equation 2.1) are recognized by their high accuracy level (Kafy *et al.*, 2021). Three important principles CA model characterise this model. These are spatial structure, local interaction and state change. The model considers the spatial heterogeneity of socioeconomic, biophysical conditions and the neighbourhood interaction of grids through self-organization in the system to determine the future of a particular cell in a dynamic way (Li and Gong, 2016).

$$S_{t+1} = f(S_t, N_t, P_t) \tag{2.1}$$

where:

S_{t+1} is is the state of the land at time t+1

S_t is the state of the land at time t

N_t represents the neighbourhood of a cell at time t

P_t are the policy or external factors influencing land use change

CA models are often combined with other methods to improve the accuracy of land use predictions (Kafy *et al.*, 2021). Among the models usually combined with CA models are Markov Chain models. These models predict the probability of transitioning from one land cover type to another based on historical land use patterns. These models are adequate for capturing the probabilistic nature of land change over time (Bashir *et al.*, 2022). However, their reliance on fixed transition probabilities may limit their ability to account for dynamic changes influenced by evolving socio-economic and environmental factors.

Another models that are combined with CA models is the Conversion of Land Use and its Effects at Small Scales (CLUE-S). It is a spatially explicit model that predicts land use changes based on local drivers, such as urbanisation and policy decisions. It integrates statistical and spatial modelling techniques to simulate land use change over time (Prasertsoong and Puttanapong, 2025). While CLUE-S is effective for predicting land use changes based on localized factors, it can be computationally intensive and may require high-quality, spatially explicit data, which might not always be available in all study regions. Given these challenges, ANNs and LR were chosen for this study to provide a more flexible and efficient approach to land use change modelling.

In this study, Artificial Neural Networks (ANNs) and Logistic Regression (LR) are chosen for LULC and LST projections due to their ability to handle complex and large datasets while offering both flexibility and interpretability.

ANNs are capable of learning complex, non-linear relationships between land cover types and influencing factors (Equation 2.2) (Id *et al*., 2016; Gupta and Aithal, 2024). Unlike traditional models such as CA-Markov Chain and CLUE-S, ANNs do not require predefined rules or fixed transition probabilities, making them more adaptable to dynamic land use systems. They can also process high-dimensional spatial and temporal data, allowing for more accurate understanding of LULC changes and their effects on land surface temperature (LST). Moreover, ANNs can identify intricate patterns in large datasets, which is especially useful in scenarios where traditional methods might fail to capture subtle transitions (Abbas *et al*., 2021).

$$f(S_t, N_t, P_t) = \sum_{i=1}^{n} W_{ij}.X_{ij} \tag{2.2}$$

WhereW_{ij} represents the weights learned by the network during training

X_{ij} are the input features, including current land use, socio-economic factors, and environmental data

$f(S_t, N_t, P_t)$ is the predicted state of the land at time S_{t+1}

On the other hand, Logistic regression provides an interpretable and straightforward framework for modelling land-use transitions, especially when the focus is on binary outcomes (Equation 2.3). By estimating the log-odds of a particular transition based on predictor variables, LR allows for a better understanding of the factors influencing land use change, which is crucial for planning and decision-making (Kafy *et al.*, 2021). Additionally, they are less computationally intensive.

$$P\left(Y = {}^{1}/_{X}\right) = \frac{1}{1 + \exp\left(-(\beta_0 + \beta_1 X_1 + \beta_2 X_2 + \cdots + \beta_n X_n)\right)} \tag{2.3}$$

$P\left(Y = {}^{1}/_{X}\right)$ is the probability of land transitioning to a new use type

$X_1, X_2, \dots, X_n$ are the predictor variables, such as population density, infrastructure presence, or climate data

$\beta_1, \beta_2, \dots, \beta_n$ are the model coefficients estimated from historical data.

2.2.3 Societal heat vulnerability framework

One of the most pressing challenges for modern society is adapting to climate change and variability. Assessing vulnerability and risk related to climate is crucial for effectively planning and preparing for current and projected climate impacts. These assessments are important for developing adaptation options and strategies (Estoque *et al.*, 2023).

Three main components of climate change vulnerability are frequently used to organize the factors that raise the risk of heat-related morbidity and mortality in individuals and population groupings. These factors include exposure, sensitivity, and adaptive capacity

(Figure 2.7). This framework is inspired by the Intergovernmental Panel on Climate Change (IPCC) Third (TAR) and Fourth Assessment Report (AR4) and has been widely used to assess and map vulnerability (Ducusin *et al*., 2019; Xu *et al*., 2020).

The concept of vulnerability is defined as “the degree to which geophysical, biological and socio-economic systems are susceptible to and unable to cope with, adverse impacts of climate change, including climate variability and extremes”. Exposure, on the other hand, is “the nature and degree to which a system is exposed to significant variations” (IPCC, 2001).Finally, adaptive capacity is defined as “the ability of a system to adjust to climate change to moderate potential damages, to take advantage of opportunities, or to cope with the consequences” (IPCC, 2007). This framework is chosen over the Risk assessment framework introduced by the Special Report on Managing the Risks of Extreme Events and Disasters to Advance Climate Change Adaptation (SREX) and AR5 report because of its simplistic approach to conducting a stand-alone vulnerability assessment and as proposed by Ishtiaque *et al*. (2022) it is essential to treat exposure ‘not only as a precondition for vulnerability but also as a secondary driver of vulnerability to capture the influence of differential exposure’, and the AR4 vulnerability framework captures this better. Additionally, evidence from the literature review conducted by (Estoque *et al*., 2023) shows that the TAR/AR4 vulnerability conceptualization is still relevant, and researchers mostly use it to assess vulnerability rather than the SREX/AR5 conceptualization of risk (52% vs. 43%).

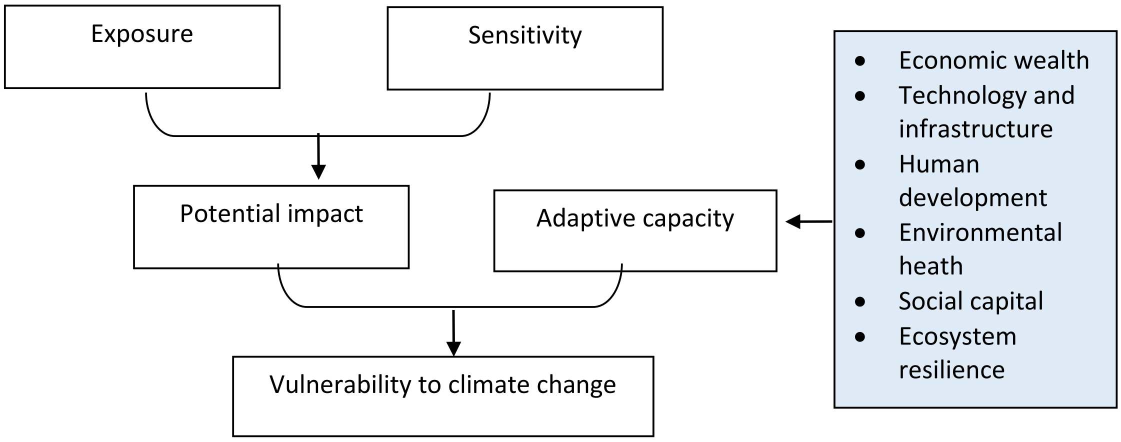

Figure 2.7 Framework for Societal Heat Vulnerability Assessment (Nakul *et al.*, 2018)

There is no single formula to calculate the vulnerability index. Several combinations of exposure, sensitivity, and adaptive capacity have been employed in the literature (Table 2.1).

Table 2.1 Diverse Vulnerability Formula Used in the Literature

S/N	Formula	Reference
1	$E + S - AC$	(Tan *et al.*, 2010)
2	$S(E - AC)$	(Voelkel *et al.*, 2018)
3	$(S \times E \times AC)$	(Manik and Syaukat, 2017)
4	$S(1 - AC + S)/n$	(Zhu *et al.*, 2014)
5	$E(1 - AC) \times S$	(Bhattacharjee *et al.*, 2019)

E is for exposure, S is for sensitivity, AC is for adaptive capacity and n is the number of indicators

2.2.4 Transactional theory of stress and coping

The Transactional Theory of Stress and Coping (TTSC) was developed by Richard Lazarus and Folkman in 1987 to illustrate how humans react to significant life events (Figure 2.8). It is a framework for assessing processes of coping with stressful events. It states that stress results from interactions between humans and their physical or social environment. The impact of the stressor on the individual depends on their appraisal of the stressor and the availability of resources and coping strategies. Hence, the level of individual stress is determined by a judgement of the ability of available resources to cope with internal and external demands (Margaret *et al.*, 2018). In this context, heat is a stressor that affects individuals at different levels depending on their resources. Individual coping strategies to heat are determined by their appraisal of heat and their available resource to cope with or mitigate the negative impact of heat. Heat stress response depends on an individual resource. While some could resolve it by taking a walk outdoors, drinking water, or spending time in a green space, other available resources allow them to use air conditioning and other techniques to deal with the stress.

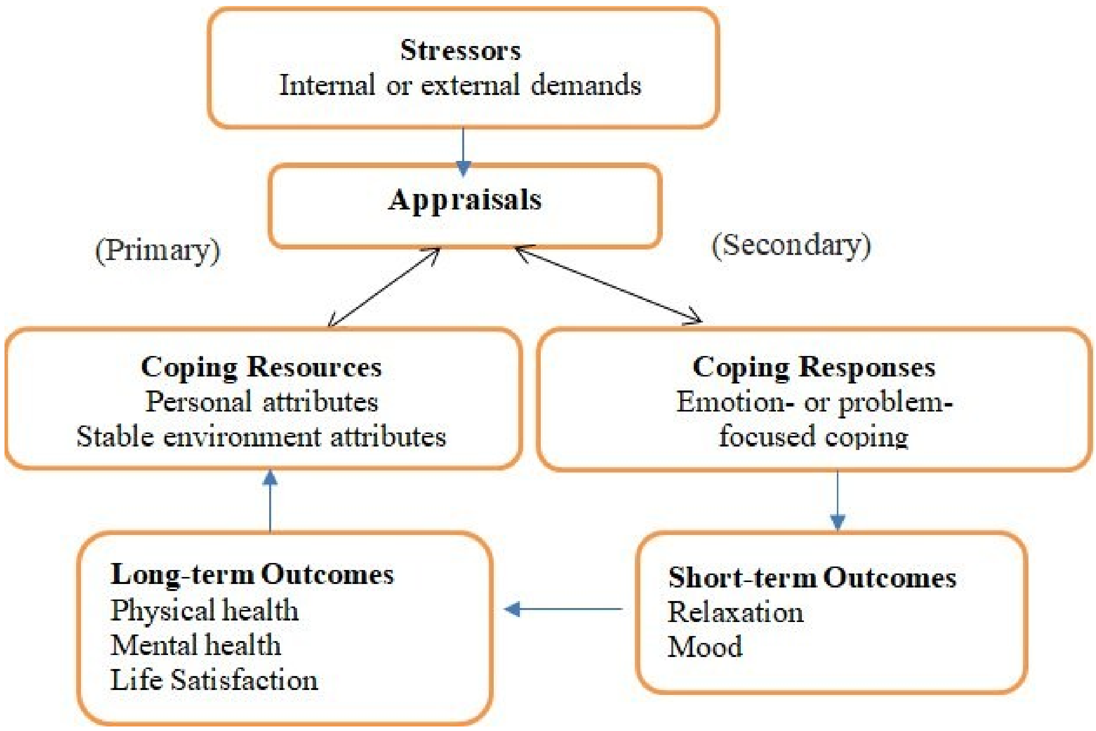

Figure 2.8 Transactional Model of Stress and Coping (Lazarus and Folkman, 1987 adapted from Margaret *et al.*, 2018)

2.2.5 Thermodynamics and heat transfer principles in urban climate studies

Thermodynamics and radiative heat transfer are fundamental theories that support the analysis of LST dynamics and their relationship with LULC changes. Thermodynamics explains the energy transformations and heat transfer processes. The first law of thermodynamics, known as the Law of Energy Conservation, states that energy cannot be created or destroyed, only transferred or converted from one form to another (Boltzmann, 1974). This principle explains how solar radiation absorbed by urban surfaces is converted into heat energy (Mansouri and Zarghami, 2025). The Second Law of Thermodynamics, which governs the natural flow of heat, adds further insight into the heat transfer processes in urban and rural areas (Boltzmann, 1974). According to this law, heat naturally moves from warmer to cooler regions to reach thermal equilibrium. However, in urban settings, this heat transfer is often hindered by low-emissivity surfaces, high-density infrastructure, and reduced airflow. This inefficiency leads to a slower dissipation of heat from urban surfaces, causing localized warming and prolonging the effects of the UHI. This principle also explains why urban centres tend to remain warmer than surrounding rural areas, particularly at night, as the release of retained heat is delayed (Oleson *et al*., 2011).

The concepts of blackbody radiation and emissivity are integral to thermodynamic processes. A blackbody is a theoretical ideal that perfectly absorbs and emits all incident radiation. Although the black body does not exist in nature, it provides a baseline for understanding real-world surfaces. Surfaces with lower emissivity, such as urban materials like asphalt and rooftops, emit less radiation than a blackbody, retaining more heat (Oleson *et al*., 2010). In contrast, natural surfaces with higher emissivity, such as vegetation, emit radiation more efficiently, contributing to lower surface temperatures (Oleson *et al*., 2011).

Emissivity refers to the ability of a surface to emit thermal radiation. It varies for different materials and surfaces, with values ranging from 0 to 1. A surface with an emissivity of 1 is considered a perfect black body, meaning it radiates energy at the maximum rate possible for its temperature (Oleson *et al*., 2010). In cities, the prevalence of artificial surfaces, such as asphalt, concrete, and glass, affects the overall emissivity of the built environment. These materials typically exhibit lower emissivity values compared to natural landscapes. For instance, asphalt has an emissivity of about 0.9, while concrete can range between 0.3 and 0.8, depending on its composition and texture (Li *et al*., 2013). The variation in emissivity among urban materials influences how they absorb and emit heat, particularly during the day and night. One of the most significant implications of emissivity is its role in urban heat islands (UHI). High emissivity surfaces, such as dark rooftops and pavements, absorb more heat during the day while not releasing it efficiently at night. This creates a persistent increase in surrounding temperatures. This principle also explains why urban centres tend to remain warmer than surrounding rural areas, particularly at night, as the release of retained heat is delayed (Oleson *et al*., 2011).

2.2.6 Thermal laws of propagation

Thermal laws of propagation explain the movement of heat through three primary mechanisms: conduction, convection, and radiation (Viskanta, 1963). These principles are critical for understanding the transfer and distribution of thermal energy in urban and rural environments. Conduction involves the direct transfer of heat through materials, such as the transfer of heat from asphalt to the air in urban areas. Convection refers to the movement of heat through air or fluids, often impeded in urban areas due to the lack of open spaces and natural ventilation. Radiation describes the emission of heat energy from surfaces, with urban materials emitting heat more slowly than natural landscapes (Viskanta, 1963; An *et al*., 2023).

The diagram in figure 2.9 highlights critical implications for urban heat, particularly in the context of the Urban Heat Island (UHI) effect. Buildings in urban areas absorb significant solar irradiance during the day, radiating heat back into the atmosphere at night, which contributes to elevated temperatures in cities. Poorly designed structures with low thermal reflectivity and high heat absorption exacerbate this effect, especially when combined with reduced vegetation cover that limit natural cooling through evapotranspiration (Li *et al*., 2022). Additionally, the heat radiated by buildings in various wavebands and the transfer of heat through conduction and convection with surrounding air amplifies local warming, especially in densely built environments with limited airflow (An *et al*., 2023).

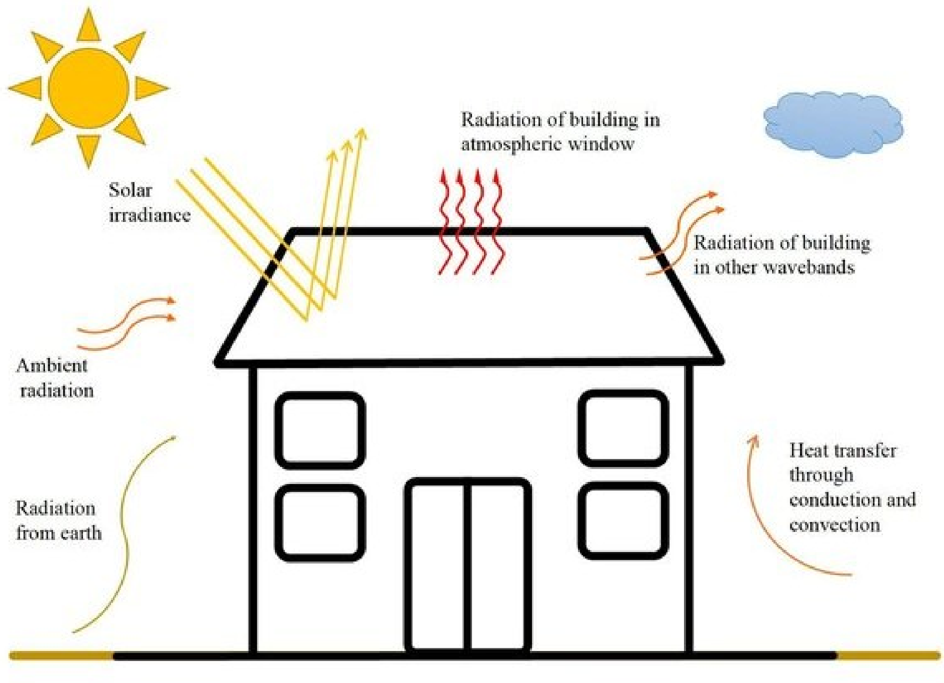

Figure 2.9 Illustration of Building Heat Transfer Mode.
Source: (An *et al*., 2023)

2.2.7 Eco-development theory

Eco-development is a framework that emphasises sustainable development by integrating ecological, economic, and social dimensions. It advocates for development strategies that are ecologically sound, socially equitable, and economically viable (Mellos, 1988). This theory aligns with the principles of sustainable development, focusing on harmonizing human activities with the natural environment to ensure long-term resilience and well-being. In the context of urban heat, eco-development principles encourage practices such as urban greening, sustainable architectural designs, and climate-resilient infrastructure to mitigate the negative impacts of urbanisation (Wu *et al*., 2024).

2.2.8 Climate trade theory

Climate trade theory examines the economic trade-offs associated with climate change mitigation and adaptation strategies. This theory highlights the tension between economic growth and the need to implement sustainable practices to address climate change (Stern, 2007). Urban areas, as hubs of economic activity, face significant challenges in adopting climate-smart policies, such as renewable energy systems, energy-efficient buildings, and green infrastructure (Vujovic *et al*., 2021). While these measures may attract short-term costs, they offer long-term benefits, including reduced urban heat, improved air quality, and enhanced resilience to climate impacts.

2.3 Review of Related Studies

2.3.1 Global overview of urbanisation

Every region of the world is expected to become more urbanised over the next decade, though it is expected that heavily urbanised regions will slow their growth rates. The less developed countries will account for 90% of urban population increase from 2018 to 2050 (UN-Habitat, 2020). It has been reported that urbanisation, no matter the form (sprawl, dispersed or peri-urbanisation), affects the physical extent of urban areas and the change is faster than that of the urban population. For example, between 1990 and 2015 a study on cities in developed countries indicated that their urban land area increased by 1.8-fold while their population increased by 1.2-fold (UN-Habitat, 2020). Setting the course of urbanisation in a more sustainable way for the benefit of present and future generations requires some understanding of the form, pace and scale of urbanisation across the world as well as the social, economic, political and environmental implications of urbanisation. However, a lack of consistent data constitutes a limiting factor for achieving this goal, particularly in the developing world. Nevertheless, that did not stop investigations.

In East Asia's Changing Urban Landscape book, the data limitation was addressed by the use of satellite imagery and other data to measure the scale and form of urban expansion across East Asia and the Pacific region between 2000 and 2010. A huge amount of free access data resulted from the study and some were presented through maps and charts illustrations. The book presented trends in urban expansion and population growth in more than 850 cities. It also discussed findings about the increase in urban population density and quantified the impact of urbanisation on administrative boundary fragmentation in urban areas. One of the key findings of the research is that the urbanisation rate experienced in the last 10 years was equivalent to that experienced in Europe over 50 years. The expected outcome is to improve the understanding of urbanisation to maximize the benefits of urban growth through some potential policy options outlined in the book (World Bank, 2015).

Africa is one of the world's fastest urbanisation regions although the continent is still largely rural, the urban population is expected to be more than triple in 40 years. In 1950, only 10% of the African population lived in urban areas and it is expected that 55% of the population will be living in urban areas by 2050. The number of megacities will increase along with the creation of new cities (United Nations, 2018). Africa's urbanisation is characterised by an unplanned expansion worsened by the legacy of colonialism, structural adjustment, and neoliberalism, which resulted in underdeveloped urban planning institutions (López-Ballesteros *et al*., 2017). Although some opportunities accompany the urbanisation rate, it also has a lot of challenges.

According to UN-Habitat (2020), changes in urban areas and population imply global environmental change through an increase in energy consumption, greenhouse gas emissions, climate change and environmental degradation. It has been reported that cities emit 70% of global greenhouse gases and consume 2/3 of global energy. In addition, the first studies that considered a demographic factor to explain the impact of urbanisation on greenhouse gases emission have revealed an intimate relationship between population and greenhouse gases emission (Weber and Sciubba, 2019).

2.3.2 Urbanisation and lessons from cities around the world

Cities around the world have faced unique challenges and have employed diverse strategies to manage urbanisation. This section explores cases from cities across different continents, highlighting key lessons learned in managing urban growth.

Tokyo, Japan, is one of the most significant examples of successful urbanisation. After World War II, Tokyo experienced rapid growth, driven by industrialization and economic recovery. The city's success in managing high population density is due to strategic urban planning, which includes efficient public transportation, a focus on green spaces, and technological innovations (Zhang and Yan, 2024). Tokyo's approach demonstrates that high-density living can be sustainable when planned effectively. One example is the city's extensive subway system and vertical living structures, which have helped accommodate millions of residents in a relatively small geographic area.

Shanghai, China, presents a more recent example of rapid urbanisation, particularly since the 1990s. The city's economic reforms and openness to global trade have fueled its rapid growth. Shanghai's urbanisation is largely government-driven, with large-scale development projects and the creation of high-rise residential buildings (Wu *et al*., 2022). The Chinese government has played a significant role in shaping the city's urban landscape, implementing strict policies to control land use and infrastructure development. Shanghai's growth demonstrates how government intervention and strong central planning can result in rapid, efficient urbanisation, although it also raises questions about social equity and displacement (Solecki and Leichenko, 2006).

In Africa, the case of Lagos, Nigeria, one of the fastest-growing cities in Africa and the world is worth noticing. Its rapid urbanisation is driven by rural-to-urban migration, as well as the city's status as an economic powerhouse in West Africa (Aweda *et al*., 2024). With over 20 million residents, Lagos faces significant challenges in infrastructure, transportation, housing, and social services. Informal settlements and slums, like Makoko, are a direct result of the city's inability to provide affordable housing for its growing population. However, Lagos is also making strides with various initiatives aimed at improving urban governance, transportation (such as the BRT – Bus Rapid Transit system), and waste management. Lagos exemplifies the challenges of managing urbanisation in a rapidly growing African metropolis, and it underscores the need for sustainable, inclusive urban planning that can address both the economic potential and social challenges of urbanisation (Abubakar *et al*., 2020).

Nairobi, the capital of Kenya, is another example of an African city which has experienced rapid urbanisation over the last few decades. It is primarily due to rural-to-urban migration and regional economic integration. The city's population has grown significantly, and informal settlements, such as Kibera, are home to a large percentage of its residents. Nairobi is also one of the fastest-growing cities in Africa, with a burgeoning middle class and a growing demand for services and infrastructure (Oyugi, 2021). The city faces several challenges related to slum development, inadequate sanitation, and poor waste management. However, Nairobi has been a leader in introducing green spaces, such as the Nairobi National Park, and embracing innovative solutions to urban challenges, including the use of technology to improve urban governance. Nairobi's efforts to balance urban growth with sustainability, particularly through initiatives like the Nairobi Green City Plan, provide important lessons for other African cities grappling with rapid urbanisation (Mwanzu *et al*., 2023).

When examining the broader themes of urbanisation, sustainability emerges as a critical consideration. Cities like Copenhagen and Amsterdam have focused on making urbanisation more environmentally sustainable (Peštová, 2022). These cities have integrated green spaces, sustainable public transport, and energy-efficient buildings into their urban designs. Copenhagen, for example, aims to become carbon neutral by 2025, offering a model for how urban centers can grow without compromising environmental health. These examples highlight that urban growth should not come at the expense of sustainability; with the right policies, cities can thrive while minimizing their ecological footprint.

Lastly, the challenge of balancing urban growth with livability is a theme that runs throughout many cities' experiences. The rapid expansion of cities often leads to overcrowding, pollution, and deteriorating quality of life. Effective governance, investment in infrastructure, and equitable policies are crucial for mitigating these negative effects. Cities that fail to balance growth with livability risk undermining their economic and social stability, as seen in the struggles faced by low-income communities in highly urbanised areas.

2.3.3 Land use and land cover change

Human activities induce changes in a natural environment among which LULC change. The study of LULC change is a priority concern of the global change research community because it is one of the primary sources of global environmental change. In the earth system, a small amount of change in the extent of urban areas can affect the climate, hydrology and biochemistry at a local level and eventually at a global level (Li *et al*., 2017).

Humans have historically modified land for survival, but the rate and amplitude of exploitation were not as high as it is today. Recent rapid exploitation has resulted in a rapid change in ecosystems and environmental processes at the local, regional, and global levels. Presently, LULC changes encompass some environmental concerns such as climate change, biodiversity loss, and water, soil, and air pollution. Although humans are key drivers of LULC change, natural events such as fire, weather, climate change, and flooding can also alter the composition of the earth's surface. Monitoring and mitigating the negative consequences of LULC change while maintaining the production of essential resources is now a major priority for researchers and policymakers worldwide. This is done by modelling spatiotemporal patterns of LULC change or by investigating the causes, impacts, and consequences of the change (Parveen *et al*., 2018).

In 2018, a global landcover change measuring was initiated by the Organisation for Economic Co-operation and Development (OECD) for monitoring pressures on ecosystems and biodiversity. The initial results of the project were: improved information about natural and semi-natural vegetated land loss and gain, conversions of land cover classes, expansion of built-up area and changes in the surface water. Globally, 2.7% of natural vegetation land has been converted to another type of land cover from 1992 to 2005. 81% of the natural vegetation land is converted to cropland, 5% to artificial surfaces, 5% to water and 9% to bare soil (OECD, 2011).

At the regional level Bagaria *et al*. (2021) used temporal satellite data to study the pattern of LULC change in the East Godavari River Estuarine Ecosystem of India from 1977–2015 and predicted the possible LULC changes by 2029. The result showed there was a creation and an increase of aquaculture areas at the expense of mangroves and all the coastal side was destroyed because of beach clearing. The study concluded that socio-economics policies greatly influence LULC change in that area. The simulation exercise used in the study allowed us to highlight that the choice of a suitable modelling approach should be based on the characteristics of an ecosystem and when the landscape is composed of smaller sub-region with some differences in the LULC composition, stratification of the region for simulation could give a better result.

At the local level, numerous LULC change studies have been conducted to understand the dynamics of different ecosystems including urban areas (Illiassou *et al*., 2015; Doulay *et al*., 2019). Illiassou *et al.* (2015) characterised the spatio-temporal dynamics of Niamey's urban area from 1975 to 2013 using Landsat images and application of landscape ecology for conservation purposes. The study revealed an expansion of built-up areas at the expense of agricultural areas throughout the study period, with a lower rate during the period 1989-1999. The analysis revealed the densification of built-up areas and sprawl around transportation lines. It concluded that the urbanisation process was the main driver of landscape dynamics in the area during the study period and that sound decisions based on available data could help city planners achieve sustainability.

Acheampong *et al.* (2017) observed a similar urbanisation process in Kumasi, Ghana. The urbanisation index was used to quantify the process of urbanisation over 28 years (1986-2014). The result shows that 72% of the expansion happened during the last 13 years of the study with a differential expansion over the city resulting from unplanned urban growth. The increase in population size is strongly correlated with urban expansion and urban populations are expected to increase in the coming years to limit unsustainable urban expansion, there is a need for a comprehensive regional growth management strategy based on effective strategic partnerships among the respective administrative districts (Das and Angadi, 2021).

There has been increasing literature about urban LULC change in the last decades. A survey of related literature on the Scopus database showed that most of the studies were conducted in the USA, China, India and Europe, with Africa having fewer documented studies, particularly in West Africa. Because Africa has the highest urbanisation rate and its cities will accommodate more than 1.339 billion in 2050 (López-Ballesteros *et al.*, 2017). More studies are needed on sound urbanisation in Africa. Additionally, most studies are conducted in capital cities and megacities, neglecting medium-sized cities. However, medium-sized cities have more potential to reverse their development pattern to be more sustainable than big cities. Moreover, this medium size city is projected to grow to accommodate the future urban populations. Hence, it is important to study their growth patterns. Part of this study will contribute to filling this gap.

2.3.4 Impact of urbanisation on urban temperatures

Many methodological approaches have been used to assess the effect of urbanisation on urban temperatures. In the existing literature. Whereas some studies use satellite imagery as a data source to Investigate the Surface Urban Heat Island (SUHI) based on land surface temperatures, some ground measurement datasets were used to study the effect of urbanisation on urban temperatures.

Using thermal bands of Landsat data from 1990 to 2019, remote sensing and GIS techniques were used to quantify the variation in land surface temperature across different LULC classes in Pune (India). The result showed a rise in mean land surface temperature over the city during summer periods (5,2%) (Gohain *et al*., 2021). In Delhi, the same type of data and method was used between 1991 and 2018. The results show that the minimum, maximum, and mean SUHII increased by 1.26°C, 4.6°C, and 1.18°C, respectively due to the effect of urbanisation (Shahfahad *et al*., 2022).

In Ghana's two biggest cities, Accra and Kumasi, the SUHII went from 1.60 °C to 2.24°C at Accra and from 2.66°C to 2.03°C at Kumasi in 2002 and 2017 respectively (Buo *et al*., 2021). Remote sensing data is an excellent tool for evaluating UHI due to its long-term spatial availability and the fact that data acquisition does not involve any cost. Nevertheless, different studies have also used station data to assess the same phenomena to a large spatial extent.

Yang *et al*. (2017) used weather observation data to assess the effect of urbanisation on the urban temperatures in the urban agglomeration of Yangtze River Delta (China). To effectively discriminate the UHI effect, the observational stations were classified into two groups namely urban and rural and summer extreme temperature indices were calculated. Overall, urbanisation contributed to more than one-third of the increase in the intensity of extreme heat events, which was comparable to greenhouse gas contributions in the study area. In Liaoning Province, using the same type of data, Hu and Li (2022) calculated the extreme temperature indices using RclimDex, and eight indices were chosen to study the impact of urbanisation on extreme temperatures. A dynamic Urban Minus Rural (UMR) method was used to quantify the impact of rural and urban areas on the temperatures and annual variations. In addition, some landscape indices were calculated at a buffer zone of 10km radius of each meteorological station to evaluate the spatial impact of urbanisation on temperatures. The result suggested that the urbanisation effect increased the frequency of daytime extreme warm events by 6.55 days and decreased the frequency of extreme cold events by 3.33 days based on the average value from 1959 to 2018. In terms of absolute indices, there was a statistically significant correlation between tropical nights and the landscape shape index, and urban landscape aggregation also had a substantial impact on the frequency of extreme temperature events in the study area.

Overall, urbanisation affected temperatures, and the changes were attributed to the impact of the UHI effect. This phenomenon occurs in the canopy layer, which is the most important for human health because it is where the majority of activity occurs and this is why some studies have gone further to investigate the effects of urban temperature on urban population comfort (Vinayak *et al*., 2022), mortality and morbidity during extreme heat events (Watson *et al*., 2020), heat risk and vulnerability (Jagarnath *et al*., 2020)

Decision-making based on data is important for sustainable development. However, data availability is a real challenge in Africa, because each country has its realities and context, the effective way to tackle a problem is to apply a bottom-up approach, that is to look at the issue from the local level. Recently, a joint project called u-CLIP financed by VITO and ACMAD has been working to implement a digital platform containing detailed urban climate projections of Niamey city. This information will be available for stakeholders and decision-makers to help in implementing climate-resilient action in Niamey. Although this information is only limited to Niamey city, it's the first attempt, to my knowledge, to vulgarise urban climate data information digitally. The findings of the present research could be an important contribution to nourishing such a platform.

2.4 Examples from Other Regions

As the urban population grows, the urban LULC pattern changes on a large scale, resulting in several environmental and ecological issues. The changing LULC pattern in urban areas also has an impact on the quality of life by altering the environment, deteriorating air quality, and increasing the frequency of extreme climatic events such as high-intensity rainfall and the development of urban heat islands (Buo *et al*., 2021). Since formal surveys of the urban atmosphere began in the early nineteenth century, hundreds of measurement studies on the city temperature effect or heat island effect have been published in the scholarly literature and it is established that urbanisation causes UHI (Yang *et al*., 2017; Buo *et al*., 2021). The integration of thermal band in the satellite images makes it possible to use the same data set to study LULC change and SUHI.

Previous research has shown that geographically weighted regression (GWR) is the best method for determining the relationship between LULC and LST (Adeyeri *et al*., 2017; Debele and Beketie, 2024). Hence, the current study will build on their findings to assess the relationship between these variables. However, the urban thermal field variation index used in their study to assess heat vulnerability was only based on the physical aspect of the landscape. Although it allowed identification of areas susceptible to heat, such an index does not relate the "place to people" it would have yielded more useful information if the characteristics of the population were taken into account.

According to Wilhelmi and Hayden (2010) vulnerability to extreme heat, events necessitate an interdisciplinary approach that includes climate information, the natural and built environment, social processes and characteristics, interactions with stakeholders, and a local level assessment of community vulnerability. The studies that have used demographic and socioeconomic characteristics of the population to investigate vulnerability used either only survey data or the physical environment along with aggregated census data (Inostroza *et al*., 2016; Nakul *et al*., 2018). Wilhelmi and Hayden (2010) stated that individual and household level field research data, both quantitative and qualitative, are required for a comprehensive analysis of a population's adaptive capacity. The Transactional Model of Stress and Coping that will be used in this study will help us collect adaptation and coping strategies data that could not be provided by population census data.

The novelty of the current study is a heat vulnerability assessment based on physical and built environments along with a household survey to assess the coping and adaptation strategies. Therefore, the present study will use a multifaceted top-down and bottom-up approach to characterise societal vulnerability in the study areas.

2.5 The Overview and Key Issues of the Study:

According to the study "Long-term Prospects for West Africa" (MEDD, 2011), the most significant development in the last thirty years is the very rapid development of cities. Niger, although long considered a predominantly rural country, has not remained on the sidelines of this dynamic. The droughts that the country has experienced, as well as the continuous degradation of the soil, have led to a massive influx of rural populations, thus affected, towards the main urban centres, notably Niamey, Zinder, and Maradi. The rate of urbanisation has increased significantly, rising successively from 5% in 1960, 12% in 1977 (RGPH77), 15% in 1988 (RGPH88) and 16% in 2001 (RGPH2001). Thus, from 1960 to 2001, the rate was multiplied by a little more than three times. The urban growth rate changed from an average of 8% between 1960 and 1977 to an average of 5% between 1977 and 1988 and 3.65% between 1988 and 2001. Even the lowest rate of 3.65% in the period 1960-2001 was a concern, as it could double the urban population in less than 20 years. From 2020 to 2050 the urban growth rate is estimated at 4.06%. IRD suggests the possibility of a further rural exodus, with a much greater growth for cities than for the rural world in Niger (MEDD, 2011). This remains a huge concern for the country.

To tackle the challenge of urbanisation, a strategic of urban planning was elaborated to tackle the challenge of urbanisation. Unfortunately, only the economic implications of urbanisation seem to attract the attention of the leader as there is no mention of urban heat in the entire document although this remains a reality in Niger. This could be explained by the scarcity of documented studies on urban heat in Niger, which this study will assist to fill the gap.

CHAPTER THREE

3.0 MATERIALS AND METHODS

3.1 Description of Types and Sources of Data

3.1.1 Description of remote sensing data used in this study

In this study, various remote sensing datasets were utilised to achieve the objectives of analyzing LULC changes, assessing LST patterns, and conducting heat vulnerability analysis. Below is a description of the datasets used:

3.1.1.1 *Description of Landsat datasets*

The Landsat satellite series has the most extended history of satellite observations. As a result, Landsat is an invaluable resource for monitoring global changes and observing the earth at medium spatial resolution in decision-making procedures Shikary and Rudra, 2020). In this study, multispectral Landsat satellite images were used for LULC change analysis. Landsat 8, launched in 2013, features the Operational Land Imager (OLI) and Thermal Infrared Sensor (TIRS), offering improved radiometric resolution and 11 spectral bands at a spatial resolution of 30 metres for reflective bands and 100 metres for thermal bands. Landsat 7, operational since 1999, is equipped with the Enhanced Thematic Mapper Plus (ETM+), which provides similar spatial resolution but with slightly fewer spectral bands. Landsat 5 and 4, launched in 1984 and 1982 respectively, are equipped with the Thematic Mapper I, offering six reflective bands and one thermal band at 30 metre spatial resolution, making them valuable for historical LULC analysis. All imagery was obtained from the United States Geological Survey (USGS) Earth Explorer platform (https://earthexplorer.usgs.gov/).

3.1.1.2 *MODIS 8-Day LST Data*

The Moderate Resolution Imaging Spectroradiometer (MODIS) is derived from sensors aboard NASA's Aqua and Tera satellites and offers consistent and reliable surface temperature measurements over time (from 2000 to present). The dataset was accessed through the Google Earth Engine (GEE) platform, which provides efficient tools for processing and analyzing large-scale geospatial datasets. The 8-day composite LST product used in this study was the MYD11A2 product, derived exclusively from Aqua's observations. This temporal resolution smooths short-term fluctuations caused by transient weather conditions, providing a consistent and stable dataset for analysis.

The choice of MODIS LST data, although having a coarse spatial resolution (1km) over Landsat-derived LST (30m) for this study, was based on its ability to provide consistent, validated, and globally processed surface temperature estimates. Additionally, the seasonal consideration of this study makes Landsat-derived LST unsuitable. Its temporal resolution of 16 days makes exploitable images rare, particularly in the rainy season due to cloud cover. Furthermore, Landsat's overpass time of around 10:30 am local solar time may not effectively represent the spatial temperature variations. In contrast, the 8-day MODIS composite from Aqua satellite's overpass time is about 1:30 pm, providing an optimum measure of temperature variation. Finally, MODIS LST data's robust quality assurance makes it a more reliable and representative choice than Landsat-derived LST, which involves complex preprocessing steps which can introduce uncertainties.

In this study, MODIS LST data were used to analyse spatial and temporal variations in land surface temperature. The dataset allowed for the identification of heat-prone areas, including urban heat islands, and enabled the exploration of seasonal temperature patterns during specific periods such as the hot-dry, cooler-dry and rainy seasons. Furthermore, MODIS LST data were integrated into the heat vulnerability analysis representing an indicator or heat exposure.

3.1.1.3 *Digital Elevation Model (DEM)*

A Digital Elevation Model (DEM) was utilized in this study to analyse the topographic characteristics of the study area, including slope, elevation, and surface roughness. This dataset was obtained from the USGS Earth Explorer platform (https://earthexplorer.usgs.gov/), which provides high-quality elevation data derived from sources such as the Shuttle Radar Topography Mission (SRTM). The DEM used in this analysis has a spatial resolution of 30 metres, offering sufficient detail for identifying variations in terrain (slope, elevation, roughness) and their impact on LULC dynamics. These derived topographic variables were critical for understanding the physical constraints and drivers of LULC changes.

3.1.2 Population dataset

The World population dataset, sourced from WorldPop (https://www.worldpop.org), was utilised as an indicator of heat exposure in the heat vulnerability analysis. This dataset provides global population distribution at a high spatial resolution of 100 metres. WorldPop integrates data from a variety of reliable sources, including population and housing censuses, IPUMS-International datasets, vital registration of births and deaths, Demographic and Health Surveys (DHS), Multiple Indicator Cluster Surveys (MICS), and official statistics reported by the United Nations and the United States Census Bureau. These diverse data sources are combined with satellite imagery and geospatial information to estimate ambient population distributions accurately (Lloyd *et al*., 2017). The data helped identify areas with higher population densities vulnerable to extreme heat conditions, providing a more precise understanding of exposure at localized scales.

Additionally, census population data was acquired from Niger's National Institute of Statistics. The data assessed the relationship between urban growth and population growth. Providing insight into drivers of urban expansion in the two cities.

3.1.3 Description of meteorological data

Daily 2m above-the-ground air temperature and rainfall datasets of Tahoua and Zinder were obtained from the National Meteorological Agency of Niger Republic in Niamey. The data was given in a tabular form, recording daily minimum and maximum temperatures in degrees Celsius and rainfall data in millimetres. The data covered 31 years and was used to describe the study areas. The minimal and maximum temperature dataset was also used to make a trend analysis of diverse extreme heat indices.

3.1.4 Description of OpenStreetMap datasets

The OpenStreetMap (OSM) data, a collaborative geospatial dataset sourced from voluntary contributions (https://www.openstreetmap.org), was utilised in this study to support spatial analysis and field surveys. The 2023 contribution of OSM provided detailed vector data on the road network and building footprints within the study area. The road network data was one of the predictors for modelling future LULC changes. Additionally, the building footprint data was employed to inform sampling strategies for the socioeconomic survey.

3.1.5 Description of survey data

A structured interview (Appendix A) was conducted in Zinder and Tahoua to assess socioeconomic characteristics, perceptions of extreme heat, and coping strategies of urban residents as part of the heat vulnerability analysis. The questionnaire captured information on household sensitivity factors as well as adaptability indicators.

Respondents provided insights into their perceptions of temperature changes, health impacts, and the effects of extreme heat on labour and household income. The survey also documented coping strategies. This data was a critical input for understanding heat vulnerability.

3.2 Description of Methods of Data Collection

3.2.1 Description of satellite image data collection

The criteria for selecting Landsat images were based on seasons, availability of the images and threshold cloud cover of less than 10%. Dry season images were used to develop and maintain consistency in identifying features. It also helps to avoid seasonal changes, which might result in changes in reflectance value (Buo *et al.*, 2021). The details of the selected images are presented in Table 3.1.

Table 3.1 Landsat Images Used in the Study

Satellite	Sensor ID	Path/Row	Spatial resolution	Cloud cover	Acquisition date
Landsat 8	OLI_TIRS	191/50	30m	0.02	15/04/2022
Landsat 8	OLI_TIRS	188/51	30m	0.02	10/04/2022
Landsat 7	ETM	191/50	30m	0	11/04/2012
Landsat 7	ETM	188/51	30m	0	20/04/2011
Landsat 7	ETM	191/50	30m	0	31/03/2002
Landsat 7	ETM	188/51	30m	5	05/04/2000
Landsat 5	TM	191/50	30m	0	28/03/1988
Landsat 4	TM	188/51	30m	0	19/03/1988

The MODIS LST dataset was filtered to focus on the study area, either Tahoua or Zinder, using a predefined shapefile. To capture seasonal variations, the data was further filtered to cover specific seasons across selected years. The cooler dry season was defined as

December to February, the hot dry season as March to May, and the rainy season as June to September corresponding to the seasonal period breakdown in Niger Republic.

3.2.2 Description of social survey data collection

A comprehensive method of interviews and observation was chosen as the data collection method. A multistage sampling technique was used to select the household to administer the questionnaire. Initially, the study intended to use urban neighbourhoods as units and population per neighbourhood as the study population. However, such information was unavailable in the two cities at that moment. Thus, the population per neighbourhood could not be assessed. Henceforth, the data of houses and their numbers from OSM was used in ESRI Shapefile format. The data comprises all the required topographical data. Buildings were used as proxy to determine the number of houses in each city, and the projected point coordinates of each house were automatically generated using the centroid of each house.

The study focused on the cities of Tahoua and Zinder, which are located in urban districts containing other villages. To define urban area units for data collection, the city parts within the urban districts were subdivided using major roads, which served as natural boundaries and area size. Each unit was then assigned a unique code to differentiate it. The code included the city name (e.g., Tahoua or Zinder), the number of the commune within which the unit was located (e.g., 1, 2, 3, or 4), and a letter to distinguish between units within the same minicipality (e.g., A, B, C, or D) (Figure 3.1). For example, a unit in Tahoua's first district might be coded as T1A. A total of 392 and 381 households were to be interviewed in Tahoua and Zinder, respectively (Table 3.2).

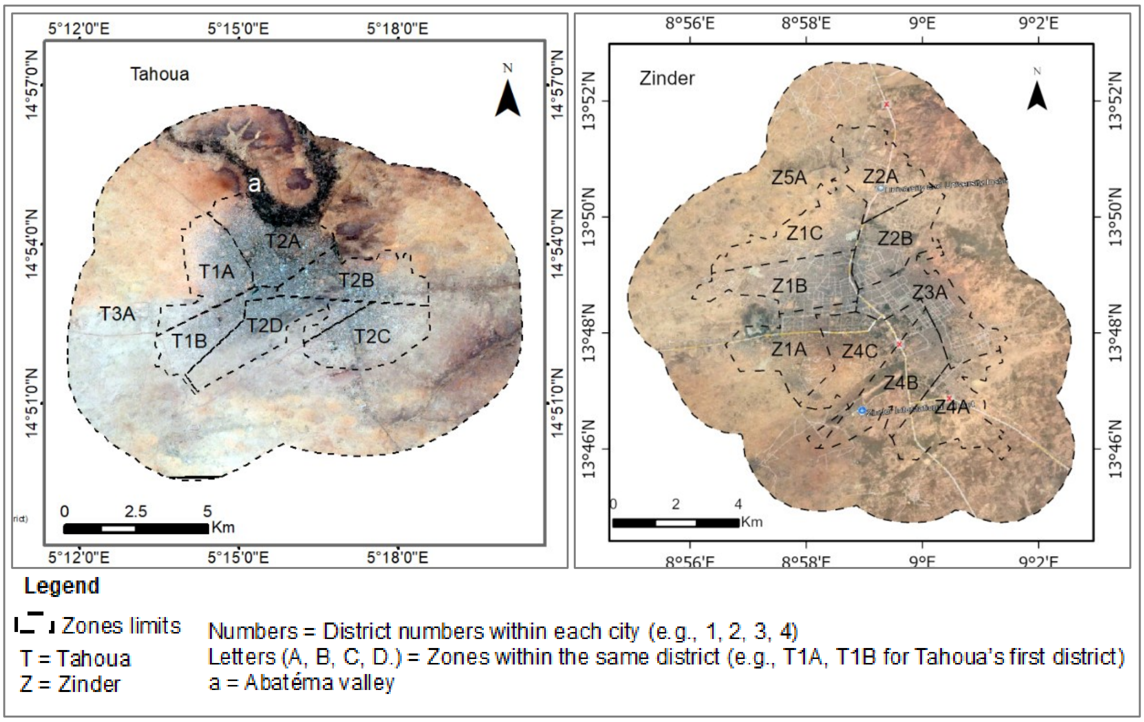

Figure 3.1 Google Map Image View and Zonal Repartition of the Urban Landscape

Table 3.2 Sample Size Per Zone in Each City and Dominant Neighbourhoods' Names

Zone	Population	Sample size
	Tahoua	
T1A (Tougoulaoua, CEG 2)	16782	142
T1B (Toudoum-Adoum, Kowet, Wadata)	3419	34
T2A (Gao, Maboya Amaré, Dioulanke)	13118	111
T2B (Kourfayawa)	5452	46
T2C (Sabon Gari)	1259	16
T2D (Nasarawa)	5143	43
Total	45173	392
	Zinder	
Z1A (Kouran Daga Extension, Kangna)	1402	38
Z1B (Karkada, Mai Tourmi, Charé)	3524	95
Z1C (Madataye)	673	19
Z2A (Garin Liman, Malam amar)	58	4
Z2B (Wadata, Djaguindi)	1819	49
Z3A (Zengou, Garin Malam, Sabon Gari)	3427	93
Z4A (Route Magaria, Route Mirriah)	313	9
Z4B (Birni, Galadima, Aéroport)	935	26
Z4C (Kangna, Yadda Kondagué)	1754	48
Total	13905	381

The sample size was calculated at the city rather than the zone level to ensure representativeness for the entire city, which is the primary focus of the study. The following parameters were used for the calculation: a 95% confidence level, a 5% margin of error, a population proportion of 50% (to ensure the most conservative sample size), and the population size defined as the total number of houses in the city. Calculating the sample size at the city level optimizes resources while ensuring statistical rigour. The total sample size for the city was then proportionally distributed across zones based on the number of houses in each zone. This proportional allocation ensured that the sample size in each zone reflected the relative size of the zone within the city, thereby maintaining representativeness at the city level while allowing for meaningful neighbourhood-level analysis. A simple random sampling technique was used to select houses where interviews were to be administered from each neighbourhood from the attribute table. The selected houses were renamed according to zone name and serial number. Henceforth, the coordinates of each appointed house were introduced into a GPS as waypoints.

Upon arriving at each city, the city hall was visited to seek permission to conduct the survey. After this was granted, houses were located, and data was collected through observation and personal interviews. When more than one household is found in a building, a number was assigned to each household, and one number was randomly selected. Figure 3.2 summarizes the sampling technique used in this study.

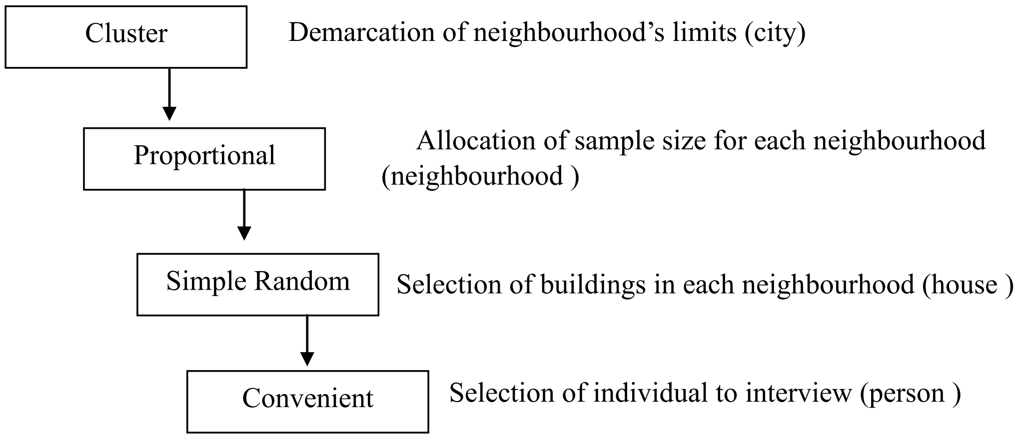

Figure 3.2 Sampling Procedure for the Selection of Respondents
Source: author, 2024

3.3 Methods of Data Analysis

3.3.1 Spatiotemporal analysis of LULC change in Tahoua and Zinder

3.3.1.1 *Landsat image processing and classification*

Image processing was performed to accurately extract LULC in the study area for 1988, 2000, 2011, and 2022 in Zinder and 1988, 2002, 2012, and 2022 in Tahoua. The Landsat images used in this study were radiometrically calibrated and orthorectified by the data provider to correct sensor-related errors and align the imagery with true geographic coordinates. Further rectification and enhancement steps were conducted to ensure the data's reliability for LULC classification. These preprocessing steps included atmospheric correction using Dark Object Subtraction (DOS), pan-sharpening, reprojection, clipping, and colour composite creation. Each step had a specific impact on data quality and interpretability (Lin *et al.*, 2015; Rokni and Komeil, 2023).

Atmospheric correction via DOS was applied to reduce atmospheric scattering and absorption effects, minimizing brightness distortions and improving the clarity of surface reflectance. This correction ensures that the reflectance values more accurately represent the land surface, enhancing differentiation between LULC types. The pan-sharpening process improved spatial resolution from 30m to 15m by merging the multispectral bands with the panchromatic band, making it possible to detect finer details. This step is particularly useful in identifying small urban features, which are essential for accurate LULC classification (Rokni and Komeil, 2023).

The images were reprojected to WGS 1984 UTM Zone 31N for Tahoua and WGS 1984 UTM Zone 32N to align with the study area's geographic region, ensuring accuracy in spatial measurements and consistency across datasets from different years. Clipping the images to the area of interest (AOI) reduced data volume and focused the analysis on relevant locations, minimizing extraneous data that could affect classification accuracy. Finally, a color composite was created by combining multiple spectral bands to improve visual interpretation, which assists in distinguishing different LULC classes by enhancing color contrast.

These preprocessing steps collectively contribute to image quality, correct distortions, and enhance visual interpretability, ultimately improving the accuracy of the subsequent (Lin *et al*., 2015). After preprocessing, representative sample data for each LULC class were selected based on visual interpretation and prior knowledge of the terrain. The Dzetsaka classification plugin in QGIS 3.34 was used to perform a supervised classification. This plugin supports multiple algorithms, including Gaussian Mixture Model, Random Forest, and Support Vector Machine (SVM), enabling users to perform efficient and accurate classifications within the QGIS environment using various classification techniques. These algorithms were tested, and the RF (Breiman, 2001) provided the highest accuracy. Therefore, it was used to perform a supervised classification of the images. The RF algorithm excels at LULC classification and remote sensing because it can handle complex datasets, is robust against overfitting, and has low bias (Ali *et al*., 2012). During the training phase, it creates an ensemble of decision trees that are trained independently; the results from all trees are then aggregated to provide a prediction (Albertini *et al*., 2024).

In Zinder, three classes of LULC have been identified: agricultural land, built-up, and vegetation. In addition to these classes, a water class was identified in Tahoua. The descriptions of the classes are presented in Table 3.3.

Table 3.3 Description of LULC Classes in the study areas

Classes	**Description**
Vegetation	Moderate vegetation cover, shrubs, and plantation
Built-up	Residential areas, including urban, industrial, commercial, all kinds of roads and airport
Water	Ponds
Agricultural land	Cropland, bare land

To further investigate the spatial pattern of urban areas from 1988 to 2022, the LULC classes were reclassified into built-up and non-built-up areas.

3.3.1.2 *Accuracy assessment*

LULC classification is susceptible to inaccuracies. Therefore, it is essential to validate the results using a reliable statistical method to ensure the accuracy of the maps (Anderson *et al*., 1976; Albertini *et al*., 2024). To assess the accuracy of the classifications, for the last years, the ground control data collected during field visits and very high-resolution Google Earth images were used (Figure 3.3), while for the previous years, very high-resolution Google Earth images corresponding to the same periods were used.

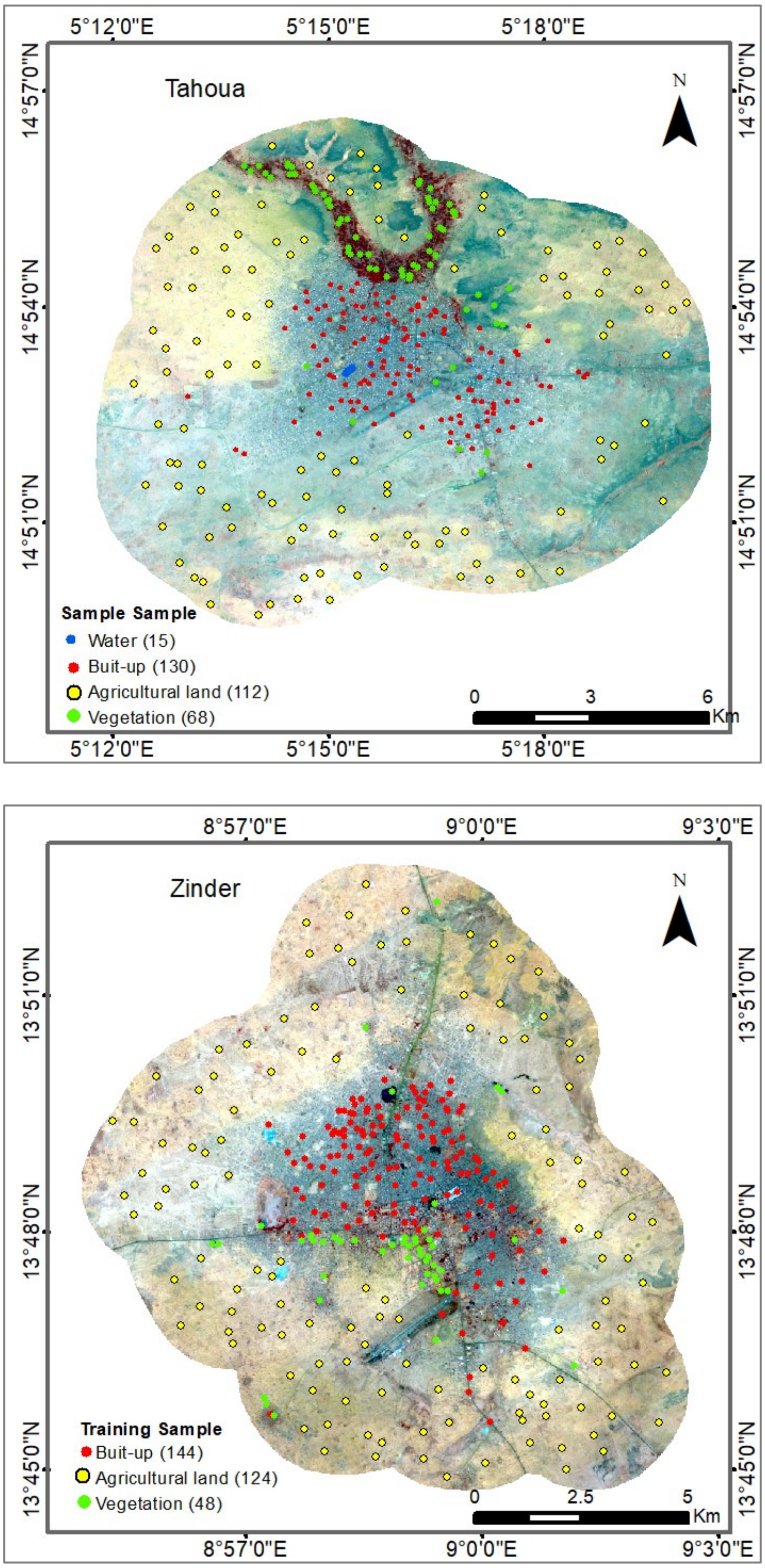

Figure 3.3 Landsat 8 images with LULC Reference Samples in Tahoua and Zinder

The statistics element was used to compute user, producer, overall accuracy, and Kappa coefficient indices. Using Equations 3.1 and 3.2, the overall accuracy and kappa coefficient were calculated

$$\text{Overall accuracy} = \frac{\sum_{i=1}^{r} x_{ii}}{N^2} \tag{3.1}$$

$$\text{Kappa coefficient } (\widehat{K}) = \frac{N(\sum_{i=1}^{r} x_{ii}) - \sum_{i=1}^{r}(x_{i+} . x_{+i})}{N^2 - \sum_{i=1}^{r}(x_{i+} . x_{+i})} \tag{3.2}$$

r is the number of rows in the matrix,

x_{ii} is the number of observations in row i and column i

x_{i+} and x_{+i} are marginal totals for row i and column i respectively

N is the total number of observations.

3.3.1.2 *Dynamics of LULC analysis in Tahoua and Zinder*

The 34-year study period (1988 to 2022) was divided into three intermediate periods: T1 (1988-2002 for Tahoua, and 1988-2000 for Zinder), T2 (2002-2012 for Tahoua , and 2000-2011 for Zinder), and T3 (2012-2022 for Tahoua, and 2011-2022 for Zinder) to facilitate LULC change detection analysis using the SCP plugin in QGIS 3.34 software. This approach involved comparing the LULC between successive periods (e.g., 1988 and 2000) to evaluate changes over time. The area for each LULC class was calculated at each time point, and a transition matrix was generated to better understand the shifts between different classes. A simple linear regression analysis examined whether population size significantly predicted the built-up area from 1988 to 2022.

3.3.1.3 *Urban growth patterns*

Urban growth direction analysis used built-up areas extracted from the LULC maps. The analysis employed sixteen gradient directions: North (N), North North-East (NNE), North-East (NE), East North-East (ENE), East I, East South-East (ESE), South-East (SE), South South-East (SSE), South (S), South South-West (SSW), South-West (SW), West South-West (WSW), West (W), West North-West (WNW), North-West (NW), and North North-West (NNW). The central business district (CBD), identified around the Grand Marché during a field visit, was used as the centre of reference for the directional analysis. A Chi-Square Goodness of Fit test was performed to assess whether urban growth in the two cities exhibits a directional preference. The test compared observed urban expansion across various directions against the expected uniform distribution of growth. Furthermore, the study areas were divided into five concentric zones using 2 km equidistant buffer rings from the city centre to evaluate whether urban growth exhibited a dispersed or compact pattern (Pradhan *et al*., 2017). For each buffer zone, the Urban Density Index (UD) was calculated using Equation 3.3 to assess the density of urban expansion. Similarly, the Urban Expansion Intensity Index (UEII) was computed for the same zones using Equation 3.4 to identify urban growth preferences during specific periods (Liu *et al*., 2010; Acheampong *et al*., 2017).

$$D_i = \frac{a_i}{A_i} \tag{3.3}$$

D_i= the density of the ring i

a_i = the built-up area of the ring i

A_i = The area of the ring i

$$UEII_i = \frac{ULA_i^{t_2} - ULA_i^{t_1}}{TLA_{\ i} \times \Delta t} \times 100 \tag{3.4}$$

Where $UEII_i$ is the Urban Expansion Intensity Index of the zone i; $ULA_i^{t_2}$ and $ULA_i^{t_1}$ are built-up area at the time t_2 and t_1 respectively; TLA_i is the total area of the zone i and Δt is the study period between the two dates. The standard division of UEII values is UEII

>1.92 is ‘‘high-speed’’; 1.05 ≤UEII ≥1.92 is ‘‘fast’’; 0.59 ≤UEII ≥1.05 is ‘‘medium speed’’; values 0.28 ≤UEII ≥0.59 is ‘‘low-speed’’; and 0 ≤UEII ≥ 0.28 is considered ‘‘slow”.

3.3.1.4 *Urban growth types*

The method proposed by Liu *et al*. (2010) was employed to identify and quantify three urban growth types: infilling, outlying, and edge expansion (Figure 3.4). This approach utilizes an urban change map to compute the Landscape Expansion Index (LEI), which provides a deeper understanding of landscape patterns and their temporal dynamics (Liu *et al*., 2010; Sapena and Ruiz, 2015).

Initially, the urban landscape was classified into two categories: newly developed objects and old objects. Old objects were present in both the initial and subsequent periods, while new objects emerged only in the later period. Secondly, the LEI values were calculated using the LEI tool in ArcGIS software. LEI is defined using buffer analysis, and the ratio between the mutual edge’s length and the object’s perimeter (Equation 3.5) differentiates between these three growth types. The selection of buffer zone size is critical as it impacts the LEI values. While (Liu *et al*., 2010) recommended a 1metre buffer to stabilize the LEI values, and (Jiao *et al*., 2015) used a 50-meter buffer based on the average width of urban roads, this study employed a 200-meter buffer zone. Choosing a 200-meter buffer was critical to align the LEI calculations with the spatial resolution and urban morphology specific to the study area. The broader buffer helps mitigate potential inaccuracies in capturing small or indistinct urban features, such as clay housing and hots, ensuring a more reliable classification of growth types. Finally, based on the LEI values, urban growth was categorized into infilling, edge expansion, and outlying types. LEI values range from 0 to 100. The infilling growth type is 100 ≥ LEI > 50; edge expansion is 50 ≥ LEI > 0, and outlying LEI=0 (Liu *et al*., 2010).

This classification allowed for a nuanced analysis of urban expansion dynamics and provided a framework for understanding how urban development has evolved in response to spatial and temporal factors.

$$LEI = \frac{l_c}{P} \times 100 \tag{3.5}$$

l_c= length of the shared edge

P = perimeter of the new object

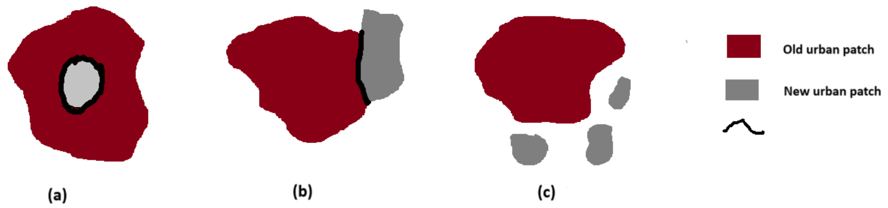

Figure 3.4 Three Types of Landscape Expansion (a) Infilling; (b) Edge Expansion; (c) Outlying

Figure 3.5 below illustrates the comprehensive workflow employed in the analysis of urban landscape change.

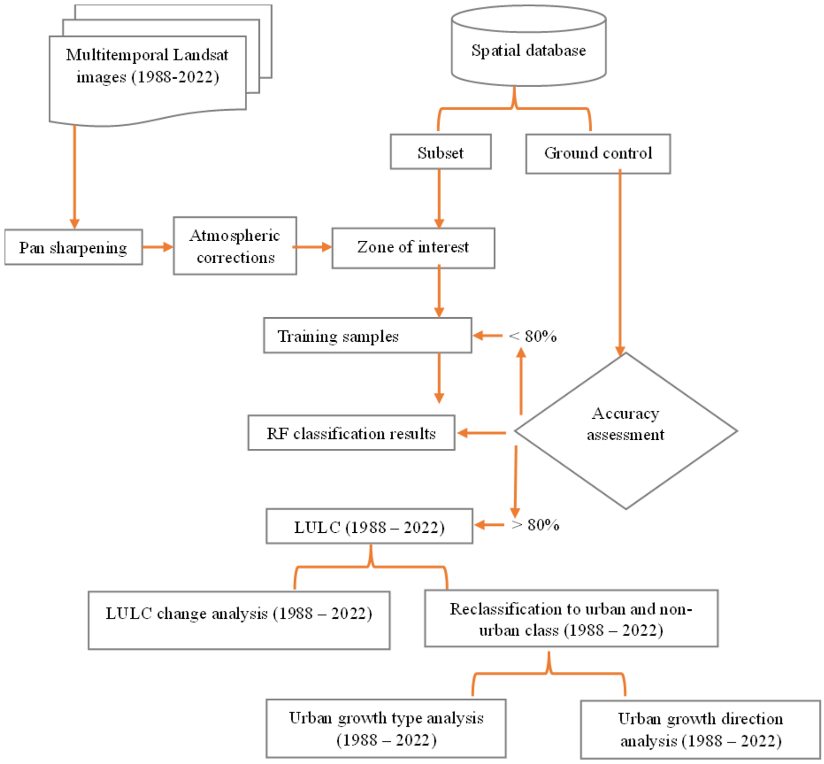

Figure 3.5 Workflow for Landscape Change Analysis (Seydou *et al*., 2024)

3.3.2 Relationship between LULC indices and LST

3.3.2.1 *Spatiotemporal distribution of seasonal LST and UHI in Tahoua and Zinder*

The assessment of missing data was a critical step in ensuring the reliability of the seasonal Land Surface Temperature (LST) analysis. For each 8-day composite, the percentage of missing data was calculated for the study areas. This was achieved by utilizing the Quality Assurance (QA) band included in the dataset, which provides information on the quality and reliability of each pixel (Neteler, 2010). The dataset was converted from Kelvin to Celsius to facilitate interpretation. Figure 3.6 highlights the percent missing data in Tahoua (a) and Zinder (b). Given the minimal missing data (less than 2%), a Nearest Neighbor Interpolation was applied. This method used a focal mode operation to replace missing values with the most frequent value from surrounding valid pixels within a defined neighbourhood. This choice minimized the impact of sparse missing data while retaining the dataset's accuracy and continuity, allowing for robust seasonal and long-term trend analysis (Qiu *et al*., 2024).

To evaluate the fit of the interpolated data against the original data, error metrics were computed, and the results showed a strong consistency between the two datasets. The calculated error metrics presented in Table 3.4 demonstrated minimal error (0.1℃ in Tahoua and 0.08℃ in Zinder) and a high correlation (0.98 both in Tahoua and Zinder), confirming that the smoothing approach preserved data integrity effectively.

Seasonal aggregation was then performed by averaging all 8-day composite LST images within each season (Cooler Dry, Hot Dry, and Rainy). The resulting seasonal LST averages were reprojected to the study area's coordinate system for consistency.

(a)

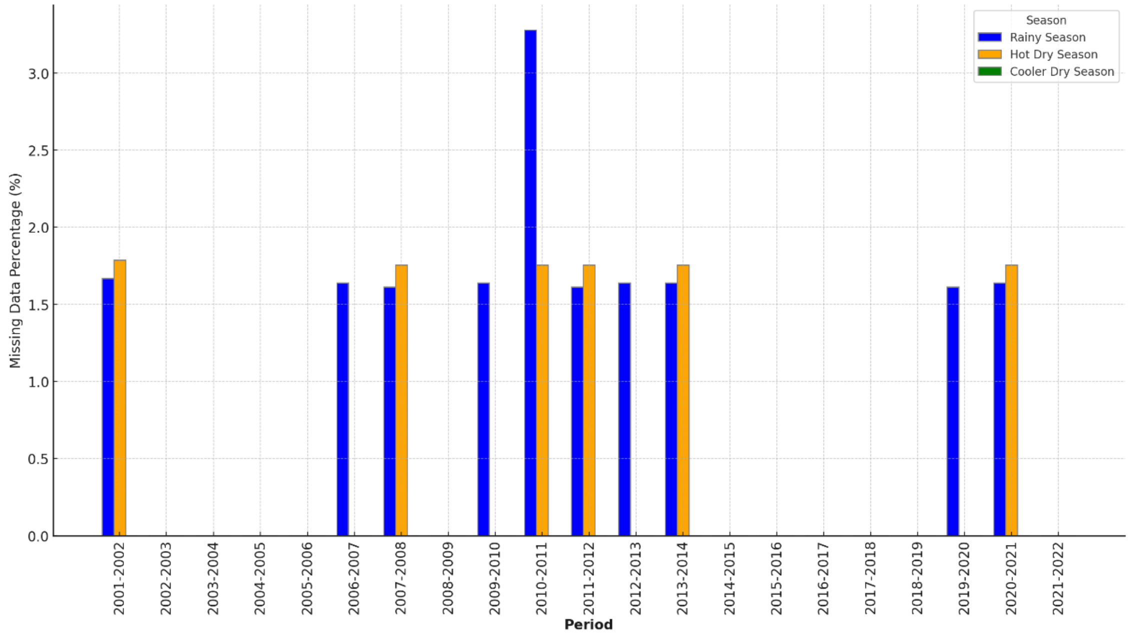

(b)

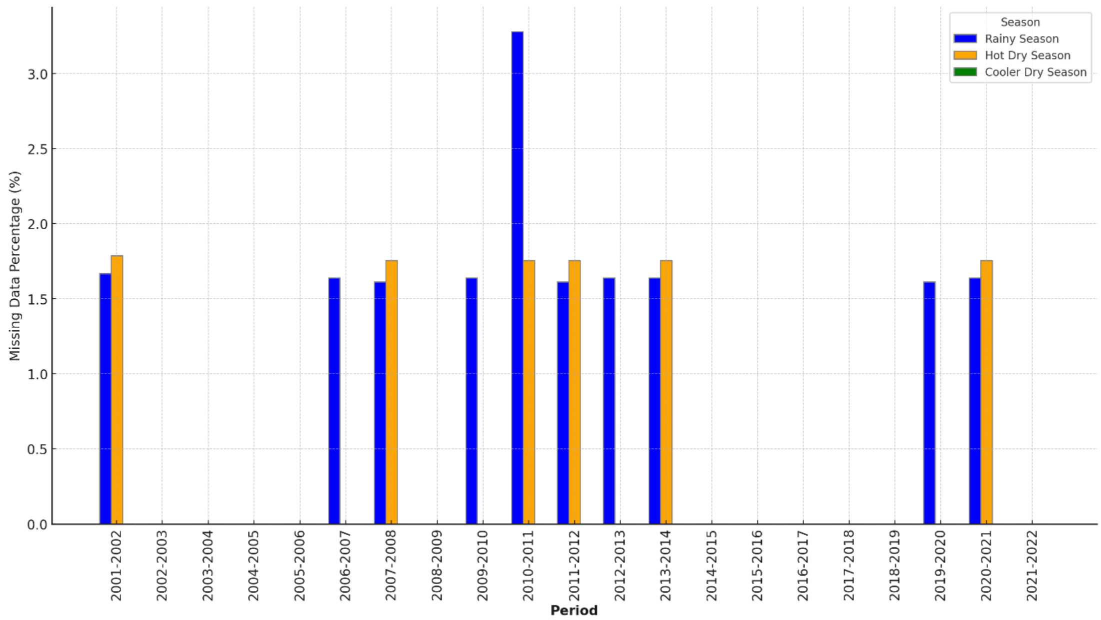

Figure 3.6 Distribution of missing data in Tahoua (a) and Zinder (b)

Table 3.4 Error Metrics of MODIS Gap-filled LST Dataset

	Bias	MAE	Pearson Correlation	RMSE
Tahoua	0.02	0.10	0.98	0.02
Zinder	0.03	0.08	0.98	0.01

The UHI intensity was derived as the deviation of local LST (pixel) values from the mean seasonal LST divided by the mean seasonal LST across the entire study area (Xu *et al*., 2013), calculated using Equation 3.6. This method facilitated the identification of areas with elevated temperatures relative to the seasonal baseline, allowing for the effective mapping of the spatial distribution and intensity of urban heat islands for each season.

$$\text{UHI Intensity} = \frac{\text{Local seasonal LST} - \text{Mean seasonal LST}}{\text{Mean seasonal LST}} \quad (3.6)$$

To quantify the effect of urbanisation on LST variation, the LST of each year were split based on LULC type. The LST of the built-up areas was considered urban LST, while the remaining classes were considered rural. Furthermore, the mean LST for both urban and rural areas is calculated, and the mean SUHI intensity for each year and season was determined by subtracting the mean rural LST from the mean urban LST. This difference represents the increase in temperature due to urbanisation. This method has been widely used in various studies, such as those by Jiang *et al*. (2022) and Sun *et al*. (2016).

3.3.2.2 *Derivation of LULC indices and regression analysis*

To examine and quantify the relationship between LULC and land surface temperature (LST), Normalised Difference Vegetation Index (NDVI), and Normalised Difference Built-up Index (NDBI) (Appendix B) were used to conduct Ordinary Least Square Regression (OLS) and Geographically Weighted Regression (GWR) as expressed by Equations 3.7 and 3.8 respectively. To account for seasonal variations, seasonal LST, NDVI, and NDBI are considered for this analysis. The average LST of each season were used as the dependent variable, and mean NDVI and the NDBI were the independent variable.

$$y_i = \beta_0 + \sum_{j}^{k} \beta_i \, x_{ij} + \varepsilon_i \qquad (3.\ 7)$$

- *yi* is the *i*th observation of the dependent variable,
- *xij* is the *j*thobservation of the *j*th independent variable,
- βj is the regression coefficient of the *j*th variable, and
- $\varepsilon_i$is the error term.

$$y_i = \beta_0(u_i, v_i) + \sum_{j=1} \beta_0(u_i, v_i)x_{ij} + \varepsilon_i \qquad (3.8)$$

- *yi* is the dependent variable,Lst in this study,
- *xij*is the *j*th independent variable at the *i*th location
- while *εi*is the random error at the *i*th location.
- (*ui,vi*) is the coordinates of pragmatic location *I*
- while *bj*(*ui,vi*) is the coefficient of the *j*th variable at location *i*.

In OLS, there is no spatial relationship between β0 and βj whereas, in the GWR model, the relationships between the dependent and independent variables vary spatially (Siqi and Yuhong, 2020). GWR uses a subset of data from surrounding observations through a series of local linear regressions to get estimates for each location in space (Siqi and Yuhong, 2020). In this study, ArcGIS Pro software was used to develop OLS and GWR models. The workflow of objective 2 is summarised in Figure 3.7.

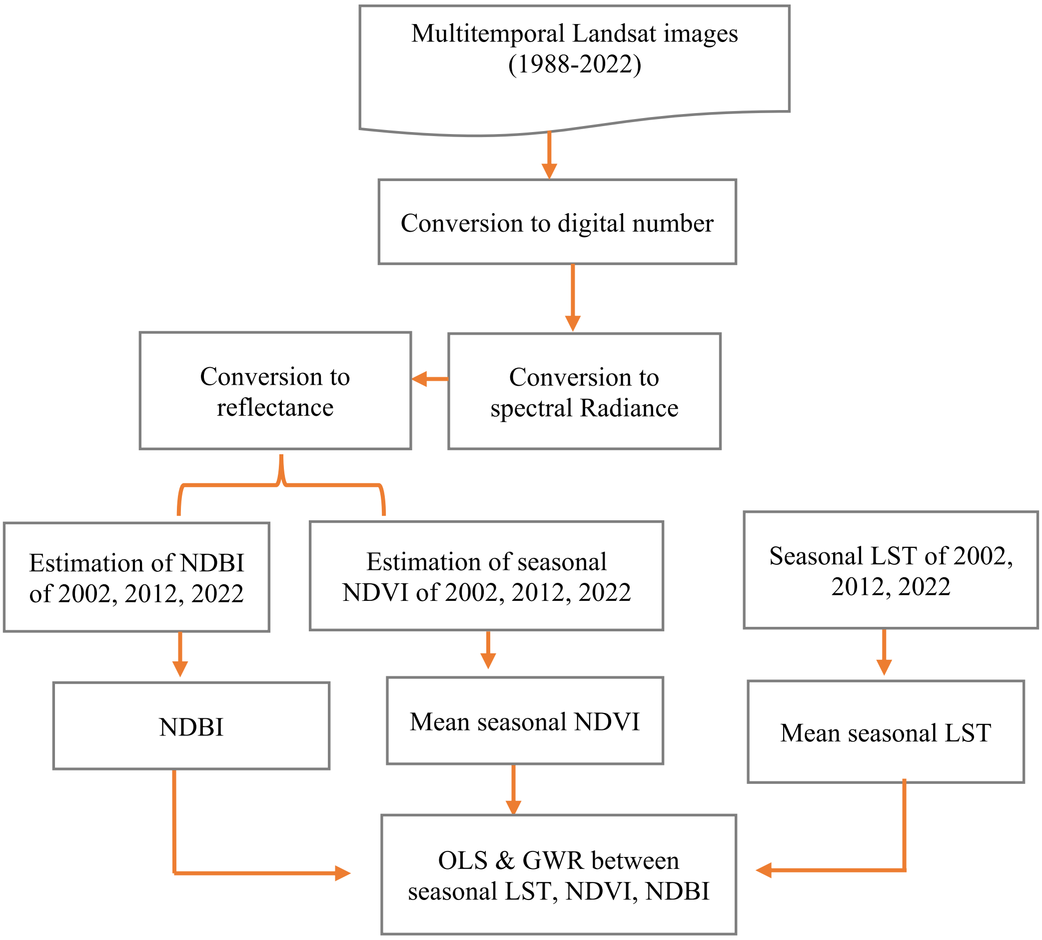

Figure 3.7 Relationship Between NDVI, NDBI and LST

3.3.3 Heat indices calculation

To assess the extreme heat events and temperature variability in Tahoua and Zinder, the Climpact2 software package in R was utilized. This tool is designed to compute various climate indices related to temperature extremes and precipitation extremes based on Expert Team on Sector-specific Climate Indices (ETCCDI) standards (Zhang *et al.*, 2011). The first step consisted of preprocessing the data to make it suitable for analysis. This process includes data homogenization and quality control. Missing data points were addressed using the nearest neighbour, and other sources of information, such as rainfall data, were used to address outliers (Gaber, 2023). Sixteen extreme heat indices related to human health were selected from the range of indices and computed for each year of the study period. The description of the selected indices is provided in Table 3.5. This allows us to capture the temporal trends and variability. Statistical tests, including trend analysis (e.g., Mann-Kendall trend test), were employed to determine the significance of observed trends in the heat indices over the study period. Sen's slope estimator was used to estimate the magnitude of the trend. The significance was tested at the 0.05 p-value threshold (Alexander *et al*., 2006).

It is important to note that Climpact2 uses geographic location (latitude and longitude) to adjust the calculation of heatwave indices based on the hemisphere, considering the different seasons in the Northern and Southern Hemispheres. Heatwave indices are typically calculated for the warm season, often from April to September in the northern hemisphere. In the southern hemisphere, the warm season is considered to be from October to March (ClimPACT2 Team, 2016). However, in the study area, the months considered by Climpact2 in computing heatwave indices do not correspond to the warm season. Hence, the heatwave indices computed by Climpact2 are not accurate. To solve this problem, R software was used to compute heatwave indices considering all the months of the year. This is necessary to capture all the needed information because in Niger, two distinct periods exist in one year.

Table 3.5 Description of The Selected Extreme Heat Indices

Index	Full Name	Definition	Units	Time Scale
TXx	Max temperature	Warmest daily maximum temperature (hottest day)	°C	Mon/Ann
TXn	Min temperature	Coldest daily maximum temperature (coldest day)	°C	Mon/Ann
TXm	Mean temperature	Mean daily maximum temperature	°C	Mon/Ann
TN10p	Cold nights	Percentage of days when TN < 10^{th} percentile	%	Ann
TN90p	Warm nights	Percentage of days when TN > 90^{th} percentile	%	Ann
TX10p	Cool days	Percentage of days when TX < 10^{th} percentile	%	Ann
TX90p	Hot days	Percentage of days when TX > 90^{th} percentile	%	Ann
TNm	Mean minimum T	Mean daily minimum temperature	°C	Mon/Ann
TNn	Min TN	Coldest daily minimum temperature (coldest night)	°C	Mon/Ann
TXgt40	Days with TX > 40°C	Number of days where TX > 40°C	Days	Ann
WSDI2	Warm Spell Duration Indicator	Annual count of days with warm spells of at least 6 consecutive days where TX > 90^{th} percentile	Days	Ann
HWN	Heatwave Number	Number of heatwave events (≥ 3 consecutive HW days)	Events	Ann
HWF	Heatwave Frequency	Number of days contributing to heatwaves	Days	Ann
HWD	Heatwave Duration	Duration (in days) of the longest heatwave	Days	Ann
HWM	Heatwave Magnitude	Mean of the mean temperature during HW days	°C	Ann
HWA	Heatwave Amplitude	Peak daily value in the hottest HW	°C	Ann

Source: ClimPACT2 Team, 2016

3.3.4 Mapping heat vulnerability

The selection of indicators for mapping heat vulnerability was based on a literature review and data availability. Table 3.6 presents the detailed description of each indicator used in this study. To ensure comparability, all indicators were normalised to a range between 0 and 1 using Equation 3.9, as follows:

$$zi = (xi - \min(x)) / (\max(x) - \min(x)) \quad (3.9)$$

Where
zi: the ith normalised value in the dataset
xi: the ith value in the dataset
min(x): the minimum value in the dataset
max(x): the maximum value in the dataset

A Tomlinson *et al*. (2011) note that vulnerability mapping can be subjective when indicator weights are arbitrarily assigned, potentially introducing bias. Therefore, this study adopted an equal-weight overlay approach. (Mushore *et al*., 2018) to combine the indicators objectively, with indicators from the same vulnerability component (sensitivity, exposure, or adaptability) averaged to ensure each had equal influence.

Table 3.6 Indicators Used for UHV Assessment

Components	Indicators	Descriptions	Reference
Exposure	LST	The normalised average temperature of each neighbourhood was obtained from Landsat 8 image band 10 using at-brightness temperature. Images from April 2022 were used. Source: https://earthexplorer.usgs.gov/	(Voelkel *et al.*, 2018)
	Population density	The normalised average population density of each neighbourhood was obtained from a gridded population dataset of 1 km resolution. Data from 2020 was used. Source: https://hub.worldpop.org/	(Wolf and McGregor, 2013)
Sensitivity	People living alone	The normalised values were obtained from the structured interview in the two cities at the neighbourhood level.	(Jagarnath *et al.*, 2020)
	The number of people per household	The normalised values were obtained from the structured interview in the two cities at the neighbourhood level	(Uejio *et al.*, 2011)
	People below 10 years	The normalised values were obtained from the structured interview in the two cities at the neighbourhood level	(Wolf and McGregor, 2013)
	People above 60 years	The normalised values were obtained from the structured interview in the two cities at the neighbourhood level	(Reid *et al.*, 2009 ; Gronlund *et al.*, 2015 ; Voelkel *et al.*, 2018)
	People with chronic disease	The normalised values were obtained from the structured interview in the two cities at the neighbourhood level	(Wolf and McGregor, 2013; Reid *et al.*, 2009)
	People with disability	The normalised values were obtained from the structured interview in the two cities at the neighbourhood level	(Jagarnath *et al.*, 2020 ; Reid *et al.*, 2009)
Adaptability	Houses with plan nearly 5 sqm	The normalised values were obtained from the structured interview in the two cities at the neighbourhood level.	(Bhattacharjee *et al.*, 2019)
	Houses with water bodies nearby	The normalised values were obtained from the structured interview in the two cities at the neighbourhood level	(Reid *et al.*, 2009)
	Houses with AC	The normalised values were obtained from the structured interview in the two cities at the neighbourhood level	(Jagarnath *et al.*, 2020)
	Houses with no change in water supply during the heating season	The normalised values were obtained from the structured interview in the two cities at the neighbourhood level	

The mean value of the indicators par zone was calculated and integrated as feature classes corresponding to sensitivity 1 and adaptability 1. The area outside the city was assumed to have 0 sensitivity and 1 adaptability since the survey covered only the city area, and the area outside the city was mainly agricultural areas, and there were no people to interview there. These layers were rasterized and the normalized adaptability 1 layer was combined with the normalized NDVI layer to get the final adaptability layer. Likewise, the first exposure layer, named exposure 1, was obtained from the interview, with zero exposure assumed for the area outside the city. The normalized LST and population density layer were added to the later normalised layer to get the final exposure layer. Equations 3.10, 3.11 and 3.12 are used to calculate each component index. These equations used overlay analysis to integrate multiple normalized indicators within each vulnerability component, maintaining balanced contributions through equal weighting. Each layer was resampled to a 30m spatial resolution, ensuring consistency for the final heat vulnerability index.

$$S = \frac{\sum normaliszed\ S\ indicators}{nomber\ of S\ indicator} \tag{3.10}$$

$$E = 0.5\ \frac{\sum normaliszed\ E\ indicators}{nomber\ of\ E\ indicator} + 0.5\ \frac{normalized\ LST + normalized\ population\ density}{2} \tag{3.11}$$

$$A = 0.5\ \frac{\sum normaliszed\ A\ indicators}{nomber\ of\ A\ indicator} + 0.5\ normalized\ NDVI \tag{3.12}$$

S: sensitivity; E: exposure; A: adaptive capacity

Furthermore, a zonal statistics tool was used in ArGis pro to determine each vulnerability component index per neighbourhood and the values were categorised into five classes (very low, low, moderate, high and very high).

It is important to note that no single, universally accepted formula for calculating the Urban Heat Vulnerability Index (UHVI). Various studies (Inostroza *et al*., 2016; Voelkel *et al*., 2018) have applied different combinations of exposure, sensitivity, and adaptability to highlight vulnerabilities.

In this study, two UHVI formulas were employed to create and compare vulnerability maps, facilitating hotspot identification and reliability assessment. The first formula, V1 (Equation 3.13), from Inostroza *et al*.(2016), incorporates adaptability as a mitigating factor, reducing vulnerability where adaptive capacity is high. The second formula, V2 (Equation 3.14) from Voelkel *et al* .(2018) uses a multiplicative approach to combine the indices.

$$V1 = E + S \pm A \tag{3.13}$$

$$V2 = E * S * A \tag{3.14}$$

The resulting vulnerability indices were classified into five vulnerability categories using the equal interval classification method, enabling a clear interpretation of areas with varying degrees of vulnerability. Are a Pearson correlation analysis comparing the indices and their components to assess consistency and highlight patterns within the data.

The characteristics of the interviewed population, their perception of urban heat and their coping strategies were analysed using descriptive statistics.

3.3.5 Simulation of future urban growth and land surface temperatures in Tahoua and Zinder under a business-as-usual scenario

3.3.5.1 *Simulation of future urban growth in Tahoua and Zinder under a business-as-usual scenario*

Using the MOLUSCE tool in QGIS, the cellular automata (CA) model was used to forecast future LULC changes in Tahoua and Zinder. This model accounts for static and dynamic features of LULC changes and is well known and has been widely used because of its high accuracy level (Al-Ahmadi *et al*., 2009; Chen, 2022) . The forecast is based on two different sets of data: independent variables like slope, elevation, and distance to roads (Appendix C), and dependent variables like previous LULC changes predicted from Landsat images from the past (Al-Ahmadi *et al*., 2009; Aithal *et al*., 2014). These variables were utilized as input in the raster format to create the models.

The first step consisted of evaluating the correlation between the variables after successfully importing all the layers and checking their geometry. During the correlation analysis steps, a layer could be removed if the user found it non-significant for the analysis. Secondly, a change analysis was performed, and a transition matrix and a change map were generated. The third step was to perform a transition potential model based on the input data. The non-linear transition functions depict the correlation between driving factors and land cover type transformation probability (Kamaraj and Rangarajan, 2022). The transition probabilities are established for the CA model. The current LULC classification of a particular cell and its neighbouring cells at time "T" are considered when predicting the transition probabilities from the current land use type to different LULC categories at the subsequent time, denoted as "T+1". Finally, using the logistic regression (LR) and Artificial Neural Network (ANN) approaches, the CA model was applied to simulate present and future LULC.

The accuracy of each model was verified by comparing the predicted LULC with the classified LULC of the same date. Furthermore, the QGIS-MULUSCE validation module was utilized to compute the total kappa coefficients and accuracy percentage between the predicted and classified LULC map for 2022. The accuracy indices generated include % correctness and Kappa coefficients (Overall, histogram and kappa location). In this study, the LR-CA produced a higher accuracy than the ANN-CA. For this reason, the LR-CA model was used to perform prediction in Tahoua and Zinder. The analytical framework adopted to achieve this objective is illustrated in Figure 3.8.

A change analysis was performed on the simulated LULC to assess the spatiotemporal change in future LULC. This was done using the SCP plugin in QGIS software. The percentage of change of each LULC at each time was calculated. Subsequently, LULC change trend analysis was carried out using the past LULC maps and the simulated LULC change.

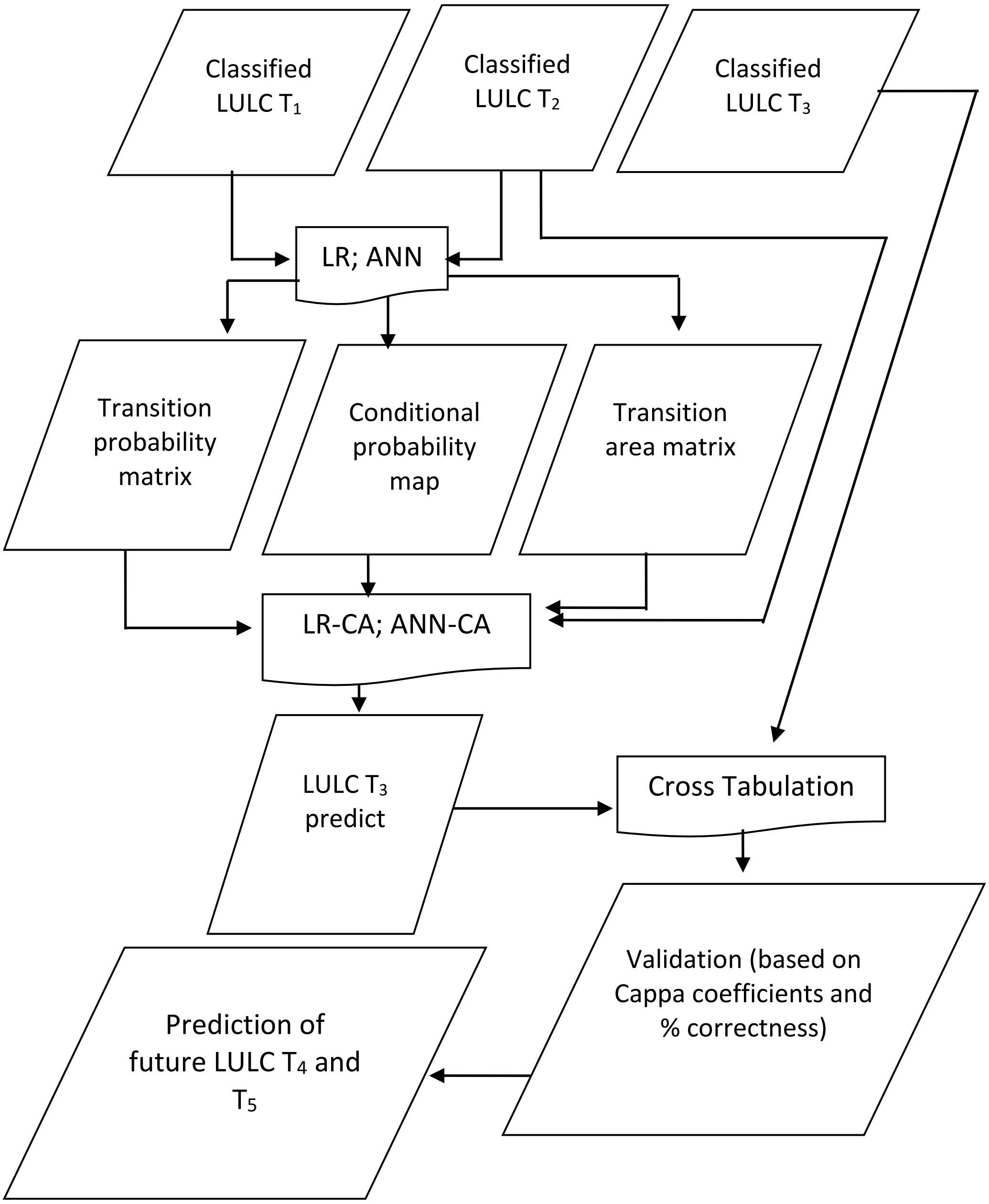

Figure 3.8 Prediction of LULC Based on LR-CA and ANN-CA Models

3.3.5.2 *Simulation of the future land surface temperatures in Tahoua and Zinder under a business-as-usual scenario*

In this study, an artificial neural network (ANN) model was employed to project seasonal land surface temperature (LST) by correlating it with landscape variables and historical seasonal LST data. This method has proven valuable in handling the spatiotemporal complexity of LST data (Id *et al*., 2016; Gupta and Aithal, 2024). The model key inputs included historical seasonal NDVI and NDBI, which are known to influence LST variation, and were computed in objective two. The historical seasonal LST values from prior periods were also incorporated to capture temporal patterns, specifically using data from 2002, 2012, and 2022 to forecast future seasonal LST.

The ANN model architecture consisted of an input layer, two hidden layers, and an output layer, with an architecture of 5:8:4:1 as shown in Figure 3.9. The input layer contained five nodes representing NDVI, NDBI, LULC, LST(t-n), and LST(t-2n), where LST(t-n) and LST(t-2n) represent seasonal LST data from two previous years. Each dataset was normalized to ensure consistency across inputs, enhancing model performance. The input and output layers were configured with the seasonal data as inputs and the target seasonal LST as output. The output layer is a function of all the input variables as shown in Equation 3.15:

$$LST(t) = f[LST(t-n), LST(t-2n), NDVI, NDBI, LULC] \qquad (3.15)$$

$LST(t)$ is the target Land Surface Temperature for the current season.

$LST(t-n)$ *and* $LST(t-2n)$ Seasonal LST values from two previous time points (e.g., from 2002 and 2012 when predicting 2022, or from 2012 and 2022 for projecting 2032)

NDVI is the Normalized Difference Vegetation Index for the current season.

NDBI is a Normalized Difference Built-up Index for the current year

LULC is land use and land cover class for the current year.

To test the model's predictive accuracy, historical seasonal LST from 2002 and 2012 was used to forecast the LST for the 2022 season. This approach allowed to validate the model by comparing its predictions for 2022 with actual seasonal LST data for that year (Gupta and Aithal, 2024). The performance of the model was assessed based on its ability to predict seasonal LST for 2022 accurately. During training, forward propagation was used to pass inputs through the layers, with weights and biases adjusted through backpropagation to minimize error, using Mean Squared Error (MSE) as the loss function. After training, the model's predictions for the 2022 seasons were compared with actual seasonal LST data, and evaluation metrics, including Mean Absolute Error (MAE) and Root Mean Squared Error (RMSE), were calculated to quantify prediction accuracy (Id *et al*., 2016). Additionally, the correlation coefficient value was determined to assess the model's ability to explain variance in seasonal LST, indicating how well the input features predicted LST changes.

After validating the model on the 2022 seasonal data, future seasonal LST for 2032 and 2042 were done. The mean seasonal LST values were then derived from the projected LST layers.

Due to the anomaly presented by 2002 as one of the hottest years on record, two scenario models were employed to project LST for 2032 and 2042, allowing for a more comprehensive range of possible future conditions. The first model incorporated seasonal LST data from 2002, thereby embedding a baseline that reflects an unusually warm year. This approach facilitates the exploration of projections under conditions influenced by elevated initial temperatures. The second model utilized seasonal LST data of 2001, providing a more typical baseline year representative of standard climate conditions.

Employing both scenarios ensures that projections account for variability in climate extremes and the potential influence of unusual warming events on future LST outcomes.

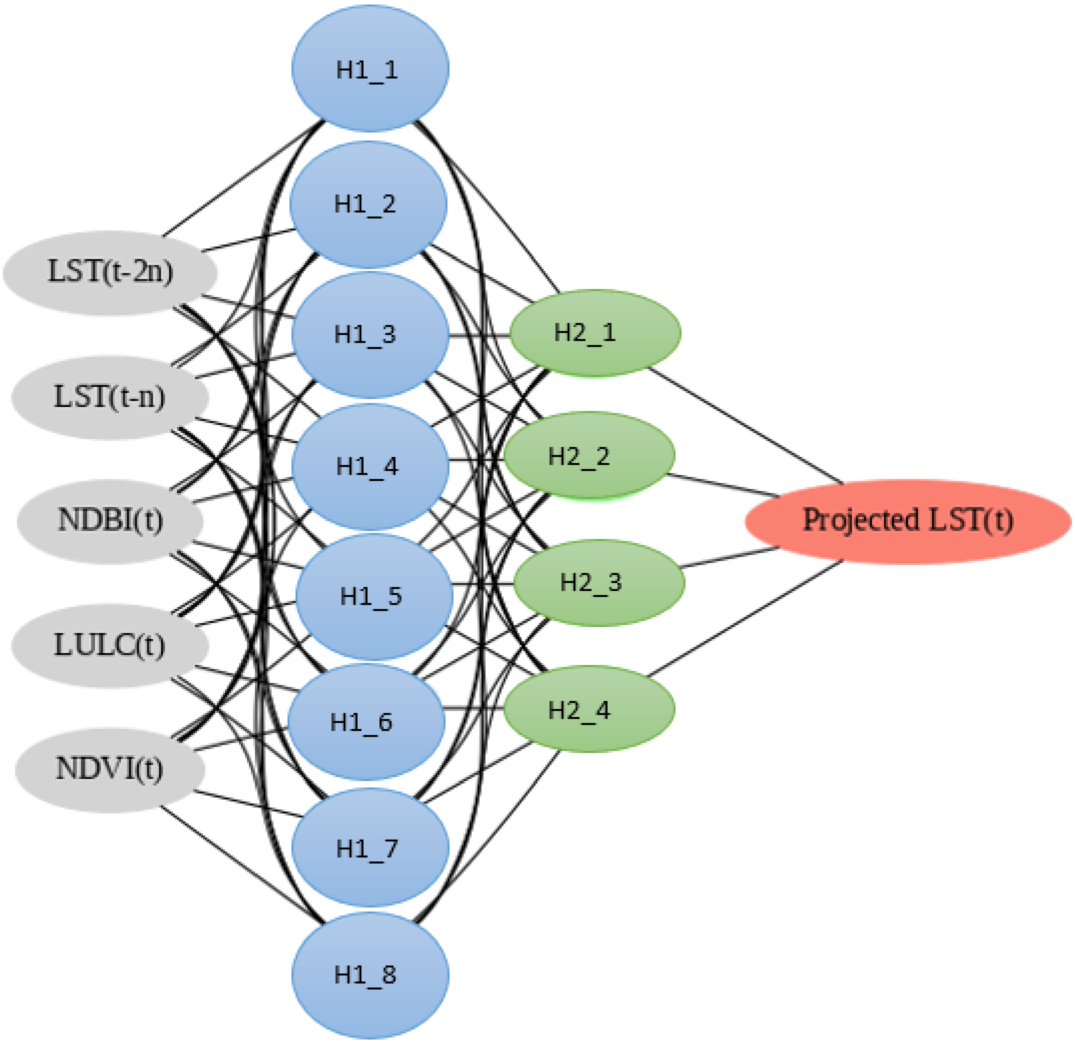

Figure 3.9 Neural Network Model for Projecting Land Surface Temperature

CHAPTER FOUR

4.0 RESULTS AND DISCUSSIONS

4.1 Results

4.1.1 Analysis of LULC changes, urban growth dynamics, and expansion patterns with population growth and infrastructure development in Tahoua and Zinder (1988-2022)

4.1.1.1 *Assessment of LULC Change*

Four macro classes of LULC have been identified in Tahoua: vegetation, built-up, water and agricultural land (Figure 4.1) and three in Zinder: vegetation, built-up, and agricultural land (Figure 4.2). The classification accuracy was evaluated using the Kapa coefficient, overall accuracy, user accuracy and producer accuracy. Kappa coefficient values varied from 97.40% to 99.21% in Tahoua, 88.6% and from 88.57% and 95.25% in Zinder (Table 4.1).

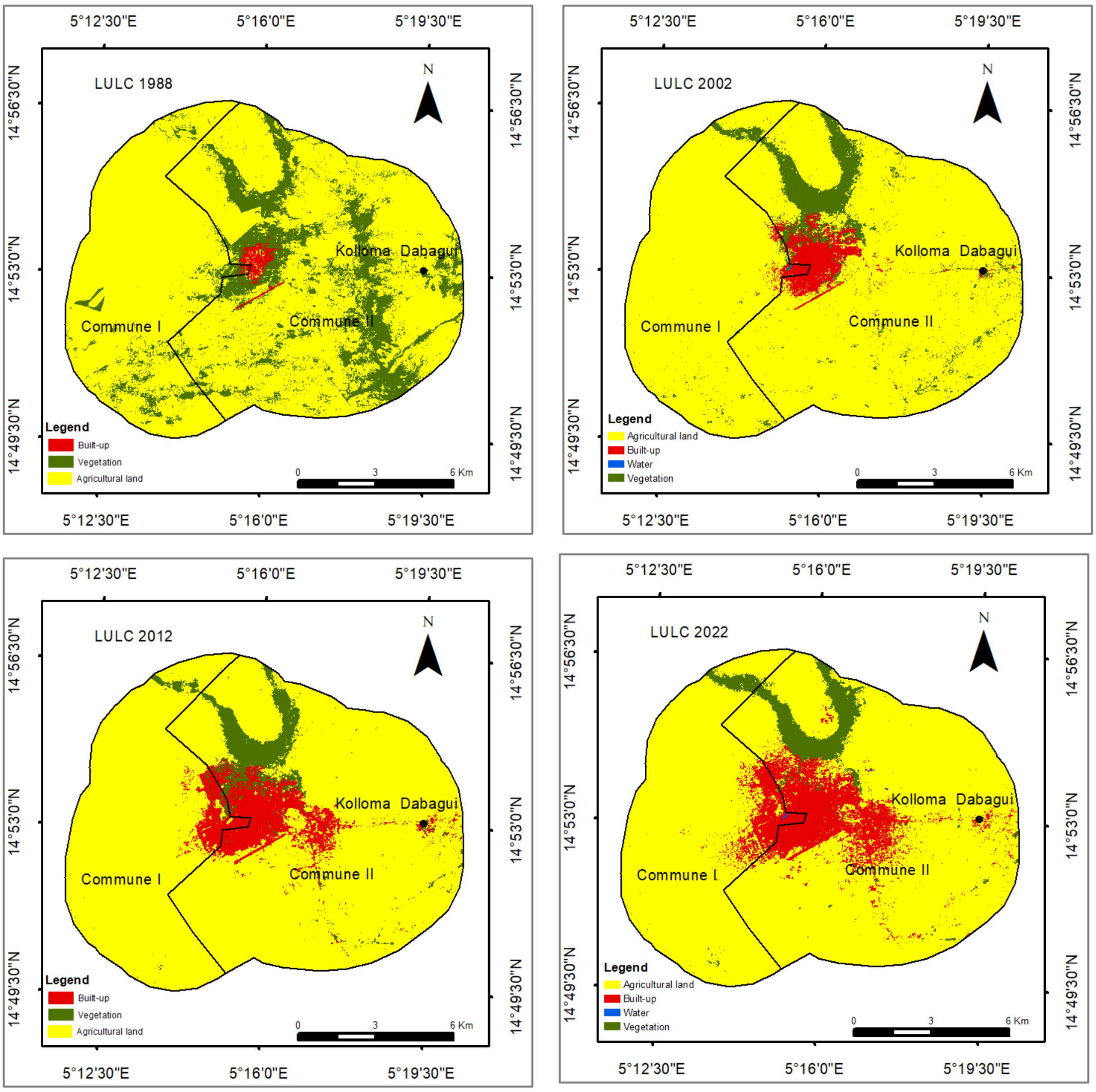

Figure 4.1 LULC in Tahoua from 1988 to 2022

Between 1988 and 2022, significant LULC changes occurred in Tahoua, particularly in the expansion of built-up areas, the reduction of vegetation, and the transformation of agricultural land. Over this period, urban growth progressed rapidly, with a clear trend of expansion towards the west. The most notable transformation is the substantial increase in built-up areas, which has progressively encroached upon vegetation and agricultural land.

In 1988, the built-up area was relatively small and concentrated mainly in the central part of the region, with dominance in the Commune II. Urbanisation was limited, with most of the surrounding land dominated by agricultural activities and patches of vegetation. By 2002, built-up areas had expanded considerably, particularly westwards towards Kolloma and within the boundaries of Commune II. This expansion coincided with a noticeable decline in vegetation cover. The trend continued into 2012 and 2022, when built-up areas covered an even larger extent, indicating a persistent and rapid process of urbanisation.

Vegetation and agricultural land experienced significant transformations over the study period. In 1988, large patches of vegetation were visible, particularly in the north and eastern parts of the region. However, by 2002, vegetation had declined significantly, particularly in the western and central areas, as land was converted to urban use. This pattern intensified by 2022 with only small remnants of vegetation remaining, primarily in the north , and along water bodies. Agricultural land remained the dominant category across all three periods, yet it became increasingly fragmented as built-up areas expanded.

Within the communes, different rates of land cover change were observed. In Commune I, urban expansion was initially slow but accelerated in later years, particularly towards the northwest and central regions. In contrast, Commune II experienced more rapid and extensive urbanisation, with a marked increase in built-up areas between 2002 and 2012. The impact on vegetation and agricultural land was particularly severe in this commune. Kolloma and Dabagui also experienced gradual urban encroachment, especially in the vicinity of Kolloma where built-up areas increased significantly over the years.

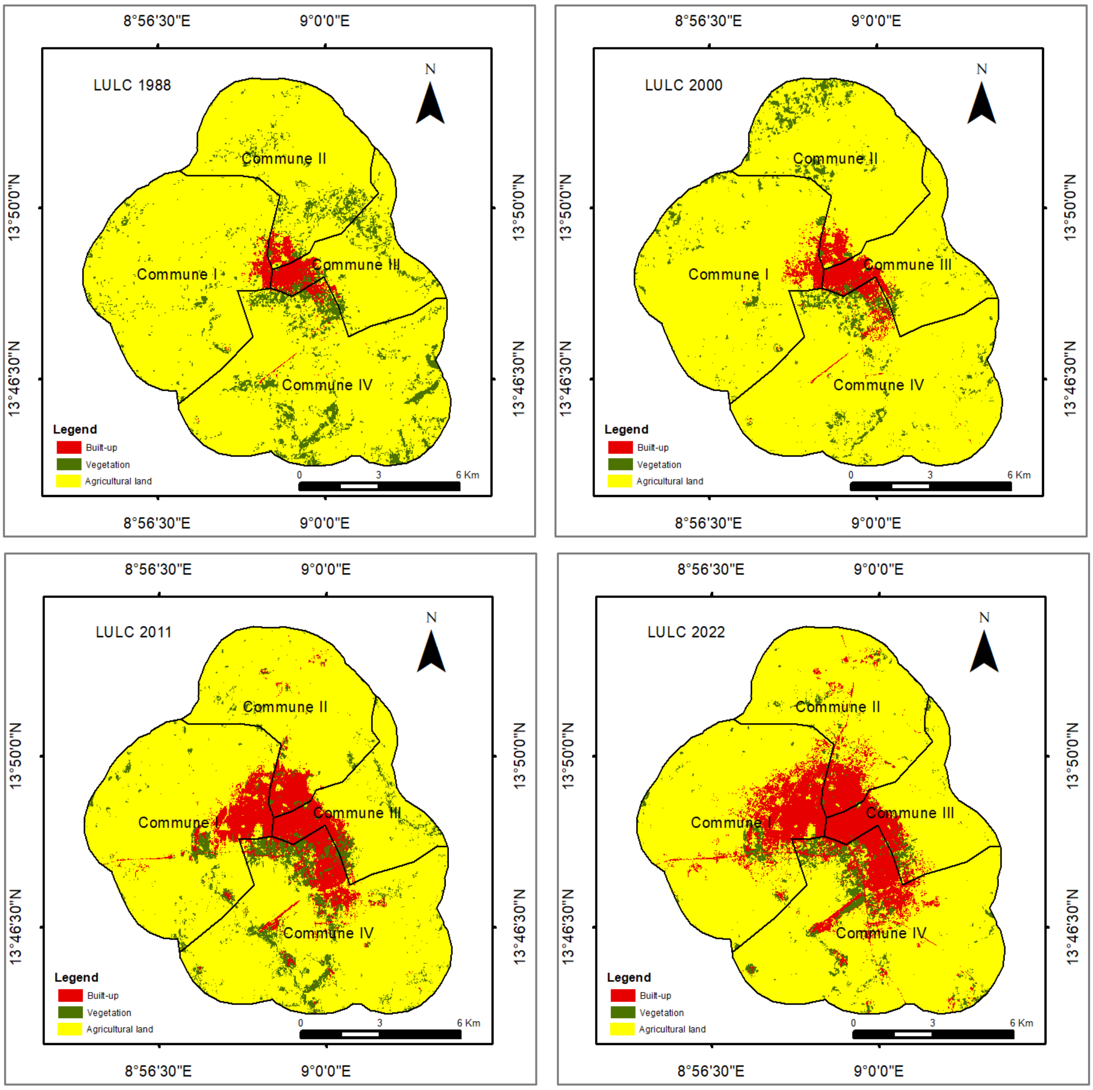

Figure 4.2 LULC in Zinder from 1988 to 2022

In Zinder, over the period 1988 to 2022, there was a drastic transformation in LULC characterised by the expansion of built-up areas, a reduction of vegetation, and the fragmentation of agricultural land. Urbanisation was a driving force, with built-up areas growing steadily across the four communes. In 1988 and 2000, the built-up area was dominant in Commune II. However, this tendency has changed in subsequent years with an outward expansion from the centre in all the communes and a south-western direction in Commune IV during the year 2022.

Table 4.1 Classification Accuracy

	Year	1988		2002		2012		2022	
	LU/LC classes	**UA**	**PA**	**UA**	**PA**	**UA**	**PA**	**UA**	**PA**
Tahoua	Vegetation	99.22	99.34	99.60	98.42	99.60	98.72	98.70	99.70
	Built-up	98.35	96.76	95.39	90.63	96.93	96.34	97.64	96.35
	Water	_	_	100	100.00	_	_	100.00	100.00
	Agricultural land	99.91	99.93	98.83	99.82	99.50	99.89	99.92	99.70
	Overall accuracy		99.79		98.76		99.32	99.44	
	Overall kappa statistics		99.21		97.40		98.57		98.84
	Year	**1988**		**2000**		**2011**		**2022**	
	LU/LC classes	**UA**	**PA**	**UA**	**PA**	**UA**	**PA**	**UA**	**PA**
Zinder	Vegetation	93.41	99.34	99.34	97.84	81.60	99.34	95.99	99.34
	Built-up	92.98	96.76	96.76	92.41	95.82	96.76	95.41	96.76
	Agricultural land	97.67	99.93	99.93	98.61	98.99	99.93	99.30	99.93
	Overall accuracy		0.97		98.21		98.26		0.99
	Overall kappa statistics		88.57		92.10		91.24		95.25

UA=User’s accuracy, PA= Producer’s accuracy

The LULC change analysis revealed that the LULC categories changed at a differential rate over time (Figure 4.3). The agricultural land class has been the landscape matrix throughout the study period, occupying over 80% of the landscape area in Tahoua and Zinder. In Tahoua, this class has increased by 8.36% during the first intermediate period (Figure 4.3a) due to drastic vegetation covert reduction. A reduction in vegetation cover was evident throughout the studied period. In Zinder, the class agricultural land experienced an increase of 1.67% during the first intermediate period (Figure 4.3c) due to the loss in the vegetation class. Subsequently, it decreased by 7.01% and 2.64% during the second and third intermediate periods (Figure 4.3.b) to the profit of the built-up area (+11.5% from 1988 to 2022). The transition matrix (Table 4.2) provides insight into the conversion of one class to another during the study period

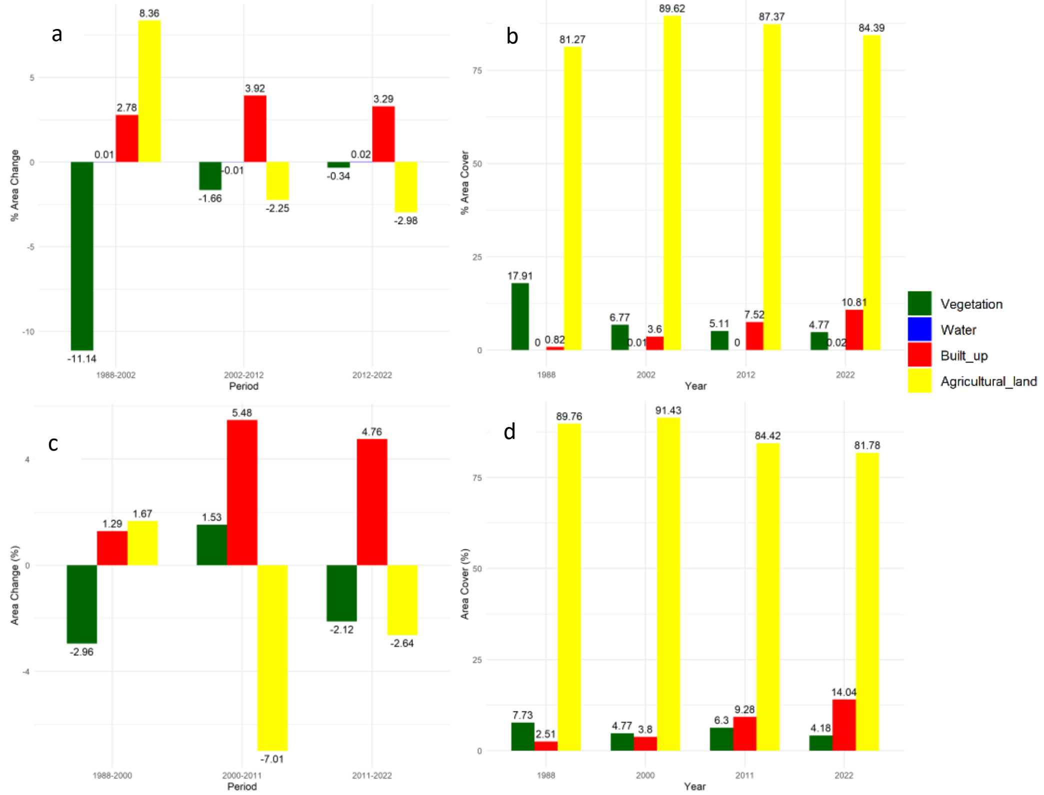

Figure 4.3 LULC Area Change and Area Proportion in Tahou (a and b) and Zinder (c and d)

Table 4.2 Transition Matrix from 1988 to 2022

Tahoua

1988	2002					
	LULC classes	Vegetation	water	Built-up	Agricultural land	Total
	Vegetation	3.81	0.01	1.83	12.26	17.91
	Water	0.00	0.00	0.00	0.00	0.00
	Built-up	0.00	0.00	0.82	0.00	0.82
	Agricultural land	2.96	0.00	0.94	77.36	81.27
	Total	6.77	0.01	3.60	89.62	100.00
	2012					
2002		Vegetation	water	Built-up	Agricultural land	Total
	Vegetation	4.20	0.00	0.36	2.20	6.76
	Water	0.00	0.00	0.00	0.01	0.01
	Built-up	0.00	0.00	3.60	0.00	3.60
	Agricultural land	0.91	0.00	3.57	85.16	89.63
	Total	5.11	0.00	7.52	87.37	100.00
	2022					
2012	LULC classes	Vegetation	water	Built-up	Agricultural land	Total
	Vegetation	3.44	0.00	0.68	0.99	5.11
	Built-up	0.00	0.00	7.52	0.00	7.52
	Agricultural land	1.33	0.02	2.61	83.40	87.37
	Total	4.77	0.02	10.81	84.39	100.00

Zinder

	2000				
1988		Vegetation	Built-up	Agricultural land	Total
	Vegetation	1.63	0.46	5.64	7.73
	Built-up	0.00	2.51	0.00	2.51
	Agricultural land	3.13	0.84	85.80	89.76
	Total	4.76	3.80	91.44	100.00
	2011				
2011		Vegetation	Built-up	Agricultural land	Total
	Vegetation	1.73	0.43	2.61	4.77
	Built-up	0.00	3.80	0.00	3.80
	Agricultural land	4.57	5.05	81.81	91.43
	Total	6.30	9.28	84.42	100.00
	2022				
		Vegetation	Built-up	Agricultural land	Total
	Vegetation	2.13	0.90	3.27	6.30
	Built-up	0.00	9.28	0.00	9.28
	Agricultural land	2.05	3.86	78.51	84.42
	Total	4.18	14.04	81.78	100.00

The analysis of built-up growth rates for the three intermediate periods revealed that the highest increase in the built-up area occurred during the second intermediate period in Tahoua (60.12%) and Zinder (144.15%) (Table 4.3). This signifies that the built-up area nearly doubled in Tahoua and tripled in Zinder between 1988 and 2000. By comparing the growth rates of the built-up area and population, it was expected that the built-up area growth rate during the last intermediate period would be more significant due to the highest population growth rate experienced during the same period (World Population Review, 2024). However, the results did not verify this expectation. Furthermore, the regression analysis conducted to investigate the relationship between the built-up area growth rate and population growth rate revealed a moderate correlation in Tahoua, although it was not significant ($r(1) = 0.67,\ p > 0.5$), and a weak and non-significant correlation in Zinder ($r(1) = 0.29,\ p > 0.5$).

Table 4.3 Built-up and Population Growth Rate

	Zinder			Tahoua		
Intermediate period	**T1**	**T2**	**T3**	**T1**	**T2**	**T3**
Built-up growth rate (%)	51.66	144.15	33.90	30.38	60.12	50.41
Population growth rate (%)*	39.16	78.44	82.21	46.1	61.40	75.68

(* source: City population)

4.1.1.2 *Analysis of urban growth types*

Three types of urban growth were identified: infill, edge-expansion, and outlying in Tahoua (Figure 4.4) and Zinder (Figure 4.5). The analysis shows that edge-expansion growth was the predominant urban growth type both in Tahoua (4.6a) and Zinder (4.6b) throughout the 34 years irrespective of the communes. This was followed by the outlying growth type, with infilling growth representing less than 1% of the total growth in the two cities.

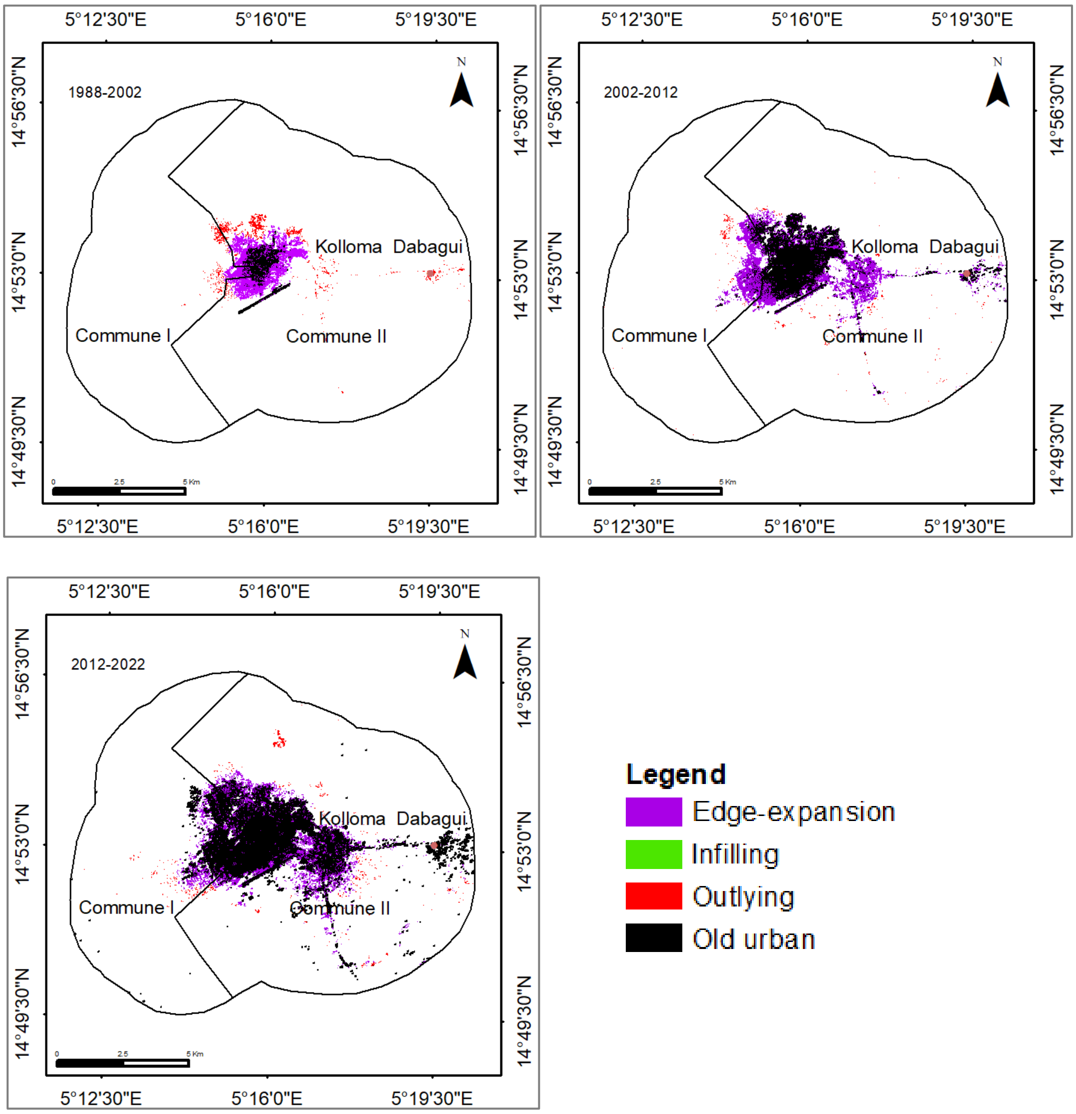

Figure 4.4 Urban Growth Types in Tahoua

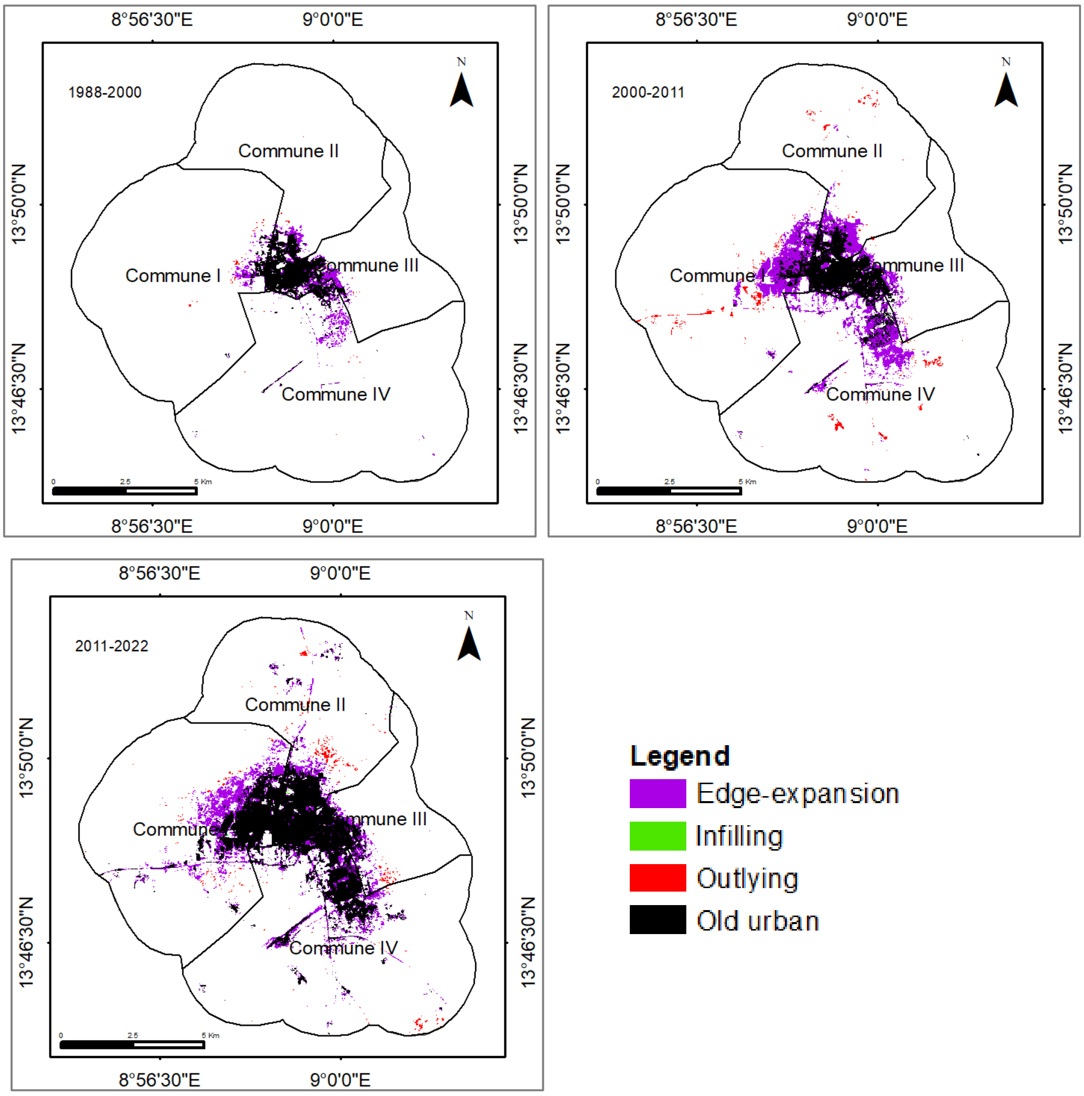

Figure 4.5 Urban Growth Types in Zinder

a) b)

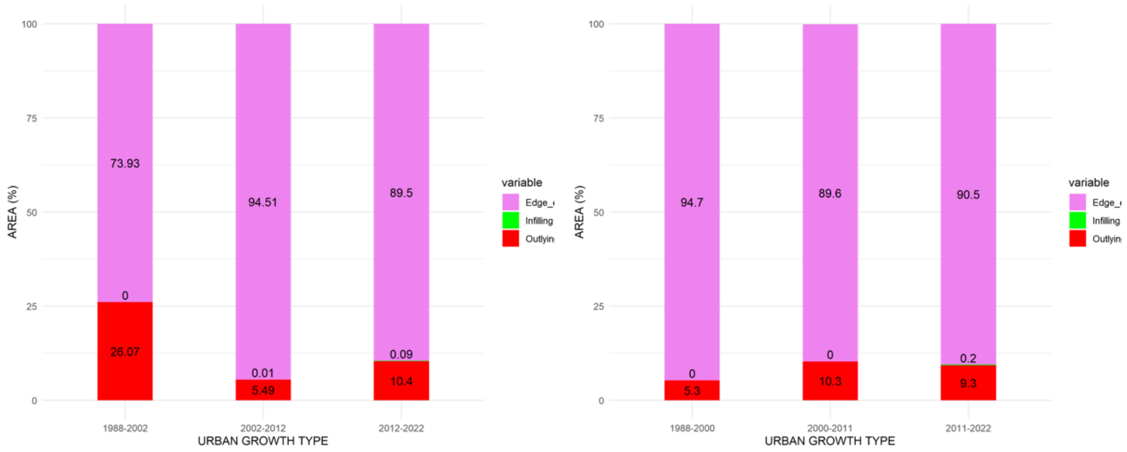

Figure 4.6 Proportion of Urban Growth Type per Intermittent Period in Tahoua (A) and Zinder (b)

4.1.1.3 *Uban growth direction and expansion preference*

The expansion direction of the built-up area from 1988 to 2022 is shown in Figure 4.7a for Tahoua and Figure 4.7b for Zinder. In Tahoua, the city is primarily growing towards the SSE-SE and WSW-W directions along National Road RN25, which also cuts through the city in the WWS-SW direction. This road intersects with RN29, entering from the SSW. Urban growth towards the E-NE is limited by the *Vallée de Abatémma*, a valley encircled by rocks and hillocks that restricts expansion.

Meanwhile, Zinder is expanding mainly towards the NNW-WSW and SE-SSW directions. To the NNW, the growth follows National Road 11 (RN11), which stretches 8.5 km through the city towards Agadez. This route includes landmarks like André Salifou University, a military camp, the Zinder Refinery (SORAZ), and schools such as Saint Joseph and Dan Bassa. In the SE and W directions, RN1, the main road that connects Zinder to Niamey, the capital city, influences Zinder's growth.

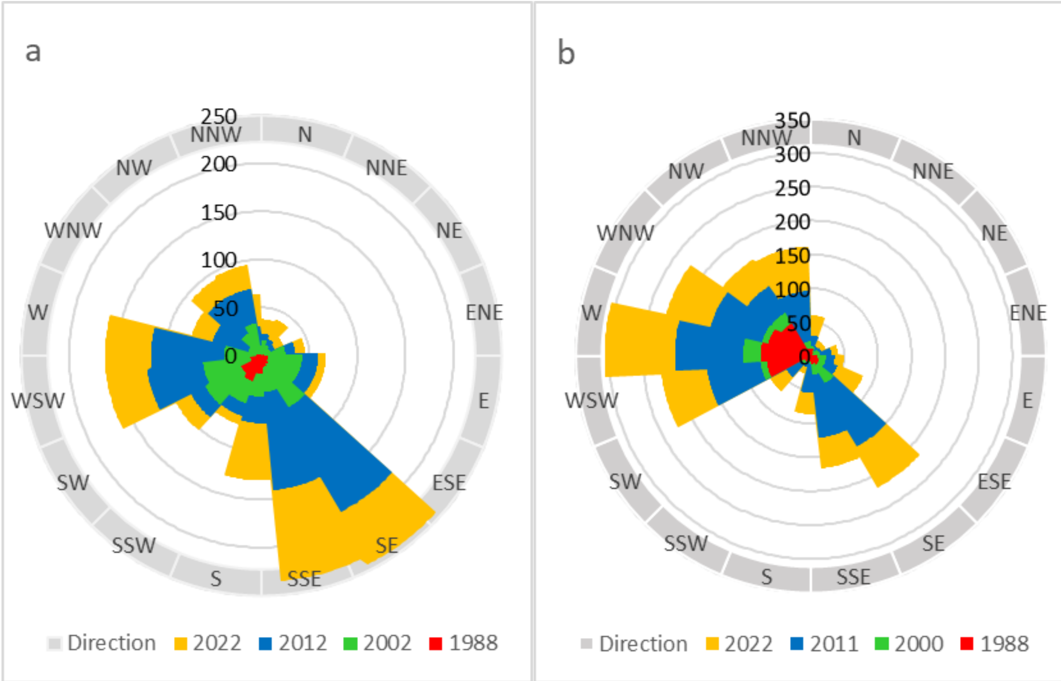

Figure 4.7 Urban Growth Direction in Tahoua (a) and Zinder (b) from 1988 to 2022

The two cities are undergoing compact growth as the built-up area density has increased in each buffer zone from 1988 to 2022, with a high value from the centre to the periphery (Figure 4.8). It also highlights the preference for the expansion of the first buffer zone. However, the UEII values gave more insight into expansion preference over time. During the first and the second intermediate periods, buffer zone 1 was the preferred area for expansion in the two cities.

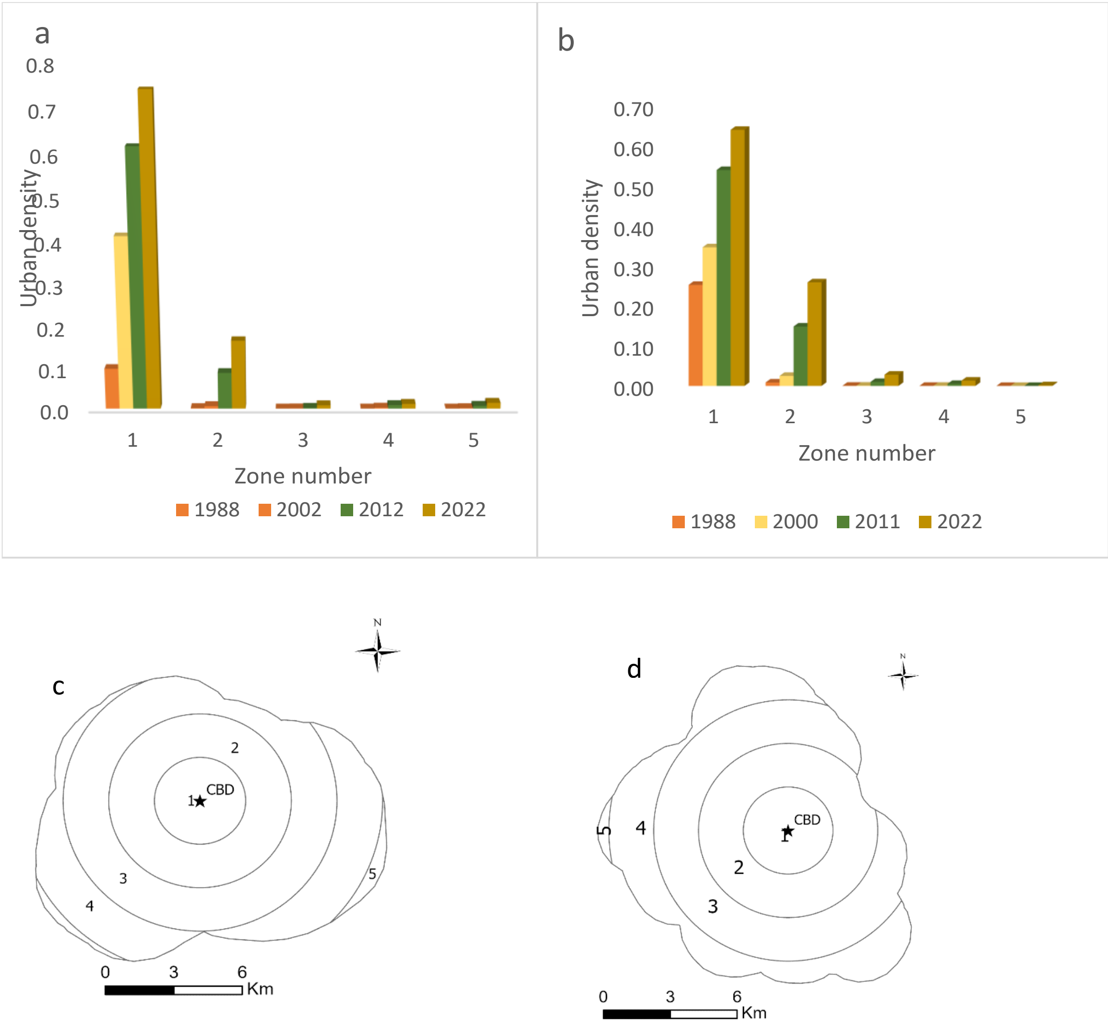

Figure 4.8 Urban Density Pattern and Buffer Zones with CBD in Tahoua (a, c) and Zinder (b, d)

In Tahoua, the UEII values of 2.25, 2.05, and 1.27 were experienced during T1, T2, and T3 respectively in zone 1, indicating a "high-speed growth". The growth rate was medium during T2 and T3 in zone 2, and "slow growth" was experienced in the remaining zones throughout the study period (Table 4.4). A similar tendency of preference is observed in Zinder, with different growth speeds. In Zinder, the UEII values of 0.78 and 0.9 obtained in zone 1 during the first and third intermediate periods denoted a "medium growth speed" while fast during the second intermediate period. During the last intermediate period, the number of vacant lands decreased to saturation in Zone 1, leading to a "medium growth speed" in Zone 2. Meanwhile, the remaining zones experienced "slow growth" throughout the study period, with increasing values from the centre to the periphery (Table 4.4). These results support the compact growth pattern in the study area.

Table 4.4 UEII by Buffer Zone per Intermediate Period

	Tahoua			Zinder		
Ring Id	**T1**	**T2**	**T3**	**T1**	**T2**	**T3**
1	2.25	2.05	1.27	0.78	1.76	0.91
2	0.04	0.82	0.78	0.01	0.05	1.00
3	0.00	0.01	0.06	0.00	0.00	0.17
4	0.02	0.06	0.03	0.01	0.01	0.08
5	0.01	0.06	0.07	0.00	0.00	0.01

4.1.2 Analysis of the spatiotemporal patterns of LST and its relationship with LULC in Tahoua and Zinder

4.1.2.*1 Spatiotemporal pattern of LST per season in Tahoua and Zinder*

The spatiotemporal pattern of LST maps per seasons represented by Figure 4.9 (Tahoua) and Figure 4.10 (Zinder) highlights distinct seasonal and temporal trends. During the hot dry season, both cities consistently exhibit high LST values, with the highest intensities recorded in built-up areas due to the heat-retaining properties of impervious surfaces. In the cooler dry season, LST values decrease overall but remained high in urban areas, reflecting the persistence of urban heat storage. The rainy season maps show a marked contrast between urban and non-urban areas, with lower LST values in vegetated regions due to their cooling effect and evapotranspiration. Over the years, the spatial extent of high LST zones has expanded, particularly in the urban centres of both cities, indicating the influence of urban growth and land cover changes on surface temperature patterns.

The mean seasonal LST in Tahoua and Zinder, represented by Figure 4.9 and Figure 4.10, show that LST not only varies across LULC types but also changes between seasons, with the hot dry season experiencing the highest temperatures and the cooler dry season the lowest LST.

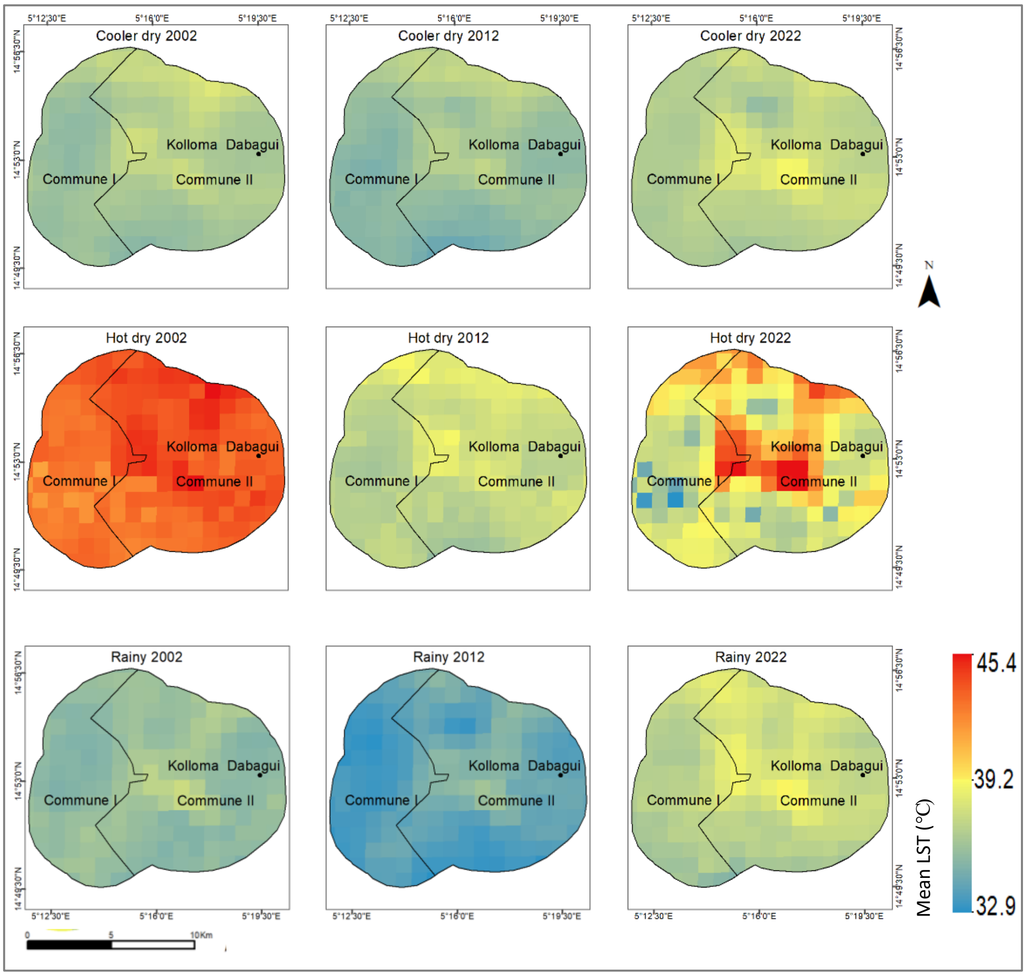

Figure 4.9 Distribution of Seasonal LST in Tahoua

In Tahoua, the cooler, dry and rainy seasons showed a similar spatial pattern of LST distribution for each corresponding year with different LST values. Commune II had a higher portion of high values of LST, which mostly fell within the built-up area. However, the hot dry period of 2022 showed a significant pattern where the highest temperature was more towards Kolloma in Commune II, unlike 2002, when all communes had relatively high temperatures approaching 45°C.

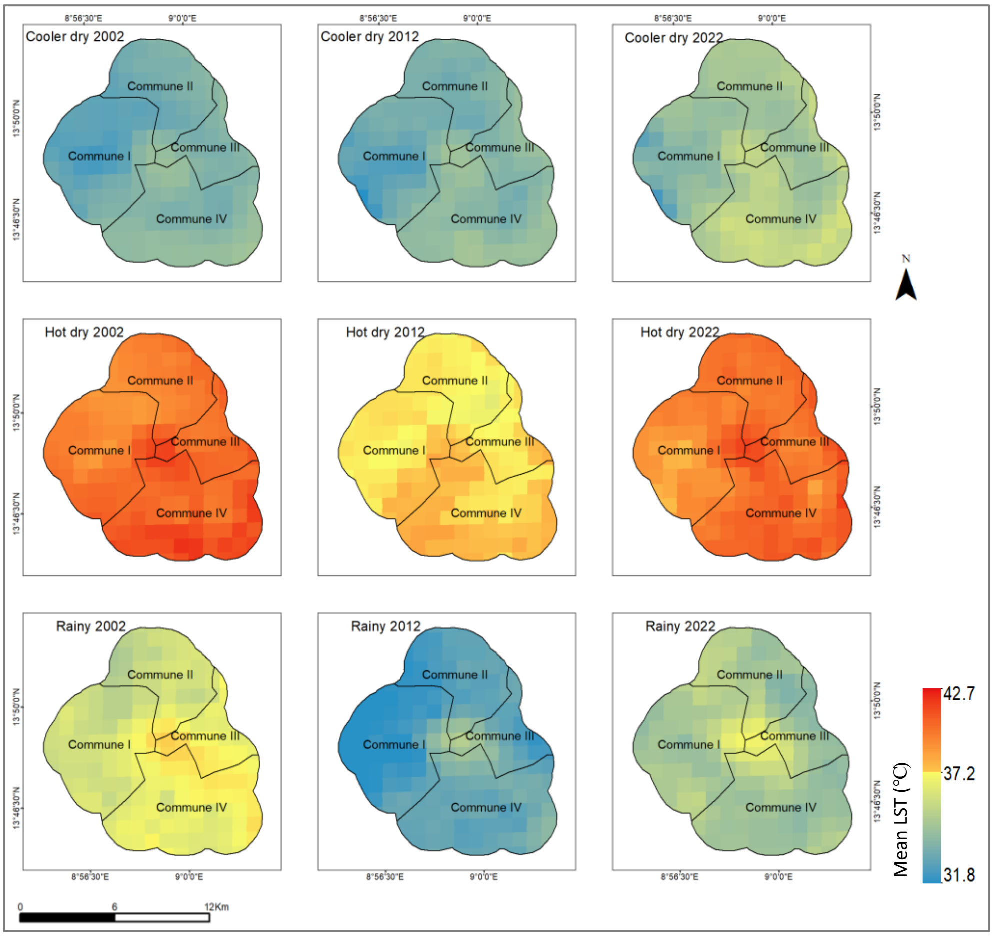

Figure 4.10 Distribution of Seasonal LST in Zinder

In Zinder, the central area, representing the built-up zone, exhibited high LST values. This area experienced an increase in LST from 2012 to 2022. Conversely, Commune IV is the most heat-exposed commune, consistently displaying the highest temperatures across all seasons from 2002 to 2022.

Generally, the mean LST values tend to decrease from 2001-2002 to 2011-2012 across all seasons in Tahoua (Figure 4:11a) and Zinder (Figure 4:11b) except for the cooler dry season in Zinder, which increased by 0.16°C. This was due to the fact that 2002 was the second hottest year in world history after 1998. There is a notable increase in seasonal LST from 2012 to 2022, with the hot dry season experiencing the highest increase both in Tahoua and Zinder. The corresponding increase during the cold, dry season and rainy season were 1.21°C and 3.14°C, respectively, in Tahoua, and were 1.06°C and 2.05 in

Zinder. This indicates a warming trend in recent years. These values indicate typical seasonal temperature variations in arid regions.

(a)

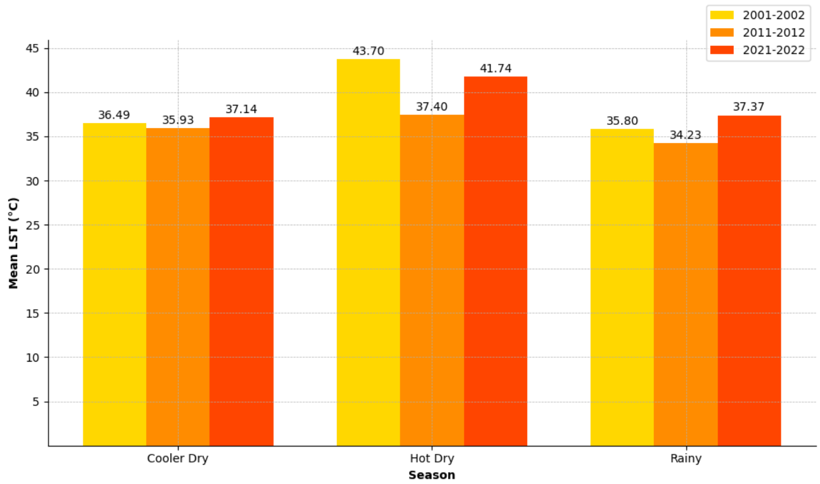

(b)

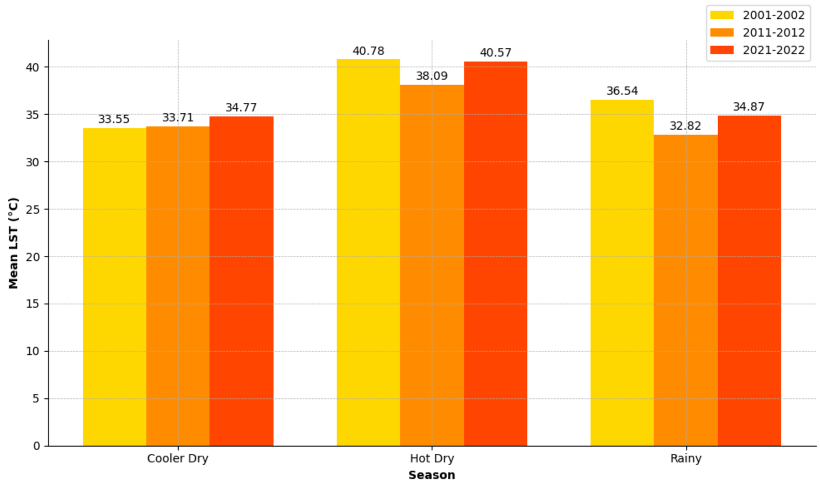

Figure 4.11 Distribution of Seasonal Mean LST in Tahoua (a) and Zinder (b)

4.1.2.1 *Spatiotemporal pattern of urban heat island per season in Tahoua and Zinder*

The seasonal UHI maps of 2001-2002, 2011-2012 and 2021-2022 for Tahoua (Figure 4.12) and Zinder (Figure 4.13) reveal a mostly central concentration of UHI in both cities, aligning with the built-up areas. Over the years, these central hotspots expanded in the two cities, indicating the direct influence of urban growth on increasing surface temperatures.

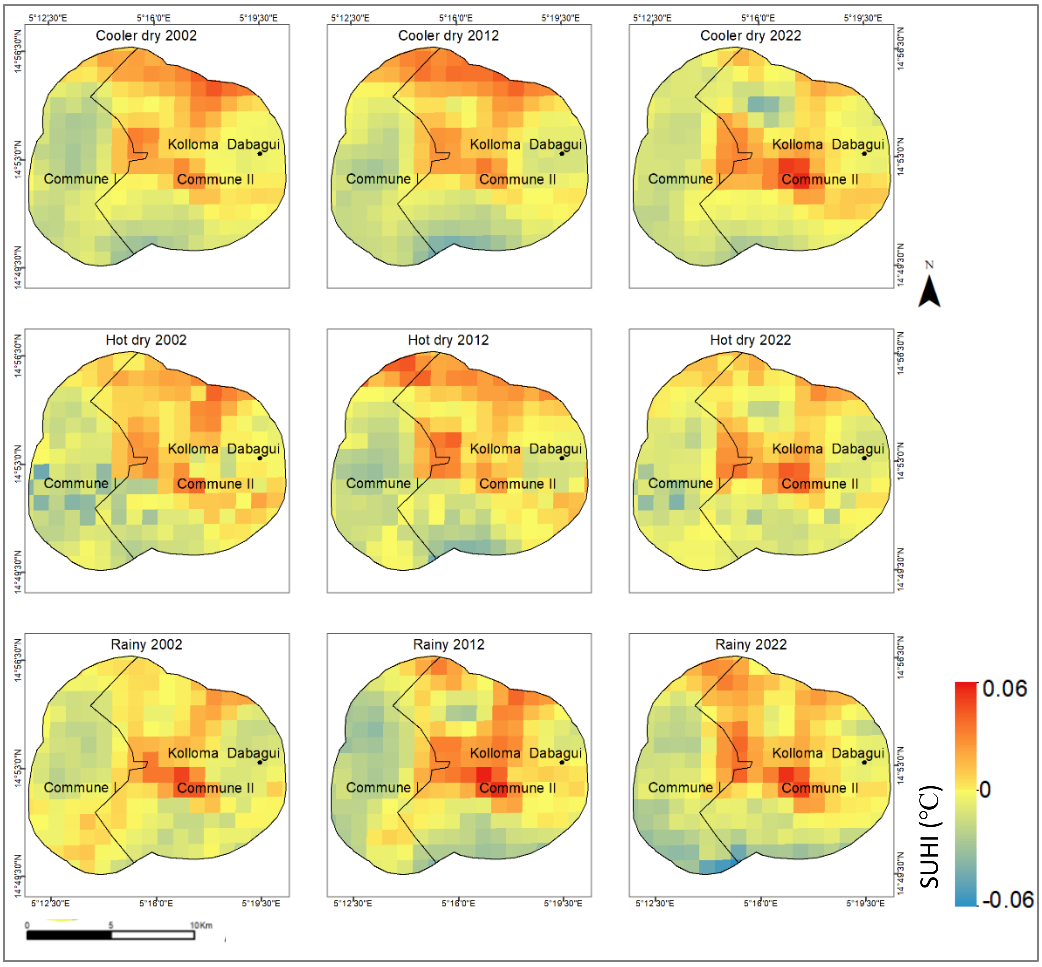

Figure 4.12 Distribution of Seasonal SUHI Intensity in Tahoua

In Tahoua, SUHI intensity is consistently higher in Commune II across all seasons. Moreover, SUHI intensity has steadily increased from 2002 to 2022, towards Kolloma reaching a peak of 0.06°C. During the hot dry and cooler dry seasons of 2002 and 2022, the northern part exhibited a distinct band of high SUHI values. However, this pattern became more fragmented in 2022 and during the rainy season, with high values of SUHI intensity no longer forming a continuous zone.

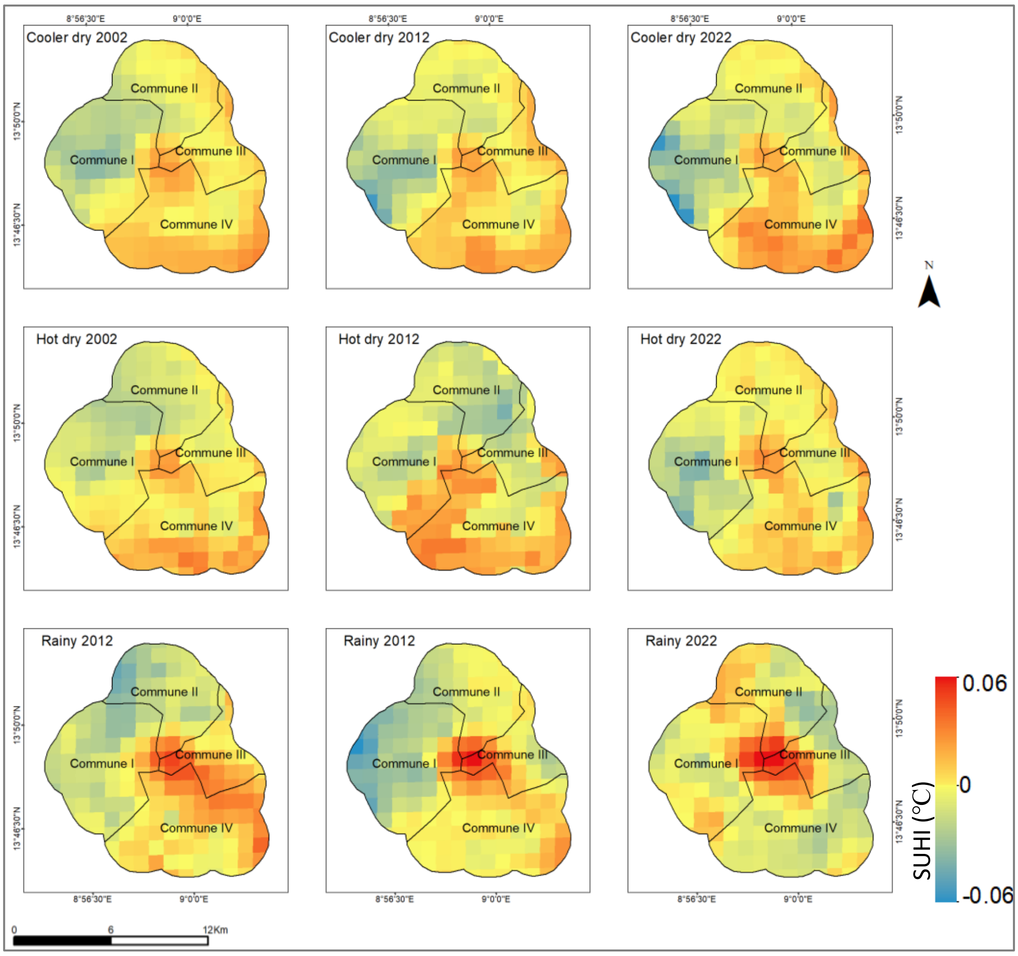

Figure 4.13 Distribution of Seasonal SUHI Intensity in Zinder

In Zinder, the SUHI intensity is higher during the rainy season and Commune IV constantly experienced higher values which were in line with the major built-up area expansion direction.

During the cooler dry season and the rainy season in 2002, SUHI was primarily concentrated in the centre and Commune IV (south), while the northern communes (I and

II) remained relatively cooler. By 2012, heat intensity had spread further into Commune III, yet Commune IV remained the hottest zone. In 2022, a noticeable cooling effect emerged in Commune I. However, Commune IV continued to exhibit high SUHI values, maintaining its status as the most heat-affected area. During the Hot Dry Season, by 2012, a cooling effect emerged in Communes II and III, temporarily reversing the warming trend observed in 2002. However, by 2022, the warming tendency intensified once again in these communes, indicating a resurgence of SUHI effects. Despite these fluctuations, Commune IV consistently remains the hottest zone, while Commune III experiences a notable rise in SUHI intensity over time. These changes are due to the built-up areas expansion and density along with variations in vegetation cover.

Another method of determining SUHI intensity, which considered the variation of the LST from the built-up area and the non-built-up area and gives more information about the urbanisation effect, shows that in Tahoua, the intensity increased over the past decade (2012-2022) (Table 4.5). The same pattern was observed in Zinder over the same decade. These results suggest a substantial rise in temperature in urban areas throughout the three seasons, reflecting an intensification of the heat island effect (Table 4.5).

Table 4.5 Variation of Urbanisation Effect Intensity in Tahoua and Zinder

	Tahoua			**Zinder**		
Year	**Cool dry**	**Hot dry**	**Rainy**	**Cool dry**	**Hot dry**	**Rainy**
2002	0.76	0.88	0.79	0.52	0.61	0.23
2012	0.72	0.80	0.99	0.23	0.2	1.09
2022	0.94	0.95	1.03	0.56	0.37	1.41

4.1.2.2 *Ordinary Least Squares Regression (OLS) between LST, NDVI and NDBI*

i. Model performance

The OLS regression between LST (dependent variable), NDVI and NDBI (explanatory variables) in Tahoua revealed that NDVI and NDBI explained only 2%, 13% and 23% of

LST variation respectively during hot dry season, cooler dry season and rainy season as indicated by the values of adjusted R^2 in Table 4.6.

Table 4.6 Summary of OLS Results in Tahoua

Season	Variable	Coef.	SE	t-Stat	Prob	Prob_SE	Robut_t	Rbust_Prob	Adj R^2
Hot_D	Intercept	40.35	0.01	2896.66	0.000*	0.01	2792.70	0.000*	0.02
	NDVI	0.78	0.04	16.31	0.000*	0.04	17.08	0.000*	
	NDBI	0.49	0.03	13.58	0.000*	0.03	13.28	0.000*	
Cool_D	Intercept	36.62	0.01	33.26.18	0.000*	0.01	3185.53	0.000*	0.13
	NDVI	-2.20	0.04	-45.42	0.000*	0.04	-48.44	0.000*	
	NDBI	0.09	0.03	2.78	0.005*	0.03	2.67	0.007*	
Rainy	Intercept	36.23	0.01	3164.39	0.000*	0.01	3043.75	0.000*	0.23
	NDVI	-4.34	0.08	-52.38	0.000*	0.08	-54.05	0.000*	
	NDBI	-0.36	0.03	-11.40	0.000*	0.03	-11.35	0.000*	

*Statistically significant p-value is less than 0.05 at 95% confidence level. (SE: standard error).

Likewise, in Zinder, NDVI and NDBI explained only 13%, 15% and 37% of LST variation during the hot dry season, cooler dry season, and rainy season, respectively (Table 4.7).

Table 4.7 Summary of OLS results in Zinder

Season	Variable	Coeff.	SE	t-Stat	Prob	Prob_SE	Robut_t	Rbust_Prob	Adj R^2
Hot_D	Intercept	37.45	0.01	2458.77	0.000*	0.01	2075.18	0.000*	0.13
	NDVI	17.06	0.02	155.66	0.000*	0.12	139.10	0.000*	
	NDBI	0.05	0.04	1.32	0.000*	0.04	1.19	0.233	
Cool_D	Intercept	32.98	0.01	2840.04	0.000*	0.01	2501.02	0.000*	0.15
	NDVI	-2.57	0.03	-76.22	0.000*	0.03	-65.15	0.000*	
	NDBI	2.60	0.04	54.42	0.005*	0.05	46.90	0.007*	
Rainy	Intercept	35.77	0.01	4105.74	0.000*	0.01	2941.75	0.000*	0.37
	NDVI	-4.37	0.06	-71.89	0.000*	0.07	-62.93	0.000*	
	NDBI	-3.77	0.05	-72.43	0.000*	0.07	-51.40	0.000*	

ii. Assessment of explanatory variables

When all other variables are held constant, the coefficient is the predicted change in the dependent variable for each unit change in the related explanatory variable. Hence, in Tahoua, the relation between LST and NDVI highlighted by the coefficient values indicates a negative relationship during the rainy season (-4.34) and cooler dry season (-2.20), while a weak positive relationship is observed during the hot dry season (0.78). In contrast, NDBI has a positive relationship with LST during hot dry season and cooler dry season (0.49, 0.09) while a negative relationship was observed during rainy season (-0.36) (Table 4.7). In Zinder, the relationship between LST and NDVI is negative during cool dry season and rainy season (-2.57 and -3.77 respectively) while a positive coefficient is observed during, he the hot dry (17.06). On the other hand, the NDBI and LST direction is also unstable across seasons.

The t-test analysis determines if the explanatory variables are statistically significant. This test is essential because the explanatory variable associated with a statistically significant coefficient is vital to the regression model assuming that there is a valid relationship between NDVI/NDBI and LST, a primarily linear relationship between these variables, and LST is not redundant to any NDVI/NDBI in the model. The results suggested that both NDVI and NBVI were statistically significant explanatory variables in all the seasons both in Tahoua and Zinder as indicated by the Robust T-test probability values (0.000*) (Table 4.6 and Table 4.7).

iii. Assessment of model significance

In all the tests and the two cities, the Koenker (BP) statistic was significant (Table 4.8 and Table 4.9). Thus, The Joint F-Statistic was not reliable for assessing the model's significance. Therefore, the Joint Wald Statistic was used to determine the overall model significance. The null hypothesis for both of these tests was that NDVI and NDBI in the model were not effective. A model is considered statistically significant if the p-value is less than 0.05 at 95% confidence level. The results indicated that the models were statistically significant with a Joint Wald probability value of 0.000 in Tahoua and Zinder (Table 4.8 and Table 4.9).

iv. Assessment of Stationarity relationships

The Koenker (BP) Statistic determines if NDVI and NDBI consistently relate to LST in data and geographic space. The results were statistically significant for both NDVI and NDBI in Tahoua and Zinder, with p-values less than 0.05 (Table 4.8 and Table 4.9), indicating a statistically significant heteroscedasticity and/or non-stationarity.

i. Assessment of model bias

The Jarque-Bera statistic indicates if the residuals are normally distributed or not. The results show that the p-values were less than 0.05 (Table 4.8 and Table 4.9), indicating that the residuals were not normally distributed, meaning that the models are biased.

Table 4.8 OLS Diagnostics Tahoua

Diagnostic Name				Probability			
	Hot_D	Cool_D	Rainy		Hot_D	Cool_D	Rainy
No. of Observations	170249	170249	170249	(AICc)	311.401.8	288617.35	294347.21
Joint F-Statistics	1693.76	271.44	1130.23	Prob(>F), (1,170262), df	0.000*	0.000*	0.000*
Joint Wald Statistic	2271.07	782.38	3247.04	Prob(>chi-squared), df	0.000*	0.000*	0.000*
Koenker (BP) Statistic	4245.47	5950.28	6963.59	Prob(chi-squared), df	0.000*	0.000*	0.000*
Jarque-bera Statistic	73.81.27	7995.19	12591.70	Prob(>chi-squared), df	0.000*	0.000*	0.000*

Table 4.9 OLS Diagnostics Zinder

Diagnostic Name				Probability			
	Hot_Dry	Cool_Dry	Rainy		Hot_Dry	Cool_Dry	Rainy
No. of Observations	156944	156944	156944	(AICc)	223626.96	249829.70	261482.82
Joint F-Statistics	12390.22	4242.79	7947.66	Prob(>F), (1,170262), df	0.000*	0.000*	0.000*
Joint Wald Statistic	19424.56	6580.00	8426.47	Prob(>chi-squared), df	0.000*	0.000*	0.000*
Koenker (BP) Statistic	4909.97	3033.80	43107.31	Prob(chi-squared), df	0.000*	0.000*	0.000*
Jarque-bera Statistic	8296.03	3243.98	8448.32	Prob(>chi-squared), df	0.000*	0.000*	0.000*

Furthermore, the Moran's I spatial autocorrelation results conducted on the residuals showed that the residuals are autocorrelated both in Tahoua (Table 4.10) and Zinder (Table 4.11) with an R2 values greater than 0. indicating a high level of autocorrelation.

Table 4.10 Moran's Residual Spatial Autocorrelation Result in Tahoua

Season	Hot dry	Cooler dry	Rainy
Moran's Index	0.83	0.87	0.91
z-score	9271.5	9873.74	9967.2
p-value	0.000*	0.000*	0.000*

Table 4.11 Moran's Residual Spatial Autocorrelation Result Zinder

Season	Hot dry	Cooler dry	Rainy
Moran's Index	0.85	0.90	0.92
z-score	9428.4	9973.74	9987.2
p-value	0.000*	0.000*	0.000*

4.1.2.4 *Geographically weighted regression between LST, NDVI and NDBI*

The GWR analysis between LST, NDVI, and NDBI shows strong adjusted R2 values ranging from 0.94 to 0.96 in both Tahoua (Table 4.12) and Zinder (Table 4.13). The model shows a very high degree of explanatory power, suggesting that the GWR model effectively explains the spatial variation in the dependent variable within Tahoua and Zinder across each season. Additionally, the AICc values of GWR were significantly lower than those of OLS. This means that GWR outperformed OLS.

As OLS coefficients, GWR also highlighted varying intensity and direction between the variables across space and seasons, as highlighted in Figure 4.13 and 4.14.

Table 4.12 Tahoua GWR Analysis Results

Year	Sigma	Effective degree of freedom	AICc	R2(adjusted)
Hot dry	0.21	169787.66	-168472.76	0.94
Cooler dry	0.11	169782.30	-270187.37	0.96
Rainy	0.01	169782.96	-23886.61	0.95

Bandwidth range used= 1000m

Table 4.13 Zinder GWR Analysis Results

Year	Sigma	Effective degree of freedom	AICc	R2(adjusted)
Hot dry	0.01	156339.48	-216740.79	0.96
Cooler dry	0.01	156341.35	-183753.46	0.94
Rainy	0.01	156344.84	-179097.94	0.96

In Tahoua, the vegetated area in the northern part of the city showed a consistently high negative correlation coefficient with NDVI and a positive correlation with NDBI at all seasons. While the urban areas and agricultural land classes showed a negative correlation with NDVI and a weak positive to weak negative correlation with NDBI

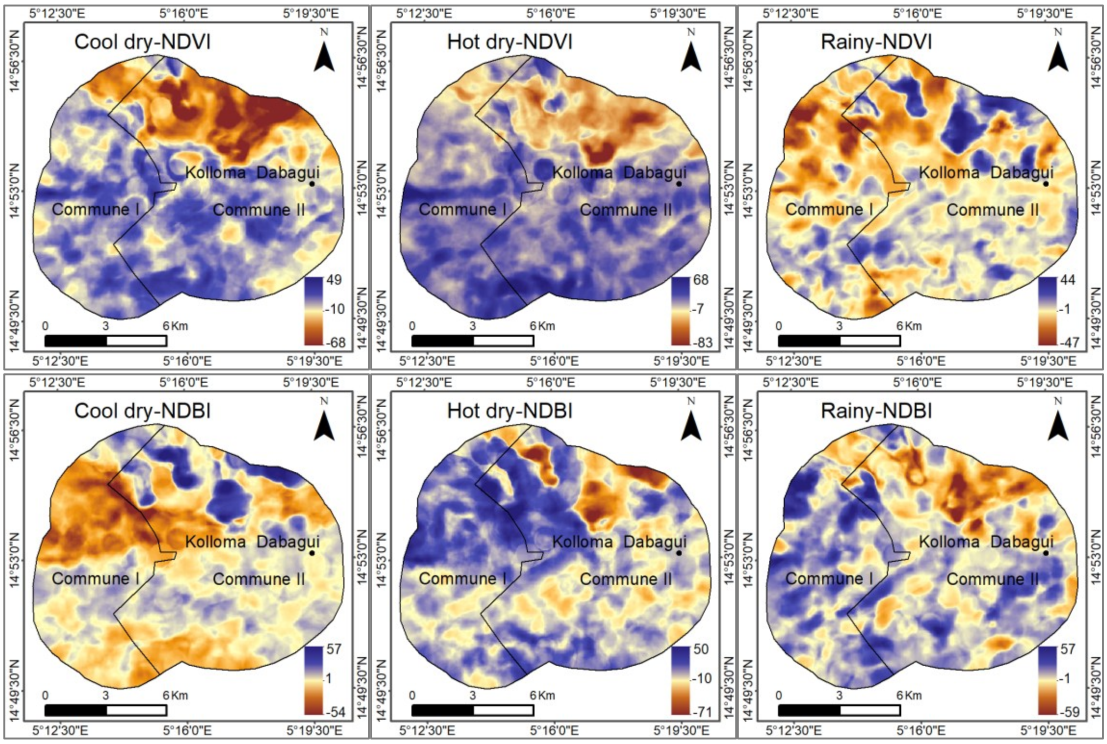

Figure 4.14 Seasonal GWR Coefficient of NDVI and NDBI In Tahoua

In Tahoua, a strong negative correlation between NDVI and LST was observed in the northern part of the study area, particularly in Commune II, across all seasons. This indicates that areas with high vegetation cover in this region consistently exhibit lower land surface temperatures. However, in the southern and central parts of the study area, the correlation was mostly positive, suggesting that vegetation has a weaker cooling effect or was less prevalent. An exception was observed during the rainy season, where the relationship becomes predominantly negative, likely due to increased vegetation growth and moisture availability enhancing cooling effects.

Notably, the settlement of Kolloma Dabagui exhibited a weak negative correlation between NDVI and LST, with seasonal variations in intensity. This suggests that while vegetation plays a cooling role in this area, its influence fluctuates across different climatic conditions because of the varying levels of vegetation cover and heath, soil moisture, and atmospheric conditions throughout the year.

The NDBI and LST relationship in Tahoua mainly showed a very weak to no relationship between these parameters except during the hot, dry season, where this relationship was predominantly positive in the northwest of Commune I and the north central region of Commune II.

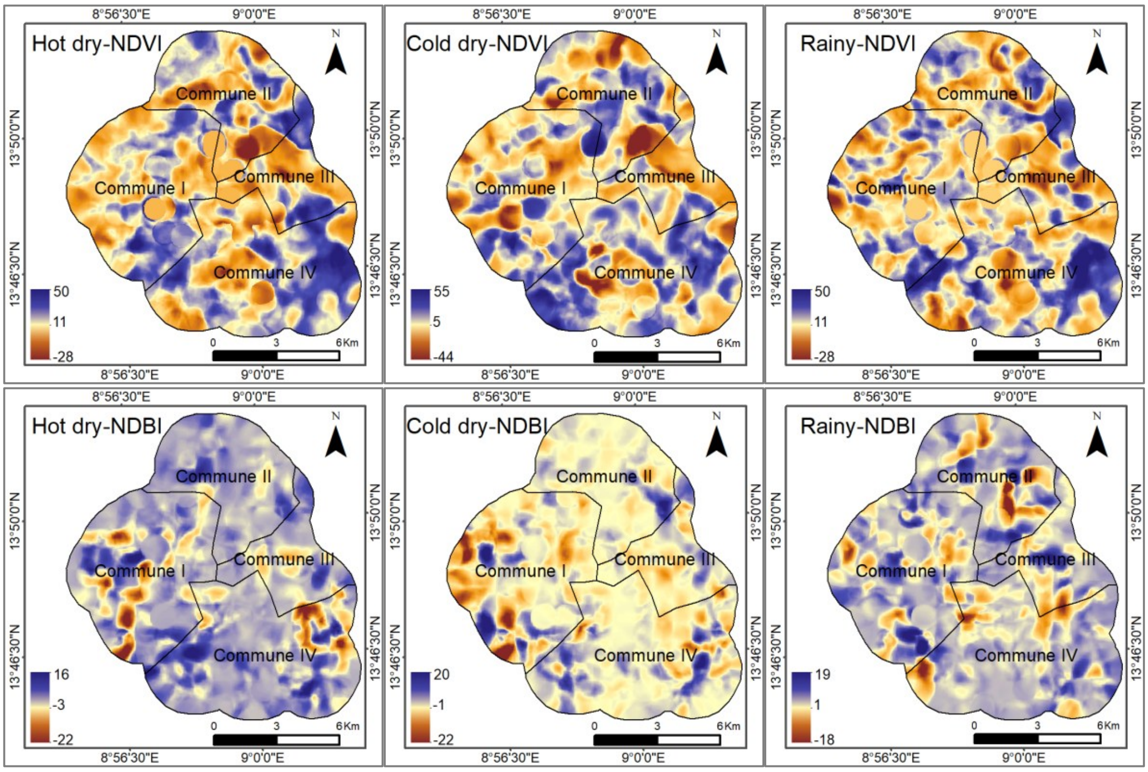

Figure 4.15 Seasonal GWR Coefficient of NDVI and NDBI in Zinder

In Zinder, the relationship between NDVI and LST varies across communes and seasons. A negative correlation (brown areas) signifies that higher vegetation cover (NDVI) is linked to lower LST, emphasising its cooling effect. This effect is most pronounced in Commune I and parts of Commune II, where distinct patches of strong negative correlations appear, particularly during the hot and cooler dry seasons. However, in much of the study area, the correlation is weaker or even positive (blue areas), indicating that vegetation plays a less significant role in reducing temperatures in these regions. This could be due to several factors, including sparse or degraded vegetation cover, which limits evapotranspiration; the dominance of non-vegetated surfaces such as bare soil or urban structures that absorb and retain heat; and possibly the presence of stress-tolerant vegetation types that do not significantly influence local microclimates. Additionally, soil properties and land management practices might further diminish the cooling effect typically associated with vegetation. Conversely, negative correlations become widespread during the rainy season across all communes, suggesting a more substantial cooling effect of vegetation due to increased moisture and plant growth.

The NDBI and LST relationship was predominantly weak across all the communes, with some high negative and positive values patches.

4.1.3 Trend of extreme heat indices in Tahoua and Zinder from 1991 to 2022

Figure 4.16 and Figure 4.17 show the trend of different heat indices in Tahoua and Zinder over 31 years. The results show that these cities have shown significant warming trends over the past three decades.

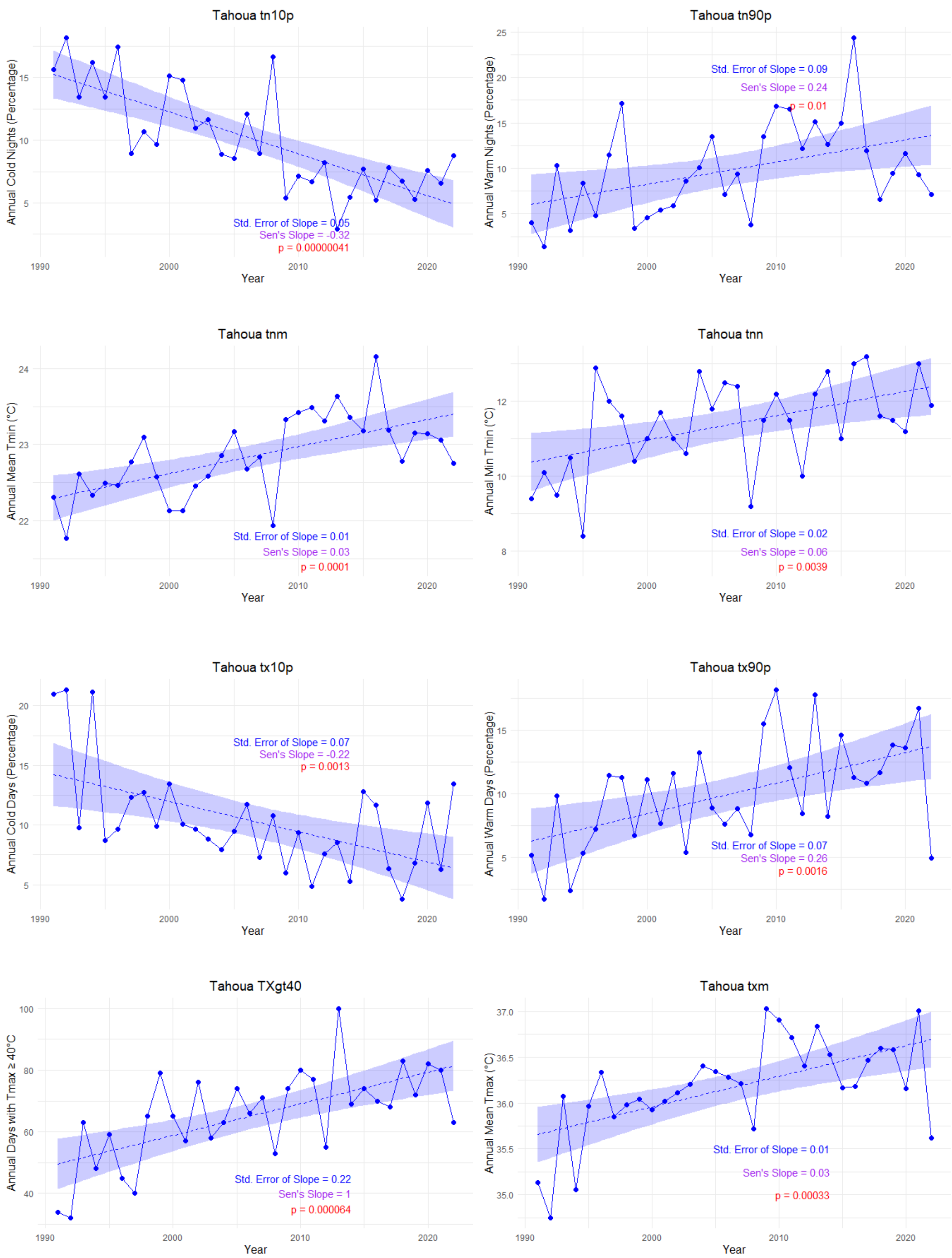

Figure 4.16 Trend of Extreme Heat Indices in Tahoua From 1991 to 2022

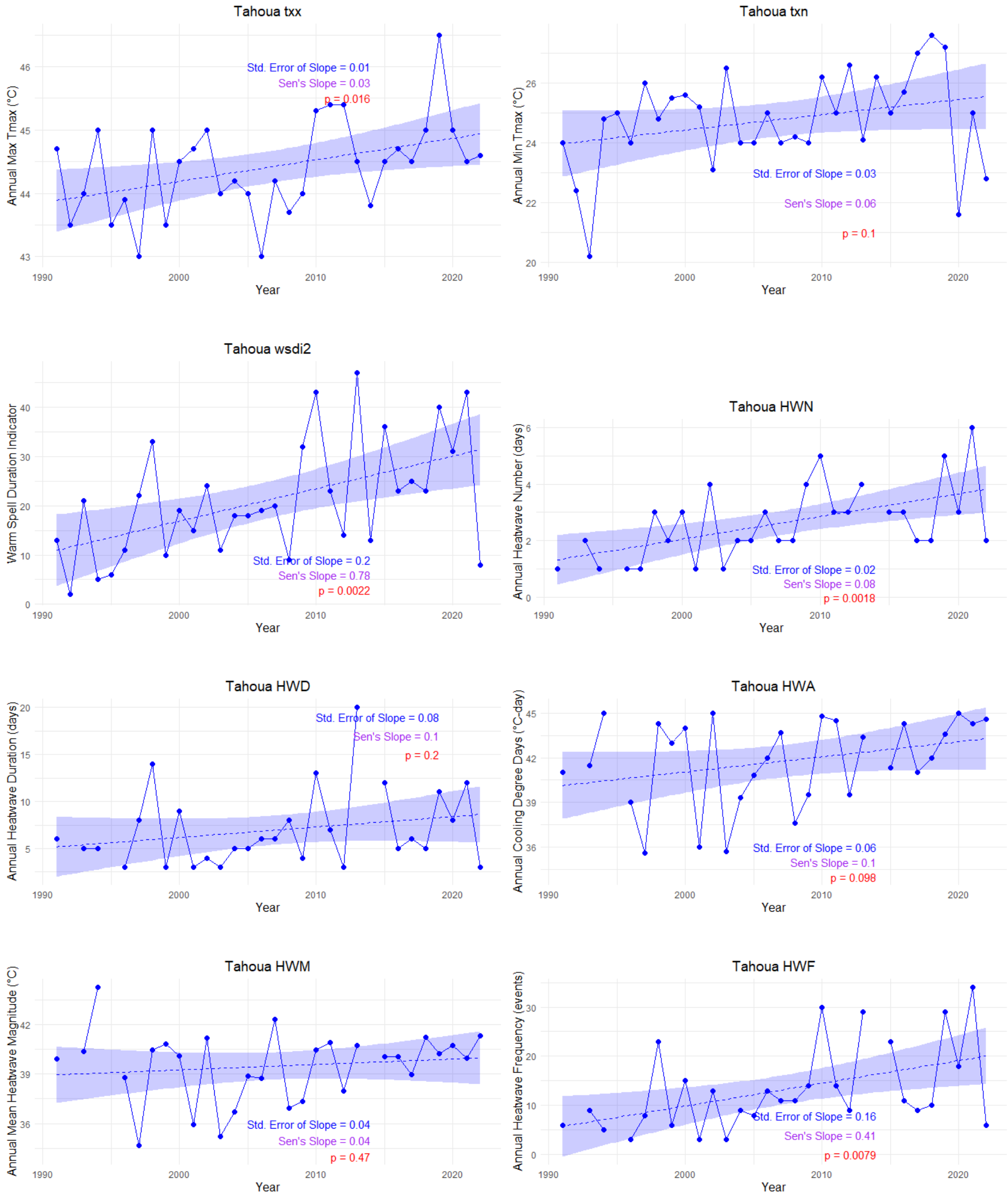

Figure 4.16 Trend of Extreme Heat Indices in Tahoua From 1991 to 2022 (Continued)

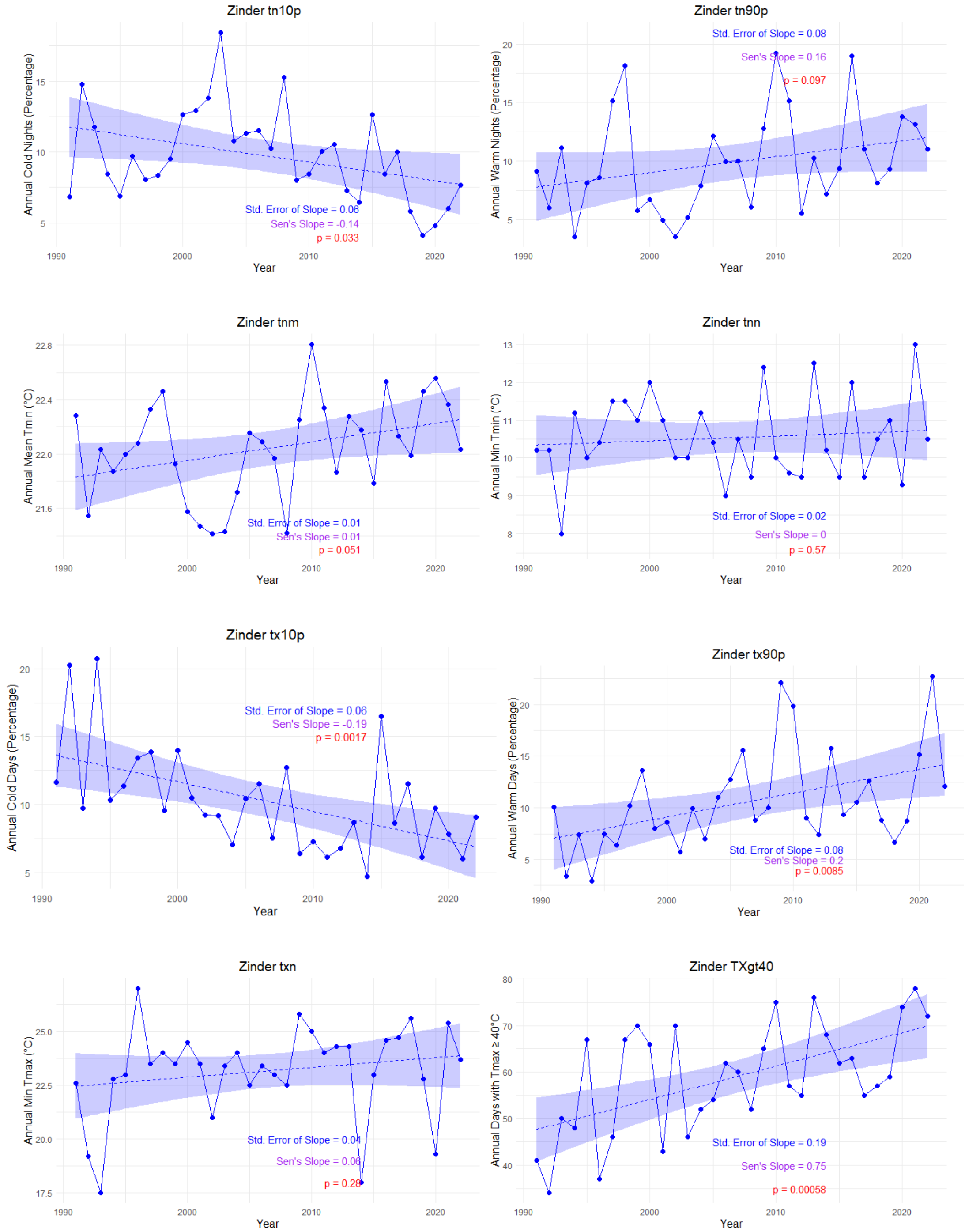

Figure 4.17 Trend of Extreme Heat Indices in Zinder from 1991 to 2022

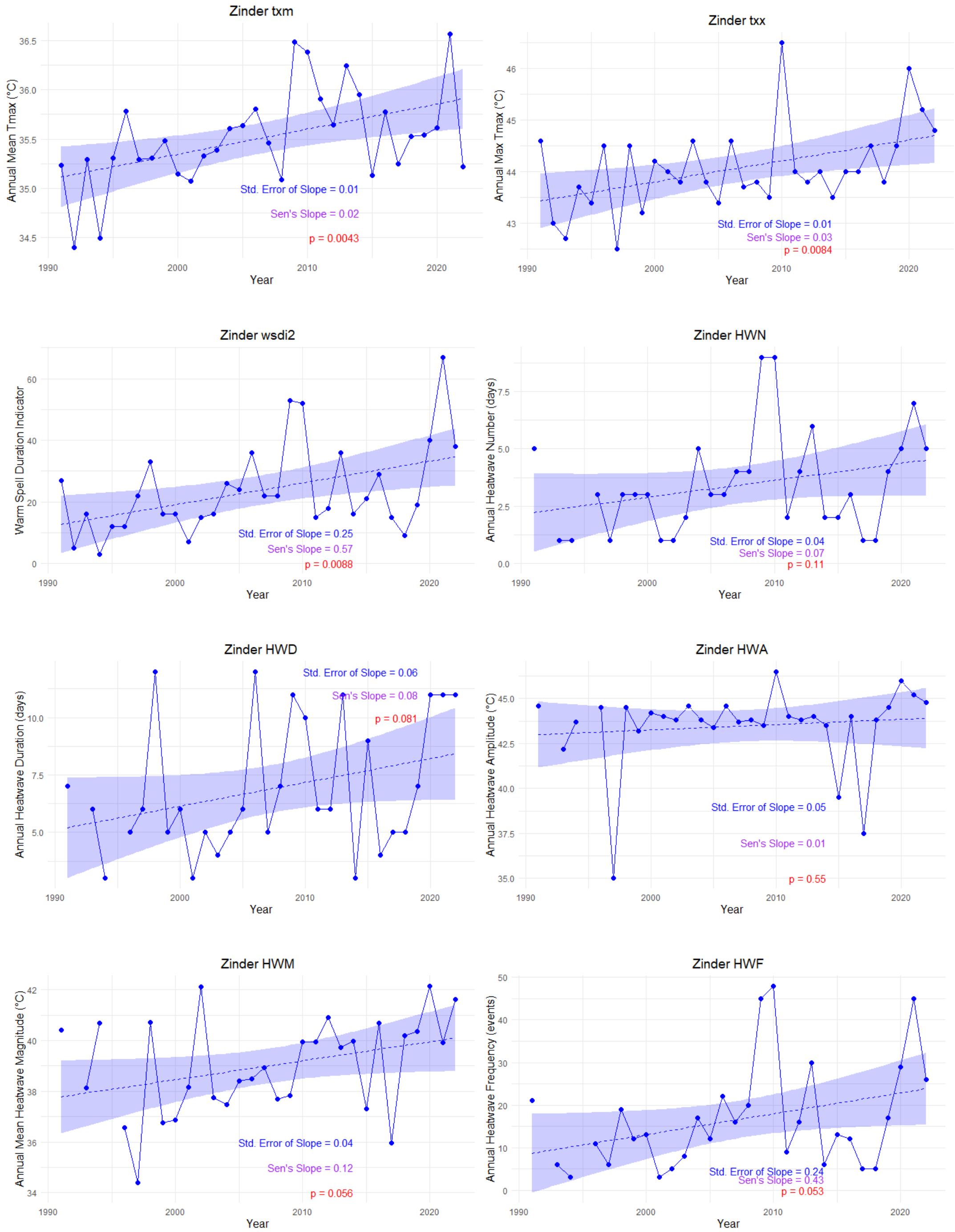

Figure 4.17 Trend of Extreme Heat Indices in Zinder from 1991 to 2022 (Continued)

For instance, both cities show a significant decrease in cold nights (tn10p), with Thaoua having a more substantial decline Table 4.14. On the other hand, warm nights (tn90p) are increasing significantly in both cities, with Tahoua having a slightly stronger trend (slope=0.24 vs 0.16). Both cities have a significant decrease in cold days (tx10p), with a sharper decline in Tahoua. Meanwhile, there is an increase in warm days (tx90p), with Tahoua showing a slightly stronger trend. In the same manner, Tahoua looks to experience more pronounced increases in the number and duration of heatwaves, as well as in extreme temperature indices. Although Zinder shows similar trends, they have slightly lower magnitudes for most indices. The number of extremely hot days (Tmax ≥ 40°C) is rising significantly in both regions, with slightly stronger trends in Tahoua.

Table 4.14 Summary Statistics of Heat Indices Trend in Tahoua and Zinder

			Tahoua			Zinder		
Indices	**Start Year**	**End Year**	**P_Value**	**Slope**	**Std_Error**	**P_Value**	**Slope**	**Std_Error**
tn10p	1991	2022	0.00*	-0.32	0.05	0.03*	-0.14	0.06
tn90p	1991	2022	0.01*	0.24	0.09	0.10	0.16	0.08
tnm	1991	2022	0.00*	0.03	0.01	0.05	0.01	0.01
tnn	1991	2022	0.00*	0.06	0.02	0.57	0.00	0.02
tx10p	1991	2022	0.00*	-0.22	0.07	0.00*	-0.19	0.06
tx90p	1991	2022	0.00*	0.26	0.07	0.01*	0.20	0.08
TXgt40	1991	2022	0.00*	1.00	0.22	0.00*	0.75	0.19
txm	1991	2022	0.00*	0.03	0.01	0.00*	0.02	0.01
txn	1991	2022	0.10	0.06	0.03	0.28	0.06	0.04
txx	1991	2022	0.02*	0.03	0.01	0.01*	0.03	0.01
wsdi2	1991	2022	0.00*	0.78	0.20	0.01*	0.57	0.25
HWA	1991	2022	0.10	0.10	0.06	0.55	0.01	0.05
HWD	1991	2022	0.20	0.11	0.08	0.08	0.08	0.06
HWF	1991	2022	0.00*	0.41	0.16	0.05	0.43	0.24
HWM	1991	2022	0.47	0.03	0.04	0.06	0.12	0.04
HWN	1991	2022	0.00*	0.08	0.02	0.11	0.07	0.04

*Statistically significant at $p<0.05$

4.1.4 Urban heat vulnerability analysis

4.1.4.1 *Urban heat vulnerability component*

The mean values of each vulnerability component indicator were calculated and used to generate maps of exposure, sensitivity, and adaptive capacity of each neighbourhood (Figure 4.18). The maps of urban heat vulnerability components show that city centres are the most exposed areas in the two cities. In Tahoua, it is the neighbourhood of Kourfayawa, while in Zinder, it is the neighbourhood of Yanda Kondagué. These areas are densely populated and have high temperatures due to the concentration of people and buildings. However, the pattern of sensitivity and adaptability depends solemnly on the socioeconomic characteristics of the population.

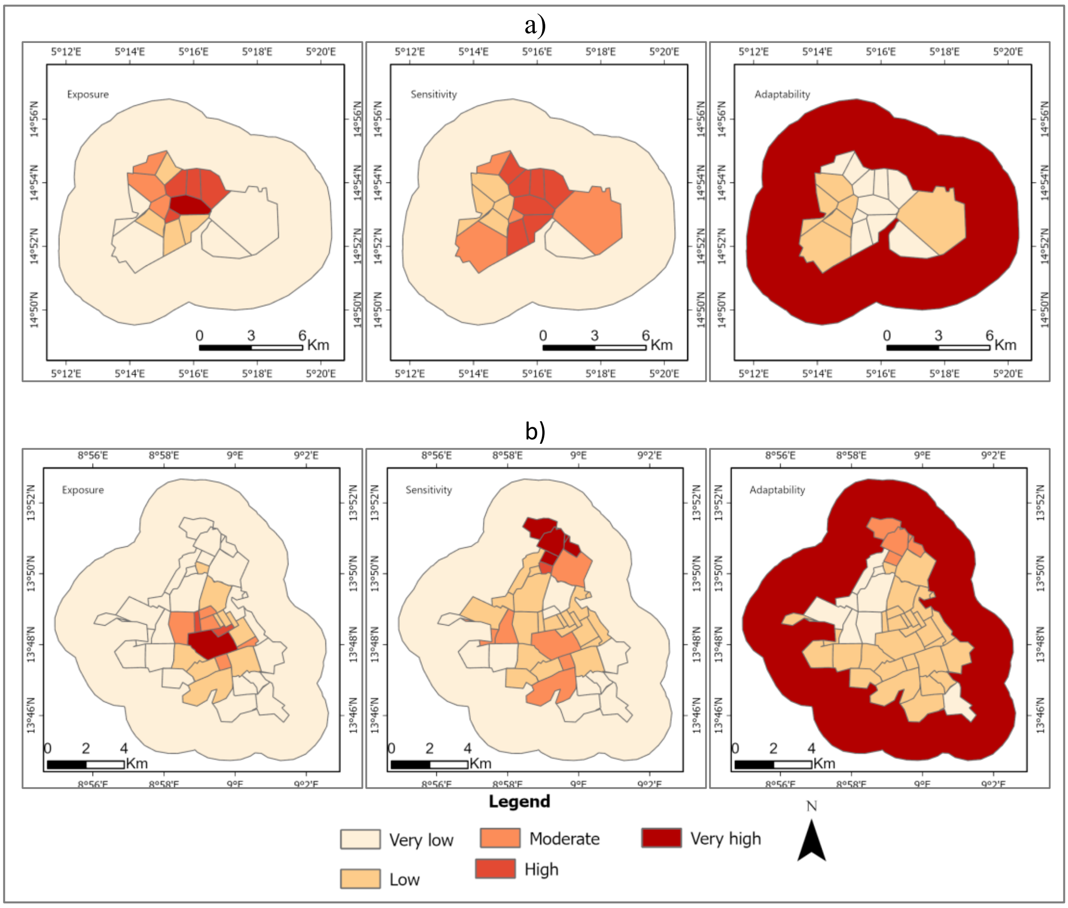

Figure 4.18 Component of heat vulnerability for Tahoua (a) and Zinder (b)

4.1.4.2 *Cartography of Urban Heat Vulnerability*

The heat vulnerabilities of Tahoua and Zinder were measured using V1 and V2, which were reclassified from very low to very high vulnerability. Figure 4.19 depicts the variations in the two cities. The most heat-vulnerable areas in Tahoua resides in the neighbourhoods of Dioulanke, Maboyaramare, Toudun Adoum, Nassaraoua and Kourfayawa. In Zinder, it includes Yada Kwandagué, Charé Zamna, Soraz, Garin Liman, Manzozo, Malan Amar, Madatey and Banguia.

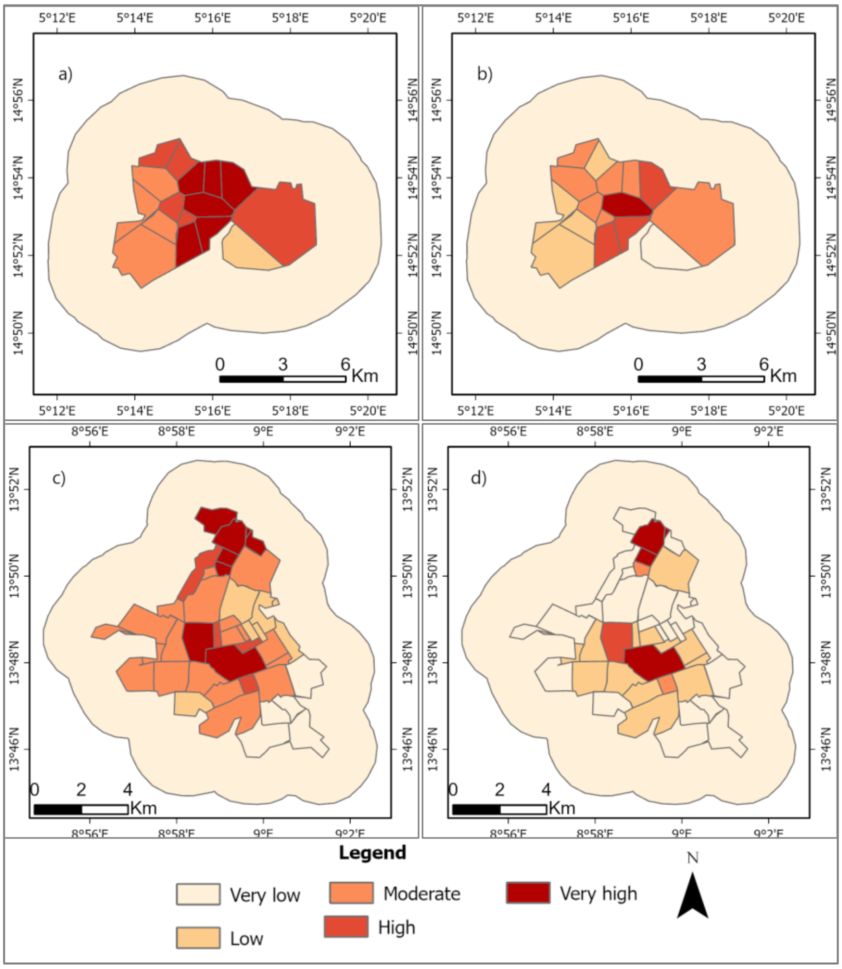

Figure 4.19 Tahoua (a and b) and Zinder (c and d) Heat Vulnerability (a and c using V1, b and d using V2)

To explore the relationship between sensitivity, exposure, adaptive capacity, and UHVI, the correlations for each formula were computed in each city and depicted in Figure 4.20.

Correlation analysis between the two heat vulnerability indices and components shows a negative correlation between the index and the adaptive capacity in the two cities (Table 4.16).

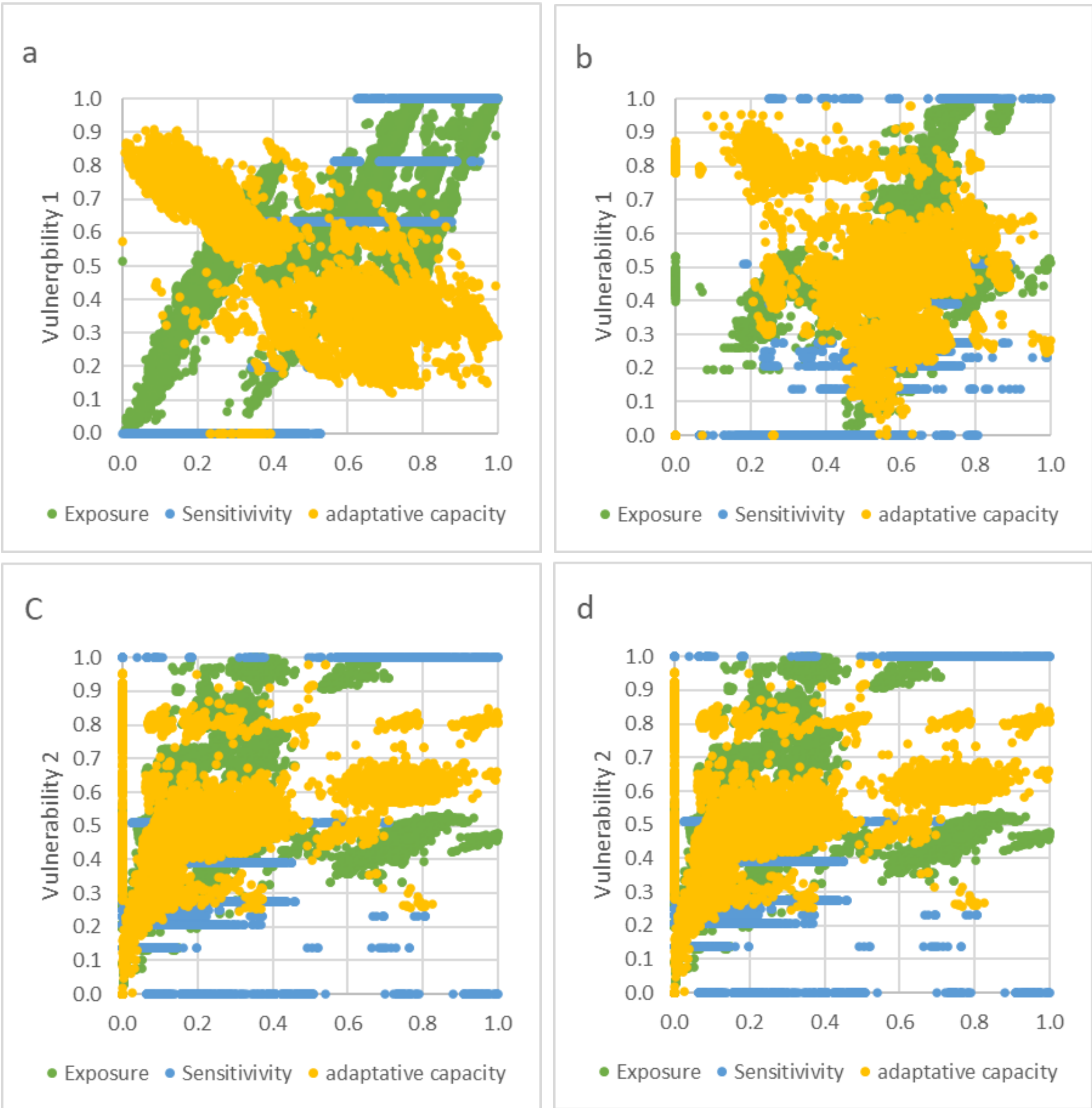

Figure 4.20 Correlation of UHVI with its Components in Tahoua (a and c) and Zinder (b and d)

All the vulnerability indices in the two cities show a robust positive correlation with the sensitive index, a moderate correlation with the exposure indices, and a strong negative correlation with the adaptability components (Table 4.15). All the p values <0.001which indicate that the correlation tests between the heat vulnerability components and indices are statistically highly significant.

Table 4.15 Correlation Between Heat Vulnerability indices and its components

Vulnerability index	Exposure	Sensitivity	Adaptability
V1T	0.45	0.93	-0.86
V2T	0.41	0.89	-0.74
V1Z	0.30	0.86	-0.80
V2Z	0.25	0.95	-0.62

4.1.4.3 *Impact of heat-stress on Tahoua and Zinder's residents and their adaptation strategies*

The interviewed targeted household heads, as mentioned in the methodology section. In Tahoua, 64% were men, and 36% were female; in Zinder, 66.4% were men and 33.6% were female (Appendix D). It is important to note that not all the females interviewed were head of household. In some cases, women were interviewed either because the men had permitted them to respond or the men were not in the house. 91.5% of the men in Zinder think that there was an increase in temperature in the city over time, while only 85% of the ladies think so. It was evident that over 99% of males and females have the same perception of the negative impact of heat on health.

Figure 4.21 illustrate the nature of heat affects the health of the population of Tahoua and Zinder. A similar pattern was observed in the two cities, with heat-induced fatigue and headache being the most frequent inconveniences caused by high temperatures. The population is using many strategies to reduce the adverse effects of heat, as shown in Figure 4.22. Because of the inconveniences caused by heat stress, the linkage between heat stress working capacity and its impact on finances has been established (Aguilar-

Gomez *et al*., 2024). To verify this in Tahoua and Zinder some questions about the population income, expenses and labour capacity during heat stress periods were asked. Only 3% and 2% of the interviewed population experienced increased income during hot periods in Tahou and Zinder respectively (Figure 4.23). This is mainly due to the ability of the responents to sell more elements related to heat stress coping strategies which include fans, batteries, cold drinks and ice. The increased expenses were due to the use of heat stress adaptation and/or coping strategies.

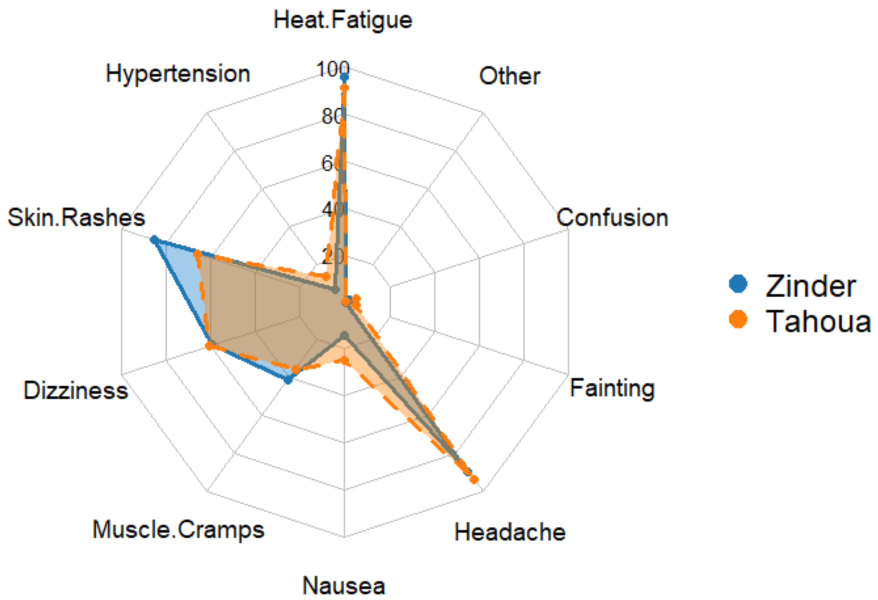

Figure 4.21 Impact of Heat on Health in Tahoua and Zinder

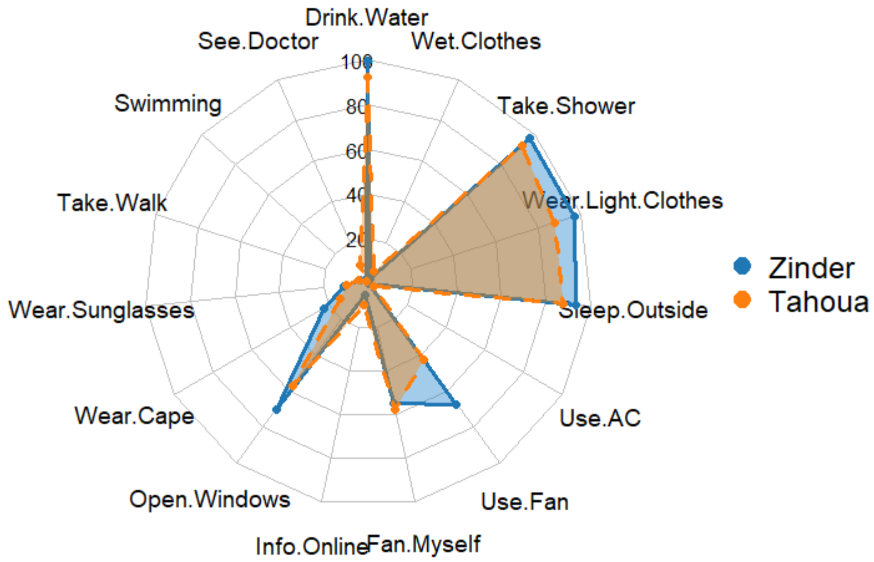

Figure 4.22 Heat Stress Coping Strategies in Tahoua and Zinder

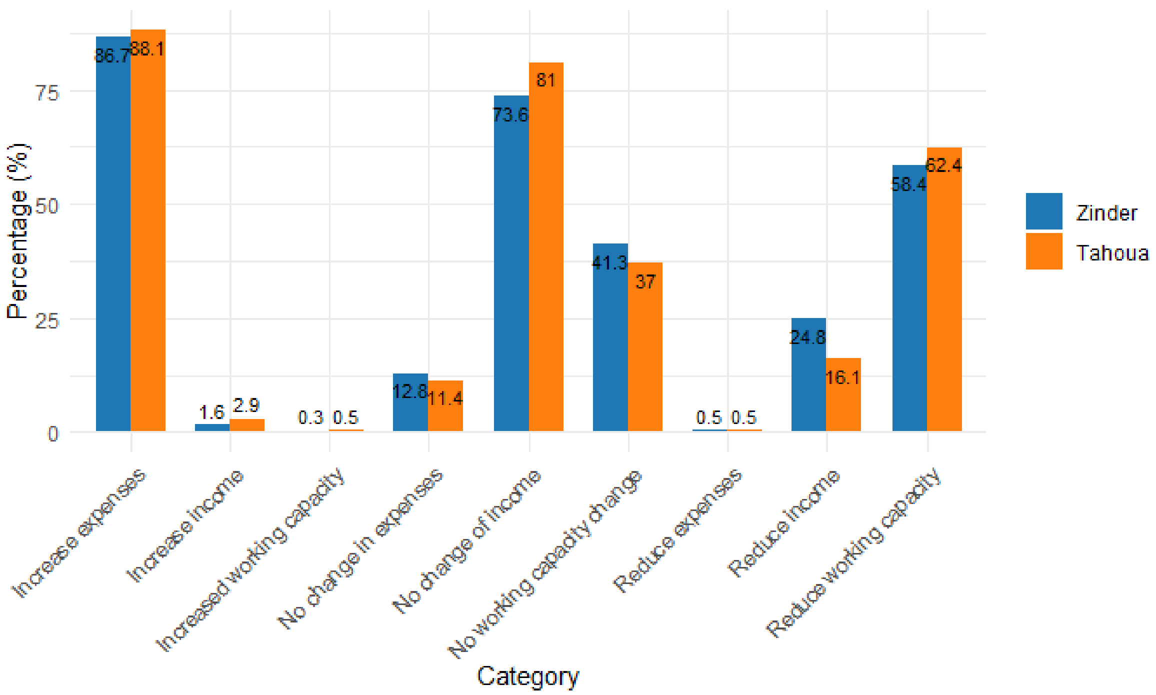

Figure 4.23 Impact of Heat Stress on Finances and Working Capacity in Tahoua and Zinder

To further investigate the relationship between residents' perception of heat based on their gender, level of education, occupation, and income, Sankey diagrams were performed for Tahoua (Figure 4.24) and Zinder (Figure 4.25).

These diagrams show the flow of responses between categories. These categories are Sex, Education Level, Employment Status, Income Level, and Heat Impact Perception. It also displays the degree of transitions between categories using link widths. The percentage of respondents who switch between different categories is indicated by the extent of the links connecting each node, which stands for a category.

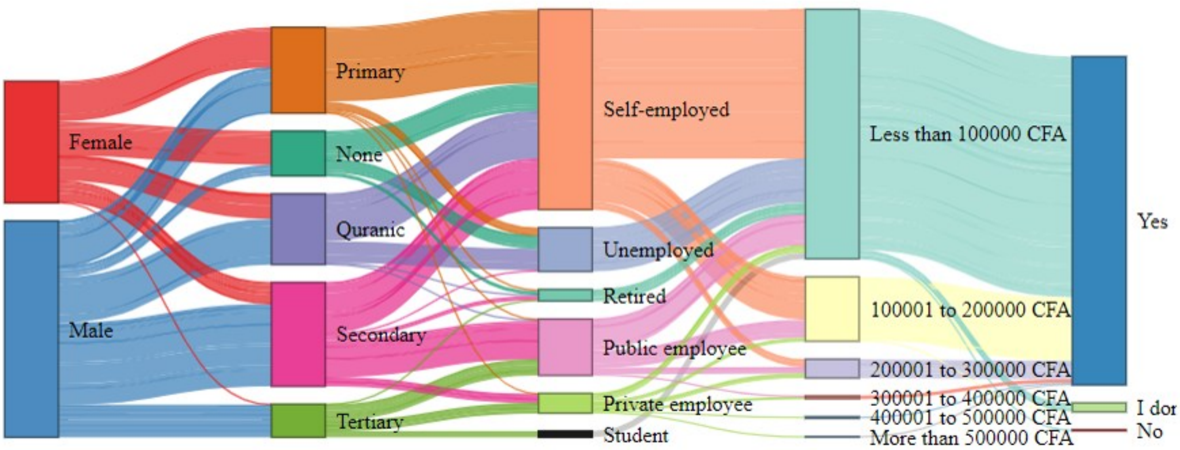

Figure 4.24 Flow from Sex to Heat Impact Perception in Tahoua

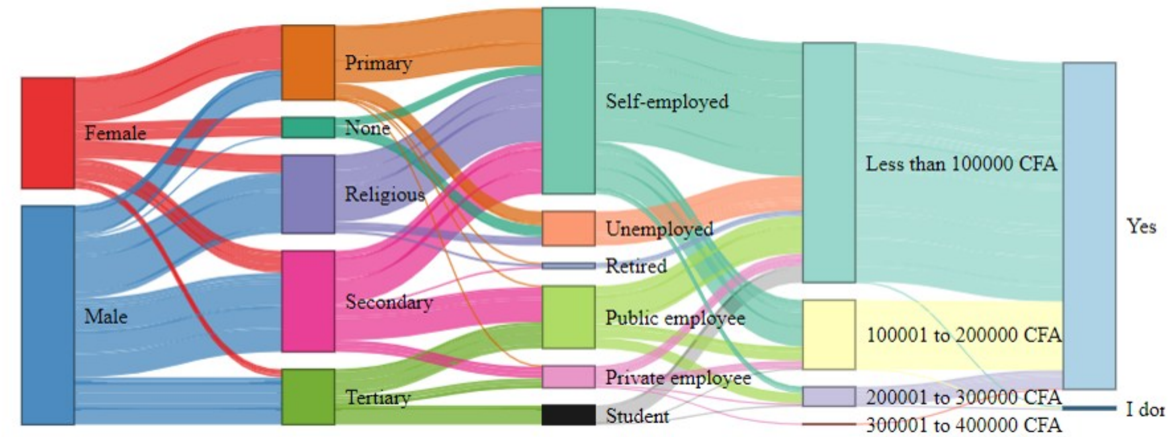

Figure 4.25 Flow from Sex to Heat Impact Perception Zinder

The results indicate that poor levels of education prevent people in these cities from obtaining formal work, which contributes to high rates of self-employment and poor income levels. Notwithstanding these variations, it was evident that over 99% of males and females in the two cities agree that excessive heat has a detrimental influence on health, suggesting that there was widespread worry about climate change and how it would affect vulnerable groups.

4.1.5 Future projection of LULC change

4.1.5.1 *Model Accuracy Assessment*

The accuracy of CA-LR and CA-ANN was determined by comparing the predicted LULC of Tahoua for the year 2022 proportions with the proportions of the classified LULC for 2022. The results show that the overall accuracy of the CA-LR model (95.73%) was higher than that of the CA-ANN model (92.53%) (Table 4.16).

Table 4.16 Model Accuracy Assessment

LULC Class	CA-ANN	CA-LR
Vegetation	84.91	81.97
Built-up	72.16	88.25
Agricultural land	95.57	97.47
Overall Accuracy	92.53	95.73
Kappa Coefficient	0.77	0.76

By evaluating the accuracy of each LULC class, it was found out that CA-LR has performed better in modelling the Built-up class (Table 4.18). This shows that the CA-LR model has a better ability to model urban expansion. While there was some underestimating of vegetation in both models and overestimation of the agricultural land class, CA-LR consistently produced forecasts that were more accurate in all categories. Although CA-ANN's Kappa coefficient was slightly higher (0.77 vs 0.76) (Table 4.17), both models demonstrated high agreement with the classified LULC. Though CA-LR was thought to be more crucial for our investigation, its greater overall accuracy was not overshadowed by the small variation in Kappa values.

Table 4.17 Area of LULC by Model

LULC Class	Actual	CA-ANN	CA-LR
Vegetation	4.77	4.05	3.91
Built-up	10.81	7.80	9.54
Agricultural land	84.42	88.16	86.56

4.1.5.2 *Future LULC change in Tahoua and Zinder*

The spatiotemporal evolution of LULC change in Tahoua (Figure 4.26) and Zinder (Figure 4.27) showed a similar pattern with differential change rate. These results revealed a slight decrease in vegetation and the agricultural land classes areas from 2022 to 2042 (Figure 4.28b), whereas the built-up area is expected to increase, going from an increase of 10.81% in 2022 to 14.98% in 2042.

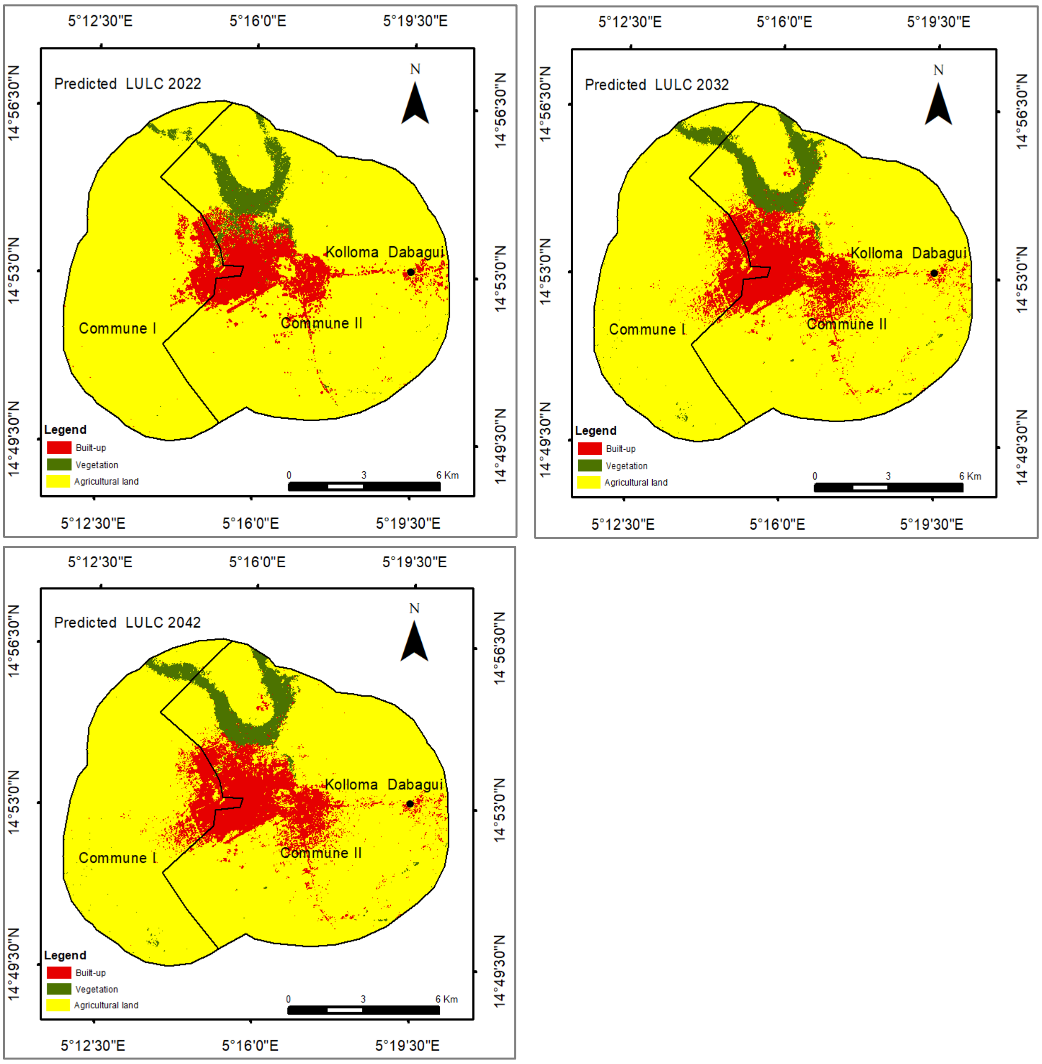

Figure 4.26 Tahoua Predicted LULC Change

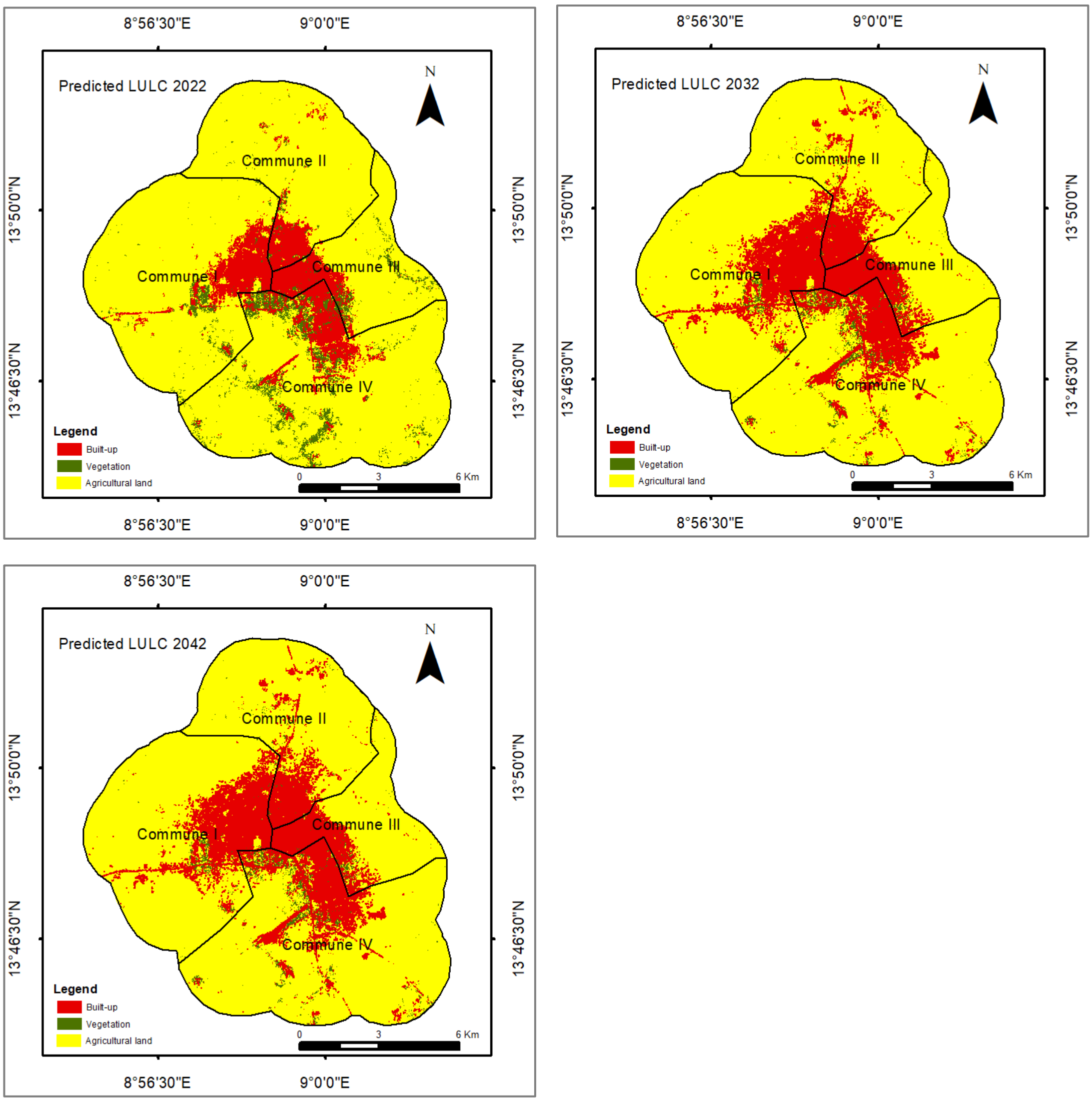

Figure 4.27 Zinder Predicted LULC Change

The same pattern of change is expected in Zinder, with a more serious decline in vegetation class. For instance, the vegetation class is expected to drastically decrease from 2022 to 2043 (Figure 4.28c). It is anticipated that during the same period, the agricultural land class will continuously decline (Figure 4.28d). Conversely, a tremendous urban expansion is anticipated, with the built-up area rising at an accelerated rate from 14.04% in 2022 to 25.28% in 2043.

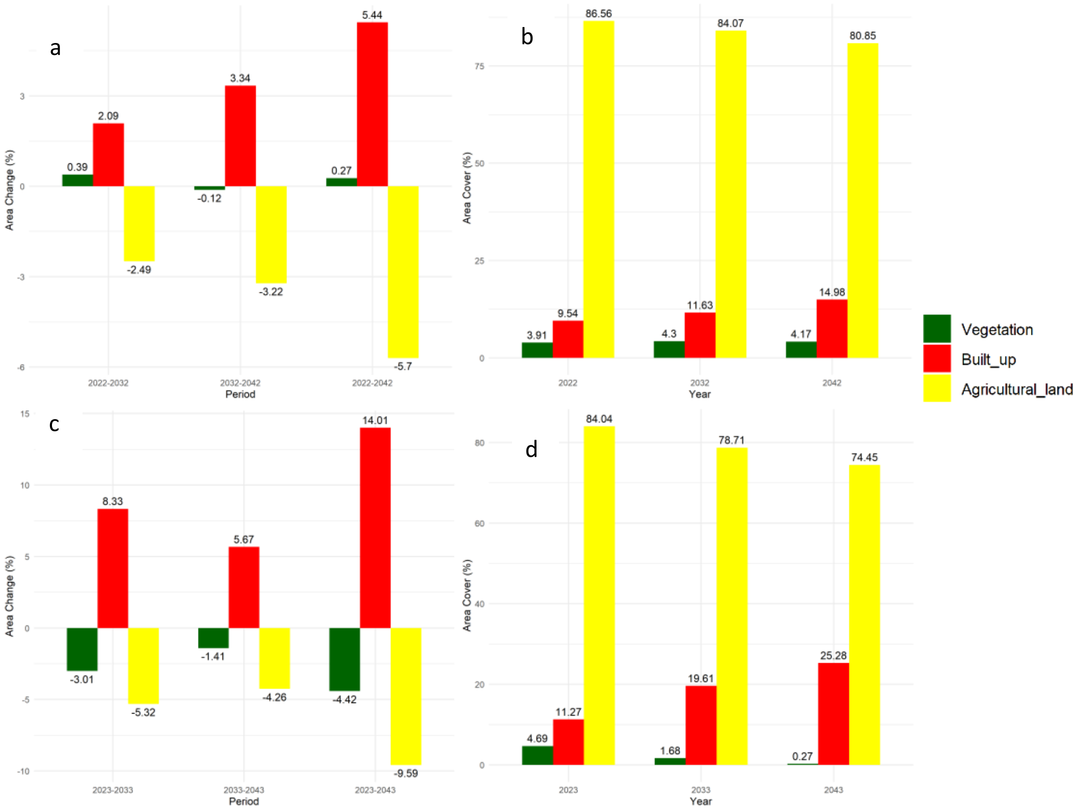

Figure 4.28 Predicted LULC Change in Tahoua (a and b) and Zinder (c and d

4.1.5.3 *Global trend of LULC change in Tahoua and Zinder*

In general, Zinder and Tahoua are facing serious problems due to the loss of their vegetation covers (Figure 4.29). By 2043, Zinder is expected to have loss almost all its vegetation (0.27%) if the present trend continues (Figure 4.29b). Controversially, urban growth is accelerating quickly, especially in Zinder. In Tahoua, the agricultural land class is comparatively steady (Figure 4.29a), whereas in Zinder, it gradually declines.

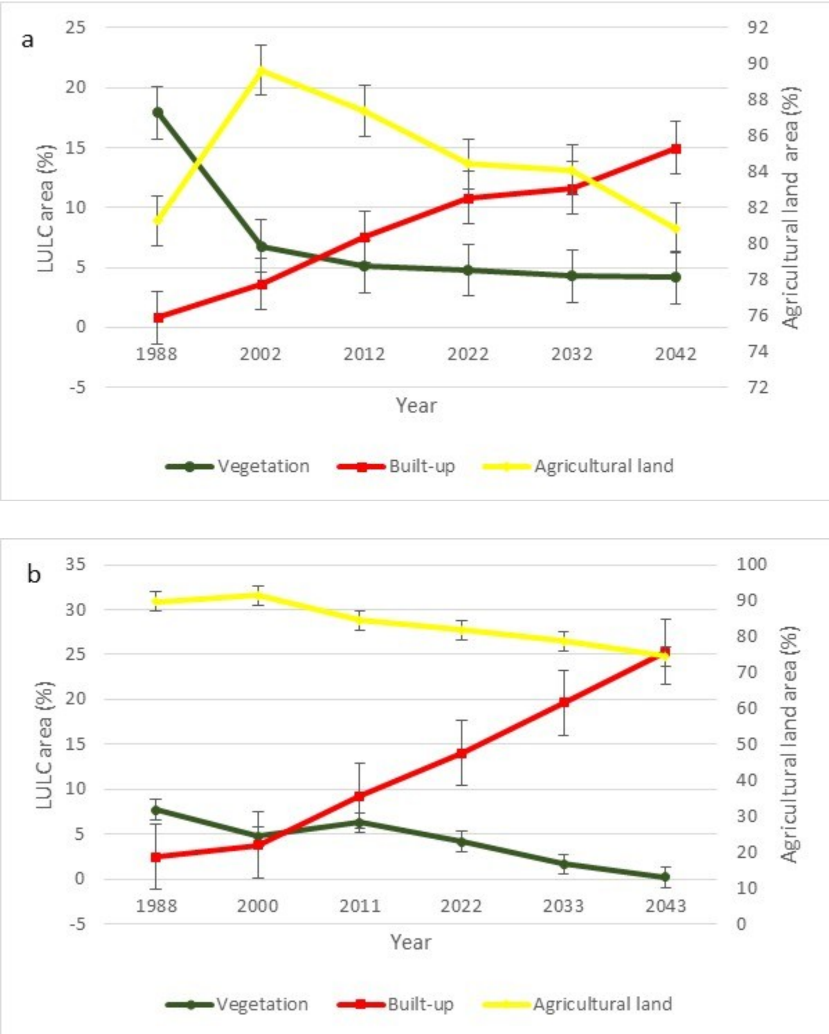

Figure 4.29 Trend of LULC Change in Tahoua (a) and Zinder (b) Under the Business-as-usual Scenario

4.1.5.4 *Future LST trend in Tahoua and Zinder*

Using 2002 (the year with anomalously high temperatures) as the baseline, projections for the period between 2032 and 2042 indicate seasonal variations in Land Surface Temperature (LST) trends across Zinder and Tahoua. In the cooler dry season, both cities are expected to experience slight increases in mean LST. However, during the hot dry season, a notable decrease in LST is projected for both regions. In contrast, the rainy season shows divergent patterns, with Zinder expected to cool while Tahoua experiences a slight increase in temperature (Figure 4.30).

Conversely, when 2001 is used as the baseline, both cities show a consistent warming trend across all three seasons from 2032 to 2042. The increases are most pronounced during the cooler and hot dry seasons, while the rainy season shows relatively moderate rises in LST (Figure 4.31). Overall, these projections underscore a general warming tendency, particularly during the drier periods of the year.

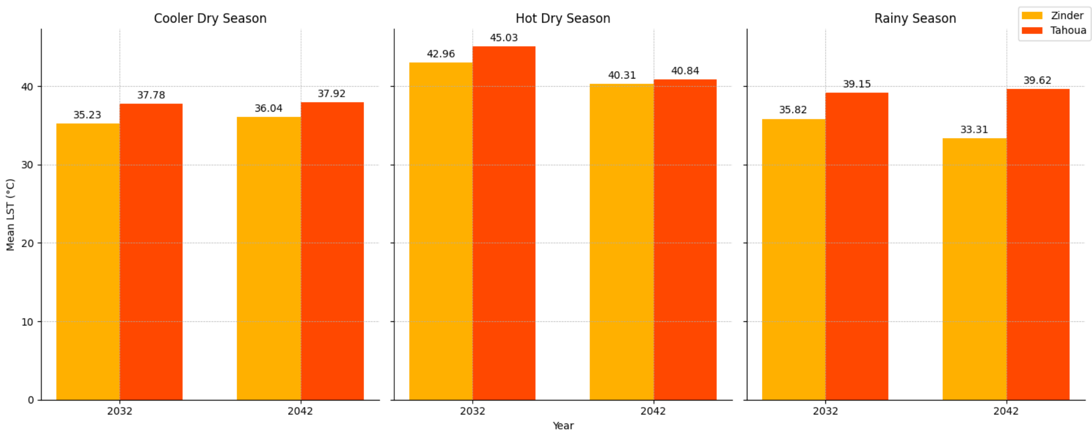

Figure 4.30 Mean Future LST in Tahoua and Zinder Using 2002 as the Baseline

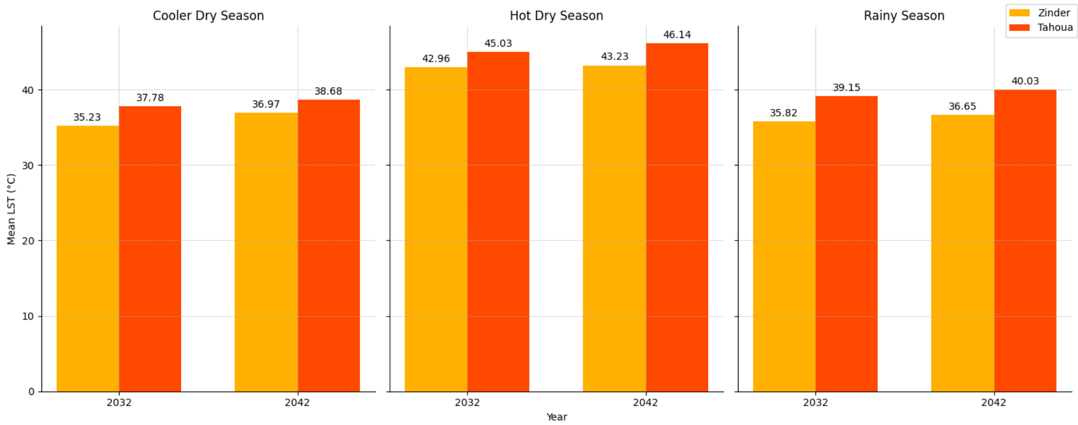

Figure 4.31 Future LST Mean in Tahoua and Zinder Using 2001 as The Baseline

4.2 Discussion of Results

4.2.1 The dynamics of urban landscape change in Tahoua and Zinder

Over the 34 years of study, the LULC in Zinder and Tahoua have shown significant changes. There has been a decrease in vegetation and agricultural classes while the built-up areas have expanded (Figure 4.3). This same pattern was observed by many researchers irrespective of the size of the city or location around the world (Abbas *et al*., 2021). In the study areas, over 80% of the population is engaged in agriculture as their primary activity (Institut National de la Statistique, 2023). This is not only for subsistence but also for generating income. The expansion of built-up areas has led to the conversion of agricultural land, impacting food security. The increase in demand due to population growth, the reduction in the number of farms, and soil degradation have further affected agricultural productivity. Another challenge caused by urban expansion and population increase includes anthropogenic pressure on natural resources, which caused a reduction of vegetation cover through abusive tree cutting and clandestine clearance. Wood is the primary energy source and is used as a building material. This negatively affects the environment and exposes the ecosystem to the harmful effects of desertification, including water and wind erosion.

Despite the fact that the vegetation covet has decreased in Zinder, an increase of 1.53% occurred during the second intermediate period (Fig 4.3c). This increase might have been achieved by the programme and development projects emphasising the massive application of assisted natural regeneration technology and irrigation schemes in the study area. The initiative was implemented under President Tanja Mahamadou's special programme to mitigate the susceptibility of Nigerien agriculture to desertification and drought (Fonds international de développement agricole, n.d.). During the same period, activities to implement an oil refinery (SORAZ) were conducted in the area, which intensified NGOs' intervention in the area. In fact, the refinery activities and associated projects might be the reason for the highest growth rate of built-up areas at 144.15 during the same period.

Data on population growth reveals the highest growth during the third intermediate period. This period experienced a critical rural-to-urban migration as a result of multiple Boko Haram attacks. Many people moved to Zinder for safety and stability. However, this increase in population size did not have a significant impact on the expansion of the built-up area as expected. This finding could be explained by the fact that these refugees lack the financial resources to fully install houses in the city. While some live in their relatives' families, others manage to make temporary housing (huts/tents) in vacant lands. The most vulnerable live along the roads (Leslie, 2015).

As part of its efforts to promote coherent development, a reference document for any development called *Plan de development communal* exists in the all the districts forming the city of Zinder and Tahoua. These documents are elaborated independently at the district rather than citywide. The districts have the authority to convert farmlands into plots and sell them, which generates income for the district. However, this has led to unregulated land conversion and plot sales reducing the agricultural areas. In all four documents, from the four urban districts forming the city of Zinder urban expansion strategies were not mentioned. Additionally, all of these documents are outdated and have not been updated, indicating a lack of planning for urban expansion. Consequently, the city continues to grow in a disorderly manner.

In Zinder and Tahoua, edge-expansion and outlying growth types are dominant (Figure 4.6). This means that these cities are experiencing a sprawl. Infilling growth, which is the least growth type, is the process of newly growing patches filling in the gaps between or within older patches. It makes good use of available land within developed areas. Moreover, it leads to efficient land resource management. Edge-expansion, on the other hand, is a pattern of progressive outward migration from the periphery of urban areas. This same type of development was called metropolitan or urban fringe development by Heimlich and Anderson (2001). The outlying growth occurs when a new patch has no neighbouring relationship with an old patch. Heimlich and Anderson (2001) qualified it as a development outside of the urban fringe. In all cases, the existing built-up area was crucial in determining the type of urban growth.

LULC change trends highlighted by this study in Tahoua and Zinder draw attention to the urgent problems that result from urbanisation and environmental deterioration. The sharp decline in vegetation cover which is more pronounced in Zinder, is consistent with larger trends in land degradation in semi-arid regions of Africa and specifically in Niger Republic (Illiassou *et al*., 2015; Doulay *et al*., 2019). This depletion in vegetation is caused not only by urban growth but also by overgrazing, deforestation, and increased agricultural production. In addition, the effects of climate change, which include changing rainfall patterns and rising temperatures, could have worsened this condition (Chapman *et al*., 2019; IPCC, 2021). Thus, causing concerns about increased soil erosion, biodiversity loss, and declining land productivity, which in turn threaten local livelihoods.

It is important to note that natural forest formations no longer exist in the two study areas. The relatively high vegetation cover in Tahoua in 1988 can be attributed to the area being part of a pastoral zone. However, this vegetation covers significantly declined between 1988 and 2002 in Tahoua particularly in commune II which was the most vegetated due to the conversion of grazing lands into agricultural land. Throughout the study period (1988 to 2022), commune II remained more urbanised than commune I. This expansion was particularly higher along main road with new settlement emergence of Kolloma Dabagui settlement at the eastern extreme of in commune I from 2002. This settlement has continued to grow to be encroached to the city of Tahoua.

In 1988, commune III of Zinder was the most urbanised area while, the commune II had less built up and was the most vegetated. However, from 2000 to 2022 this commune has experienced an increase in the built-up areas through the conversion of the agricultural lands and the vegetation therein. Nevertheless, commune III remained the most vegetated throughout the study period. This could be explained by its high-water scarcity.

In both cities, remaining patches of vegetation are mostly found in the peripheral built-up areas. This trend can be partly explained by the growing interest among local populations in planting trees around their homes. When land is divided for development, it is no longer actively cultivated, allowing vegetation to grow in the interim before construction begins. Eventually, these trees are typically cleared to make way for new buildings.

Additionally, the vegetation patches found in agricultural areas are largely the result of NGO and government-led interventions, aimed at land restoration and reforestation. These areas are typically protected or left untouched only for the duration of the projects. Once the projects conclude, however, local communities tend to exploit these areas, leading to the degradation of the vegetation cover and contributing to the shifting location of vegetation patches on maps.

Another important tendency is the transformation of agricultural lands into built-up areas. The higher growth of built-up areas in all the communes of Zinder and Tahoua during the first intermittent period compared to the first (Figure 4.3) can be attributed to the decentralisation of urban planning and land management after the year 2000 in Niger. Prior to the decentralisation, the major cities of Niger were provided with Master Plan for Urban Planning (MPUP), which is a framework that governs urban development and planning. However, the MPUP expired in the early 2000s due to decentralization, which reallocated powers to local authorities (Djibo, 2019). This decentralisation meant that local councils had more control over land management. Since the decentralisation, these cities have evolved with no operational MPUP, although Law n°2008-03 of April 30, 2008, in its chapter 2, discussing urban planning documents, Articles 6 and 7 address the necessity of urban planning documents such as the Urban Reference Plan (PUR) and the Land Use Plan (POS).

City halls were engaged in the exchange of parcels, often resulting in land use that was not directly tied to organised urban planning. Additionally, the 2002 government initiative called the "Arrears of Wages Against Parcels" program, aiming to resolve unpaid salaries by giving land parcels to workers, further contributed to urban sprawl (Adamou, 2012). These factors resulted in a significant expansion of urbanised areas in Tahoua and Zinder from 2002-2012, more so than in the previous decades. Djibo (2019) also found that, similar to the findings in this study, the urbanised area in Zinder expanded significantly, from approximately 2,170 ha in 2000 to 6,146 ha in 2017, with a notable decline in population density from 94 inhabitants per hectare in 2000 to 63.91 inhabitants per hectare in 2017. He highlighted that the increase in land area was not accompanied by an equivalent demand for housing, as reflected in the drop in density, further highlighting the issue of unplanned subdivisions.

4.2.2 Spatiotemporal pattern of LST and SUHI

The results of this study show that the initial period 2001-2002 shows elevated mean LST values, which could align with global patterns observed in 2002. In fact, in 2002, global temperatures rose by 0.56°C above the long-term average from 1880 to 2001, making it the second warmest year on record after 1998; this resulted from a strong El Niño event. Land temperatures were 0.87°C above the historical average, while ocean temperatures exceeded the 1980-2001 mean by 0.42°C. Both land and ocean temperatures for 2002 rank as the second-highest recorded (NOAA, 2003). This global change might have been a contributing factor to the higher mean LST observed in 2002 as a general increase of temperatures was observed globally. Although Zinder and Tahoua may not directly experience El Niño impacts, broader atmospheric dynamics influenced by global events can contribute to the warming trends observed. This warming effect in 2002 contrasts with the cooling trend observed in the subsequent period (2011-2012), suggesting a temporary atmospheric anomaly rather than a sustained trend, followed by a notable warming trend through 2021-2022 period in the two cities.

In Tahoua and Zinder, the presence of hotspots of heat outside the built-up areas (Figures 4.12 and 4.13) can be attributed to the unique geological and environmental characteristics of these regions. In Zinder, the granite bedrock is exposed in certain areas, and these rocks emit significantly more thermal infrared radiation (Mineo and Pappalardo, 2021). Similarly, in Tahoua, the hotspot areas are primarily lateritic plateaus, where the soil is rich in iron with less to no vegetation cover. The combination of iron-rich soil and sparse vegetation leads to higher heat emissions, contributing to the formation of these hotspots. Theses hotspots are observed in all the communes of the two cities with dominance in commune II of Tahoua (Figure 4.12) and commune IV of Zinder (Figure 4.13).

It is important to note that the settlement of Kolloma Dabagui in Tahoua did not experience high temperatures at the image of the two cities' centres (Figure 4.12). This could be attributed to the village's lower building density, which allows for better airflow and reduces the urban heat island effect typically observed in denser urban areas. Additionally, the traditional architecture and materials used in building in Kolloma Dabagui might provide better insulation and reflectivity, further contributing to its relatively cooler temperatures than Tahoua and Zinder's city centres.

4.2.3 Relationships between LST and LULC

The relationship between LST and LULC using OLS and GWR evaluated in this study showed an inconsistent relationship between these parameters across space and time, as shown by the OLS coefficients in Table 4.7 and Table 4.8 and GWR coefficient in Figure 4.13 and Figure 4.14. However, GWR model provides a better prediction than the OLS. In GWR, more than 90% of the change in NDVI and NDBI explained the variation in LST, while the OLS model explained less than 40% of the variation in LST and a smaller Akaike Information Criterion in GWR (Table 4.7, Table 4.8 and Table 4.13 and Table 4.14). This prevalence of GWR over OLS in determining the relationship between LST and LULC was emphasised by previous studies (Debele and Beketie, 2024) . These results are not uncommon, although the majority of studies evaluating the relationship between these parameters found a negative relationship between NDVI-LST and a positive relationship between NDBI-LST(Guha and Govil, 2020; Hussain *et al*., 2022).

By comparing the degree of relationship between LST and LULC indices over different seasons in Raipur City of tropical India, Guha and Govil, (2020) found that the least correlation coefficient was observed during winter, while the best correlation was found during post-monsoon. Additionally, a small to moderately positive correlation between LST and Modified Normalized Difference Impervious Surface Index (MNDISI) was found in Chhattisgarh State of India. The correlation was higher in the autumn, meaning that seasonal and environmental factors have an impact on the relationship's intensity and direction (Govil *et al*., 2020). Similarly, a positive correlation between LST and NDVI was found in areas with little vegetation cover and in urban settings where the presence of vegetation is insufficient to counterbalance heat effects due to the urban heat island effect (Alademomi *et al*., 2022). Additionally, water stress during dry seasons reduces vegetation's ability to cool the surface, which can change the usually negative connection to a positive one, especially in semi-arid and arid situations. Some other factors, such as the spatial resolution of the data used, could also affect the relationship between these parameters. While coarser resolutions may smooth out these fluctuations and produce inconsistent results, finer resolutions may be able to capture local variations more accurately. In this study, NDBI and NDVI exhibited a similar pattern. NDBI was not effective in capturing built-up areas alone. This has also affected the direction of its relationship with LST. This issue about NDBI not reflecting built-up areas accurately in some regions was also observed by (Zha *et al*., 2003). The authors found that NDBI is more efficient in places where the NDVI value is greater than 1. Henceforth, examining the relationship between LST and other built-up area indexes such as Dry Built-up area Index (DBI) or MNDISI could yield a better result.

4.2.4 Trend of extreme heat indices

The findings from Tahoua and Zinder indicate increased frequency and duration of heat waves (Figure 4.16 and 4.17). This aligns with the patterns seen throughout West Africa and highlighted by IPCC (Weber *et al*., 2018; IPCC, 2021) emphasizing that humaninduced climate change is a factor behind the increase of heat occurrences. The rise in both TXgt40 and tx90p is consistent with earlier research conducted by (Dunn *et al*., 2020)They suggested that the rise in extreme heat days has direct impacts on health, farming, and infrastructure. The notable increase in these factors in Tahoua reflects weather patterns and heightened susceptibilities to heat-related issues. In Tahoua and Zinder heatwaves have become more frequent and last longer in the past three decades there is no significant increase in their intensity. These findings are in line with the study conducted by (Weber *et al*., 2018).

It's interesting that both regions have experienced an increase in warmer nights (tn90p). Warmer nights are particularly problematic as they affect the human ability to rest. Contrary to Tahoua, there was a non-significant change in nighttime temperatures (tnn). This could indicate that local urban and environmental factors may be at play in reducing nighttime temperature extremes. The increase in theses heat indices can worsen public health problems, particularly in cities without proper copping/adaptation capacity, such as Tahoua and Zinder. Additionally, the statistically significant increase in the warm spell duration index (wsdi2) suggest that more extended heat events may have detrimental socioeconomic and health effects. This is similar to the results of Filho *et al*. (2020) in Guangdong.

4.2.5 Urban heat vulnerability

The two formulas used to map UHVI gave different results, as depicted in Figure 4.20. Using these two formulas, the expectation was that the heat vulnerability index for each city would differ slightly across the formulas. However, if an area is highly vulnerable to extreme heat, all formulas should yield a higher heat vulnerability index. Another expectation was that the adaptive capacity component would be inversely related to heat vulnerability. The results confirm these two expectations irrespective of the city involved, although V1 yielded higher correlation scores in the two cities. The similarity of the results given by the two formulas was also observed by Bhattacharjee *et al*. (2019) in Milan, Italy**.**

Due to the absence of indicators such as heat-related morbidity at neighbourhood level, this study did not proceed to a validation analysis. Similar limitations were noted by Oh *et al*. (2017), and Verdonck *et al*. (2018). We therefore suggested that the neighbourhoods highlighted by V1 and V2 maps could be considered the most vulnerable. Henceforth, the most heat-vulnerable neighbourhood highlighted by the two V1 and V2 maps in Tahoua is Kourfayawa. In Zinder, the most vulnerable population resides in the neighbourhoods of Yanda Kwandagué, Banguia, Manzozo and Garin liman.

To cope with heat conditions, personal strategies such as taking a drink, bathing, sleeping outside open windows and wearing light or loose clothing are standard heat adaptation techniques (Figure 4.22). These strategies are directly related to maintaining body temperature and comfort, particularly in environments where exposure to heat is inevitable. Notably, drinking water emerges as one of the most common responses (about 97% in Tahoua and 99% in Zinder), which is consistent with previous studies emphasizing the role of hydration in preventing heat-related illnesses (Zander *et al*., 2024). Bathing or showering, particularly with cool water, helps provide immediate relief, thus mitigating the physical stress caused by high temperatures. Wearing light or loose clothing, on the other hand, reduces the risk of heat retention. It facilitates the body's natural cooling process through sweating, underscoring the importance of personal attire choices in heat management. Another heat-copping strategy involves making environmental adjustments, such as using air conditioning, fans, and opening windows. Although air conditioning is one of the most effective methods for regulating indoor temperature and providing a controlled cooling environment, reliance on it is not without challenges, especially regarding energy consumption and environmental impact.

Air conditioning consumes large amounts of electricity and contributes to the UHI effect by releasing heat into the surrounding environment. Furthermore, energy consumption patterns can exacerbate the challenges of grid overload during heatwaves, leading to potential power shortages and increased greenhouse gas emissions if the electricity is sourced from non-renewable sources.

4.3 Summary of Findings

This study highlighted a rapid urban expansion and a trend towards urban sprawl in Tahoua and Zinder. From 1988 to 2024, the built-up area has passed from 0.82% to 10.81% and from 2.52% to 14.04% in Tahoua and Zinder respectively. The correlation analysis between built-up areas growth and population growth shows a statistically no correlation between these two parameters. However, although the relationship was not significant the degree of correlation is higher in Tahoua ($r = 0.67$) than Zinder ($r =0.29$). The study also highlights that urban growth direction is influenced by infrastructure development as in the two cities new development occurred mainly along roads and public services. The study shows an unstable relationship between LST, NDVI, and NDBI, indicated by both OLS and GWR analysis. This is due to the different biophysical conditions and environmental factors in arid and semi-arid regions compared to other climatic zones. The increasing trend of extreme temperature indices over the last three decades shows evidence of climate change in the two cities, with Tahoua experiencing higher values than Zinder. Under the business-as-usual scenario, by 2043, Zinder is expected to have lost almost all of its vegetation (0.27%) under a business-as-usual scenario. This is accompanied by accelerated urban growth, making the built-up area to occupy 25.28% of the landscape area. The same pattern is observed in Tahoua by 2042, with built-up area being 14.97% of the landscape area and vegetation representing 4.17%. This calls for adequate urban planning that take into account urban development without compromising the environmental sustainability.

CHAPTER FIVE

5.0 CONCLUSIONS AND RECOMMENDATIONS

5.1 Conclusions

This study used remote sensing, GIS techniques, and the urban growth model to comprehensively characterise and quantify urban landscape change in Tahoua and Zinder City over 34 years. Furthermore, the relationship between built-up area growth and urban population growth was assessed using simple linear regression analysis based on population data. The results showed that LULC changes experienced mainly resulted from reduced vegetation and agricultural lands to the profit of built-up area. Reducing agricultural land has some implications for food security, as agriculture is the main activity practised by more than 80% of the population in the study area. Although population growth is a general driver of urban area expansion, a non-significant relationship was found between these two variables in Zinder. The correlation between these two parameters is higher in Tahoua and the level of significance too. Throughout the 34 years of study, the edge-expansion growth type has been dominant, which is known to be inefficient in land resource management. The main attractions for urban development were the presence of paved roads, which facilitate mobility in and out of the city, and proximity to essential public services like schools, markets and hospitals. The fact that there was no mention of urban expansion in the strategic plan of all four districts forming the city of Zinder and the two districts forming the city of Tahoua insinuates that the city is growing at the rate of the population's housing and infrastructural needs.

The varying correlations between NDVI and LST across different locations reflect the complex nature of the vegetation-temperature relationship, influenced by spatial heterogeneity, land cover types, and seasonal changes. This study highlights the importance of using spatially explicit models like GWR to capture these local variations, which can provide more nuanced insights into the interactions between land cover and surface temperatures. Future research could further explore these dynamics by integrating additional environmental variables, such as soil moisture and albedo, to refine the understanding of NDVI-LST relationships.

Tahoua and Zinder are experiencing an increase in extreme temperatures, as highlighted by the upward trend of some calculated heat indices such as HWF, HWN, TX, and Tn. With the projected increase in global temperature and the UHI effect, the residents of these cities may be negatively affected by heat stress. The urban heat vulnerability analysis in the cities of Tahoua and Zinder identifies the most heat-vulnerable areas and examines the relationships between different vulnerability indices and their components. Some specific neighbourhoods in both cities are particularly susceptible to extreme heat, necessitating targeted interventions to mitigate these risks. The results underscore the importance of considering exposure, sensitivity, and adaptive capacity when assessing urban heat vulnerability. The negative correlation between the vulnerability indices and adaptive capacity components further emphasises the need to enhance the adaptive capacity of vulnerable communities to reduce their susceptibility to extreme heat.

5.2 Recommendations

i. To enhance the performance of urban development in Tahoua and Zinder, it is essential to address the current lack of coordinated planning and the unstructured nature of urban expansion. One of the key steps toward improving performance is to elaborate a cohesive city-level urban planning document such as the Urban Reference Plan (URP) mandated by Law n°2008-03, which has been non-existent in the two cities since 2000. Currently, the only planning documents called district development plans are fragmented and exist only at the district level, with each district having its own plan. However, these district plans do not address urban expansion, leading to uncoordinated growth contributing to environmental degradation. Therefore, it is recommended that a comprehensive urban planning framework be established for each city. This framework should include specific provisions for urban expansion, land use management, infrastructure, and services, which have been shown to influence urban expansion direction. Such a document will provide a unified vision for both cities, guiding future urban growth more sustainably and organised.

ii. In addition to developing a unified planning framework, performance improvement can be achieved by promoting infill development in vacant areas within the built-up zones of the cities. Encouraging development within these existing urban areas, instead of expanding outward, will reduce the environmental strain caused by urban sprawl. This will also make more efficient use of existing infrastructure, reduce pressure on surrounding ecosystems, and help mitigate the adverse effects of sprawling development patterns.

iii. To address rising temperatures and mitigate the urban UHI effect, it is crucial to leverage geospatial technologies to monitor LST and identify emerging heat hotspots. This ongoing monitoring system will allow authorities to act proactively by implementing interventions in real time to address areas with the highest heat exposure, improving both public health and overall urban liveability.

iv. Improving existing policies is essential to ensuring the sustainability of urban development in Tahoua and Zinder. A key area for policy improvement is protecting the cities' remaining vegetation and promoting urban greening initiatives. As highlighted in the study, both cities have experienced significant loss of vegetative cover, which exacerbates environmental and climatic challenges. To reverse this trend, incorporating national efforts such as the 3N Initiative, Niger's comprehensive program aimed at combating desertification and promoting land restoration, into local urban development strategies can provide a model for urban greening. The 3N Initiative's success in mobilising large-scale tree planting during Niger's Independence Day celebrations in a particularly selected region highlights the potential for nationwide engagement in environmental restoration. Local governments in Tahoua and Zinder could replicate similar initiatives, utilising national observances or creating their own localised tree-planting days, encouraging public participation in preserving and enhancing green spaces.

v. Urban greening projects should be implemented in vulnerable neighbourhoods, such as Adoum, Tougoulaoua, and Kourfayawa II in Tahoua and Garin Liman, Karkada, Charé Kolia, and other exposed areas in Zinder. These projects, which could include parks, tree-lined streets, and green roofs, will not only enhance the urban landscape but also help mitigate the UHI effect by providing cooling benefits to the cities.

vi. Moreover, it is crucial to integrate urban heat mitigation strategies into national and local urbanisation policies. This aspect is not mentioned in the national strategic document to combat the negative effect of urbanisation. Therefore, policies should mandate the inclusion of green spaces, tree planting, and other cooling solutions within urban planning frameworks. These measures can improve overall urban livability, reduce energy consumption (especially for cooling), and enhance public health, particularly for vulnerable populations.

vii. Further research is needed to address the health impact of rising temperatures in urban areas. Although the study focuses on the relationship between land use and surface temperatures, the implications for public health, particularly in terms of heat stress, morbidity, mortality, and healthcare costs, warrant deeper exploration. Understanding how increasing temperatures affect vulnerable populations will help inform more targeted interventions that protect public health and reduce the socio-economic costs associated with heat-related illnesses.

viii. Another important area for further research is the economic analysis of urban heat mitigation strategies. While urban greening projects and heat resilience measures are vital, it is equally important to assess their economic viability and long-term benefits. Future research should examine the cost-effectiveness of various mitigation measures, such as tree planting, park creation, and the promotion of cool roofs. This analysis can guide policymakers in making informed decisions about resource allocation and prioritising interventions that deliver the most significant impact for the cities' long-term sustainability.

ix. Finally, there is a need for ongoing monitoring and research into urban growth and LST patterns over time. As employed in this study, geospatial techniques should be expanded to establish an ongoing monitoring system for LST. This system would help track the effectiveness of implemented mitigation measures and provide timely data to identify emerging heat hotspots. Long-term monitoring will also allow urban planners and policymakers to adapt and refine strategies as the cities continue to grow and face new challenges related to climate change.

5.3 Contribution to Knowledge

This study provided new insights into the spatial and climatic impacts of urban expansion in semi-arid cities of Niger. Between 1988 and 2022, built-up areas increased by 10% in Tahoua and 11.5% in Zinder, largely replacing vegetation and agricultural land. Urban growth was more closely associated with infrastructure development than population increase, as indicated by weak correlations between population growth and built-up expansion ($r = 0.67$ in Tahoua; $r = 0.29$ in Zinder, $p < 0.05$). This implied that urban form and its thermal impacts are shaped more by planning and investment decisions than by demographic pressure. The relationship between vegetation cover (NDVI) and land surface temperature (LST), evaluated using Ordinary Least Squares (OLS) and Geographically Weighted Regression (GWR), showed clear spatial and seasonal variations. OLS coefficients ranged from 0.78 to −2.20 in Tahoua and from 17.06 to −2.57 in Zinder, from the rainy to the dry season, respectively. These results indicate that vegetation amount, health, and surface emissivity significantly influenced the NDVI–LST relationship, challenging the commonly assumed consistently negative association in the literature. Additionally, Surface Urban Heat Island (SUHI) intensity increased from 0.04°C to 0.88°C in Tahoua and from 0.17°C to 0.61°C in Zinder over the 34-year period. Projections for 2042 under a business-as-usual scenario show further warming, with LST expected to rise by 1.74°C in Zinder and 1.11°C in Tahoua. The findings imply that current urban development patterns intensified localised climate stress and urban heat disparities, and potentially led to long-term vulnerability in fast-growing Sahelian cities.

REFERENCES

Abbas, Z., Yang, G., Zhong, Y., & Zhao, Y. (2021). Spatiotemporal change analysis and future scenario of LULC using the CA-ANN approach: A case study of the Greater Bay Area, China. *Land*, 10(6) doi.org/10.3390/land10060584

Abdoulaye, A. (2019). Croissance urbaine et dysfonctionnements : cas de l'arrondissement communal Zinder III. Annales de l'Université de Parakou, 2(1). Retrieved from https://www.researchgate.net/publication/341057269

Abubakar, I. R., Lawanson, T. O., & Usman, A. S. (2020). Urban planning practices in Lagos. In *The Routledge handbook of planning megacities in the global south* (pp. 382-396). Routledge.

Acheampong, R. A., Agyemang, F. S. K., & Abdul-Fatawu, M. (2017). Quantifying the spatio-temporal patterns of settlement growth in a metropolitan region of Ghana. *GeoJournal*, 82(4), 823–840, doi.org/10.1007/s10708-016-9719-x

Adamou, A. (2012). *L'étalement urbain dans la ville de Niamey*. [Unpublished doctoral dissertation], Université Abdou Moumouni de Niamey, Niger.

Adeyeri, O. E., Akinsanola, A. A., & Ishola, K. A. (2017). Investigating surface urban heat island characteristics over Abuja, Nigeria: Relationship between land surface temperature and multiple vegetation indices. *Remote Sensing Applications*: Society and Environment, 7, 57–68, doi.org/10.1016/J.RSASE.2017.06.005

Aguilar-Gomez, S., Gutierrez, E., Heres, D., Jaume, D., & Tobal, M. (2024). Thermal stress and financial distress: Extreme temperatures and firms' loan defaults in Mexico. *Journal of Development Economics*, 168, 103246, doi.org/10.1016/J.JDEVECO.2023.103246

Aithal, B. H., Vinay, S., Ramachandra, T. V, & Area, S. (2014, July 13). *Landscape Dynamics Modeling Through Integrated Markov, Fuzzy-AHP And Cellular Automata*. Geoscience and Remote Sensing Symposium (IGARSS), 2014 IEEE International, (pp. 3160–3163)

Alademomi, A. S., Okolie, C. J., Daramola, O. E., Akinnusi, S. A., Adediran, E., Olanrewaju, H. O., Alabi, A. O., Salami, T. J., & Odumosu, J. (2022). The interrelationship between LST, NDVI, NDBI, and land cover change in a section of Lagos metropolis, Nigeria. *Applied Geomatics*, 14(2), 299–314, doi.org/10.1007/S12518-022-00434-2/METRICS

Al-Ahmadi, K., See, L., Heppenstall, A., & Hogg, J. (2009). Calibration of a fuzzy cellular automata model of urban dynamics in Saudi Arabia. *Ecological Complexity*, 6(2), 80–101, doi.org/10.1016/j.ecocom.2008.09.004

Albdour, M. S., & Baranyai, B. (2019). Water body effect on microclimate in summertime: A case study from PÉCS. *Pollack Periodica*, 14(3), 131–140, doi.org/10.1556/606.2019.14.3.13

Albertini, C., Gioia, A., Iacobellis, V., Petropoulos, G. P., & Manfreda, S. (2024). Assessing multi-source random forest classification and robustness of predictor variables in flooded areas mapping. *Remote Sensing Applications*: Society and Environment, 35, 101239, doi.org/10.1016/J.RSASE.2024.101239

Alexander, L. V., Zhang, X., Peterson, T. C., Caesar, J., Gleason, B., Klein Tank, A. M. G., Haylock, M., Collins, D., Trewin, B., Rahimzadeh, F., Tagipour, A., Rupa Kumar, K., Revadekar, J., Griffiths, G., Vincent, L., Stephenson, D. B., Burn, J., Aguilar, E., Brunet, M., & Vazquez-Aguirre, J. L. (2006). Global observed changes in daily climate extremes of temperature and precipitation. *Journal of Geophysical Research Atmospheres*, 111(D5) doi.org/10.1029/2005JD006290

Ali, J., Khan, R., Ahmad, N., & Maqsood, I. (2012). Random Forests and Decision Trees. International Journal of Computer Science, 9(5), 272.Retrieved from www.IJCSI.org

An, Y., Sun, J., Ji, C., & Wang, J. (2023). Cooling Coating for Buildings Based on the Daytime Radiative Cooling Technology. *Journal of Physics: Conference Series*, 2566(1), 012094, doi.org/10.1088/1742-6596/2566/1/012094

Anderson, J. R., Hardy, E. E., Roach, J. T., & Witmer, R. E. (1976). *A land use and land cover classification system for use with remote sensor data*. New York, NY: US Government Printing Office.

Arias, P. A., N. Bellouin, E. Coppola, R.G. Jones, G. Krinner, J. Marotke, v. Naik, M.D. Palmer, G.-K. Plattner, J. Rogelj, M. Rojas, J. Sillmann, T. S. P. W. T. B., & Trewin, K. A. R. B. A. and K. Z. (2021). Technical Summary. In Climate Change 2021: *The Physical Science Basis. Contribution of Working Group I to the Sixth Assessment Report of the Intergovernmental Panel on Climate Change*. New York, NY: Cambridge University Press

Aweda, E. D., Okhimamhe, A. A., Obateru, R. O., Schürmann, A., Teucher, M., & Conrad, C. (2024). Assessing the Impacts of Migration on Land Degradation in the Savannah Region of Nigeria. *Sustainability*, 16(18), 8157, doi.org/10.3390/SU16188157

Ayeni, B. (2018). *Urban Population. In Concepts and Techniques in Urban Analysis* (pp. 34–57). New York, NY: Routledge

Azhdari, A., Soltani, A., & Alidadi, M. (2018). Urban morphology and landscape structure effect on land surface temperature: Evidence from Shiraz, a semi-arid city. *Sustainable Cities and Society*, 41, 853–864, doi.org/10.1016/J.SCS.2018.06.034

Bagaria, P., Nandy, S., Mitra, D., & Sivakumar, K. (2021). Monitoring and predicting regional land use and land cover changes in an estuarine landscape of India. *Environmental Monitoring and Assessment*, 193(3), 193, doi.org/10.1007/s10661-021-08915-4

Baggnnian, I., Sanda Seydou, N., & Adam, T. (2021). Diversité floristique et vulnérabilité de la végétation ligneuses dans le département de Illela, région de Tahoua, Niger.

Journal of Environmental Science, Toxicology and Food Technology, 15(9), 15–27, doi.org/ISSN: 2319-2399

Bashir, O., Bangroo, S. A., Guo, W., Meraj, G., T. Ayele, G., Naikoo, N. B., Shafai, S., Singh, P., Muslim, M., Taddese, H., Gani, I., & Rahman, S. U. (2022). Simulating Spatiotemporal Changes in Land Use and Land Cover of the North-Western Himalayan Region Using Markov Chain Analysis. *Land*, 11(12), 2276, doi.org/10.3390/LAND11122276

Bhattacharjee, S., Gerasimova, E., Imbert, C., Tencar, J., & Rotondo, F. (2019). Assessment of Different Methodologies for Mapping Urban Heat Vulnerability for Milan, Italy. *Earth and Environmental Science*, 290(1), doi.org/10.1088/1755-1315/290/1/012162

Boltzmann, L. (1974). *The second law of thermodynamics. In Theoretical physics and philosophical problems: selected writings* (pp. 13-32). Dordrecht: Springer Netherlands, doi.org/10.1007/978-94-010-2091-6_2

Breiman, L. (2001). Random Forests. *Machine Learning*, 45(1), 5–32, doi.org/10.1023/A:1010933404324

Buo, I., Sagris, V., Burdun, I., & Uuemaa, E. (2021). Estimating the expansion of urban areas and urban heat islands (UHI) in Ghana: a case study. *Natural Hazards*, 105(2), 1299–1321, doi.org/10.1007/s11069-020-04355-4

Burgess, E. W. (2015). "The Growth of the City: An Introduction to a Research Project". *The City Reader,* 212–220, doi.org/10.4324/9781315748504-34

Chaolin, G. (2020). Definitions of Urbanisation. *International Encyclopedia of Human Geography*, 12, 112–118, doi.org/10.1016/B978-0-08-102295-5.10355-5

Chapman, S., Thatcher, M., Salazar, A., Watson, J. E. M., & McAlpine, C. A. (2019). The impact of climate change and urban growth on urban climate and heat stress in a subtropical city. *International Journal of Climatology*, 39(6), 3013–3030, doi.org/10.1002/joc.5998

Chen, Y. (2022). An extended patch-based cellular automaton to simulate horizontal and vertical urban growth under the shared socioeconomic pathways. *Computers, Environment and Urban Systems,* 91, 101727, doi.org/10.1016/j.compenvurbsys.2021.101727

City population. (2018). *Niger: Regions, Cities & Urban Centers* - Population Statistics, Maps, Charts, Weather and Web Information. Retrieved from https://www.citypopulation.de/en/niger/cities/, 2nd June, 2022

ClimPACT2 Team. (2016). ClimPACT2 User Guide: A software package for calculating climate extremes indices from daily data. Retrieved from https://climpact-sci.org/assets/climpact2-user-guide.pdf, 28th September, 2024

Das, S., & Angadi, D. P. (2021). Land use land cover change detection and monitoring of urban growth using remote sensing and GIS techniques: a micro-level study. *GeoJournal* 2021 87:3, 87(3), 2101–2123, doi.org/10.1007/S10708-020-10359-1

Debele, G. B., & Beketie, K. T. (2024). Studying the spatial non-stationary relationships of some physical parameters on the Earth's surface temperature using GWR in Upper Awash basin, Ethiopia. *Scientific African*, 23, e02052, doi.org/10.1016/j.sciaf.2023.e02052

Deilami, K., Kamruzzaman, M., & Hayes, J. F. (2016). Correlation or causality between land cover patterns and the urban heat island effect? Evidence from Brisbane, Australia. *Remote Sensing*, 8(9), 716, doi.org/10.3390/rs8090716

Djibo, A. K. (2019). History of the urban planning of the city of Zinder in the Niger Republic. In *Routledge Handbook of Urban Planning in Africa* (pp. 30-43). Routledge.

DMN. (2023). *Observations Météorologiques. Direction de La Météorologie Nationale Du Niger*. Retrieved from meteo-niger.org, 23rd January, 2025.

Doulay, K., Diouf, A., Sadda, A.-S., & Yakubu, I. B. (2019). Landuse/landcover change process in a tropical semi-arid zone: case of two rural communes (Chadakori and Saé-Saboua) in Maradi region, Republic of Niger. *Landscape & Environment*, 13(1), 1–12, doi.org/10.21120/le/13/1/1

Ducusin, R. J. C., Espaldon, M. V. O., Rebancos, C. M., & De Guzman, L. E. P. (2019). Vulnerability assessment of climate change impacts on a Globally Important Agricultural Heritage System (GIAHS) in the Philippines: the case of Batad Rice Terraces, Banaue, Ifugao, Philippines. *Climatic Change*, 153, 395–421, doi.org/10.1007/S10584-019-02397-7

Dunn, R. J. H., Alexander, L. V., Donat, M. G., Zhang, X., Bador, M., Herold, N., Lippmann, T., Allan, R., Aguilar, E., Barry, A. A., Brunet, M., Caesar, J., Chagnaud, G., Cheng, V., Cinco, T., Durre, I., de Guzman, R., Htay, T. M., Wan Ibadullah, W. M., … Bin Hj Yussof, M. N. A. (2020). Development of an Updated Global Land In Situ-Based Data Set of Temperature and Precipitation Extremes: HadEX3. Journal of *Geophysical Research: Atmospheres,* 125(16), e2019JD032263, doi.org/10.1029/2019JD032263

Estoque, R. C., Ishtiaque, A., Parajuli, J., Athukorala, D., Rabby, Y. W., & Ooba, M. (2023). Has the IPCC's revised vulnerability concept been well adopted? *Ambio* 52(2), 376–389, doi.org/10.1007/s13280-022-01806-z

Filho, W. L., Icaza, L. E., Neht, A., Klavins, M., Morgan, E. A., Shooshtarian, S., Kwong, C., Lam, C., Kenawy, I., Bi, P., Williams, S., Loughnan, M., Lloyd, G., Hansen, A., Kjellstrom, T., Vinayak, B., Soo, H., Gedam, S., Latha, R., … Gebreslasie, M. (2020). Associations between risk perception, spontaneous adaptation behavior to heat waves and heatstroke in Guangdong province, China. *BMC Public Health*, 13(2), 807–829, doi.org/10.1186/1471-2458-13-913

Fonds international de développement agricole. (n.d.). *Programme Spécial pour le Niger* (PSN) Retrieved from https://www.ifad.org/en/web/operations/-/project/1100000441, 11th July, 2024

Gaber, E. (2023, October). *Trends of Extreme Events in Precipitation and Temperature during the 1986-2015 Period at Cairo, Egypt*. Presented at The 6th International Electronic Conference on Atmospheric Sciences Vol. 15, (pp. 30).

Gohain, K. J., Mohammad, P., & Goswami, A. (2021). Assessing the impact of land use land cover changes on land surface temperature over Pune city, India. *Quaternary International*, 575, 259–269, doi.org/10.1016/j.quaint.2020.04.052

Govil, H., Guha, S., Diwan, P., Gill, N., & Dey, A. (2020). *Analyzing linear relationships of LST with NDVI and MNDISI using various resolution levels of Landsat 8 OLI and TIRS data*. In Data Management, Analytics and Innovation: Proceedings of ICDMAI 2019, Volume 1 (pp. 171-184).

Gronlund, C. J., Berrocal, V. J., White-Newsome, J. L., Conlon, K. C., & O'Neill, M. S. (2015). Vulnerability to extreme heat by socio-demographic characteristics and area green space among the elderly in Michigan, 1990–2007. *Environmental Research*, 136, 449–461, doi.org/10.1016/J.ENVRES.2014.08.042

Guha, S., & Govil, H. (2020). Land surface temperature and normalized difference vegetation index relationship: a seasonal study on a tropical city. *Applied Sciences*, 2(10), 1–14, doi.org/10.1007/S42452-020-03458-8/FIGURES/7

Guigma, K. H., Todd, M., & Wang, Y. (2020). Characteristics and thermodynamics of Sahelian heatwaves analysed using various thermal indices. *Climate Dynamics*, 55(11–12), 3151–3175, doi.org/10.1007/s00382-020-05438-5

Guo, J., Yu, Z., Ma, Z., Xu, D., & Cao, S. (2021). What factors have driven urbanisation in China?. *Environment, Development and Sustainability*, 24(5), 6508-6526, doi.org/10.1007/s10668-021-01714-4

Guo, L., Di, L., Zhang, C., Lin, L., Chen, F., & Molla, A. (2022). Evaluating contributions of urbanisation and global climate change to urban land surface temperature change: a case study in Lagos, Nigeria. *Scientific Reports*, 12(1), 14168, doi.org/10.1038/S41598-022-18193-W

Gupta, N., & Aithal, B. H. (2024). Urban land surface temperature forecasting: a data-driven approach using regression and neural network models. *Geocarto International*, 39(1), 2299145, doi.org/10.1080/10106049.2023.2299145

Hanana, M., Bejia, A., Amri, I., Gargouri, S., Jamoussi, B., & Hamrouni, L. (2021). Socio-economic characteristics of households in the region of Tahoua in Niger. *Journal of New Sciences*, 83, 4805-4812. Retrieved from https://www.jnsciences.org/agri-biotech/119-volume-83/682-socio-economic-characteristics-of-households-in-the-region-of-tahoua-in-niger.html

Harris, C. D., & Ullman, E. L. (1945). The nature of cities. *The Annals of the American Academy of Political and Social Science*, 242(1), 7–17, doi.org/10.1177/000271624524200103/ASSET/000271624524200103.FP.PNG_V03

Hassed, J. (2017). *Multiple Nuclei Model in Urban and Regional Planning*. Retrieved from http://mail.aboutcivil.org/multiple-nuclei-model, 7th November, 2022.

He, B. J., Wang, J., Liu, H., & Ulpiani, G. (2021). Localized synergies between heat waves and urban heat islands: Implications on human thermal comfort and urban heat management. *Environmental Research*, 193, 110584, doi.org/10.1016/j.envres.2020.110584

Heasahel. (2016). Profil des moyens d'existence région de Zinder Magaria et Dungass-Zone agricole centrale de culture de céréales et des légumineuses, Retrieved from https://hea-sahel.org, 4th November, 2022.

Heimlich, R. E., & Anderson, W. D. (2001). *Development at the Urban Fringe and Beyond: Impacts on Agriculture and Rural Land.Washington*, DC: U.S. Department of Agriculture. Agricultural Economic Report No. 803

Hertel, W., Snyder, P. K., & Twine, T. E. (2012, December). *Factors Contributing to Urban Heat Island Development: A Global Perspective*. In AGU Fall Meeting Abstracts (Vol. 2012, pp. B43H-0526). Retrieved from https://ui.adsabs.harvard.edu/abs/2012AGUFM.B43H0526H/abstract

Hu, Z., & Li, Y. (2022). Effect of urbanisation on extreme temperature events in Liaoning Province, China, from a spatiotemporal perspective. *Urban Climate*, *41*, 101025. https://doi.org/10.1016/j.uclim.2021.101025

Hussain, S., Lu, L., Mubeen, M., Nasim, W., Karuppannan, S., Fahad, S., Tariq, A., Mousa, B. G., Mumtaz, F., & Aslam, M. (2022). Spatiotemporal Variation in Land Use Land Cover in the Response to Local Climate Change Using Multispectral Remote Sensing Data. *Land*, 11(5), 595, doi.org/10.3390/land11050595

Ibn, A.-R., Rudith, I., & King, S. (2017). The Contribution of Rural Urban Migration to Migrants' Economic Development in Tamale. *Research on Humanities and Social Sciences*, 7(24), Retrieved from www.iiste.org

Id, M., Yun, Z., & Patrick, B. (2016). Simulation and Prediction of Land Surface Temperature (LST) Dynamics within Ikom City in Nigeria Using Artificial Neural Network (ANN). *Journal of Remote Sensing* & GIS, 05(01), 1–7, doi.org/10.4172/2469-4134.1000158

Illiassou, A. S., Boubacar, M. M., Abou Soufianou, S., Ali, M., & Mahamane, S. (2015). Dynamics of a third world city: Case of Niamey, Niger. *Journal of Geography and Regional Planning*, 8(5), 120–130, doi.org/10.5897/jgrp2015.0491

Inostroza, L., Palme, M., & Barrera, F. De. (2016). A Heat Vulnerability Index : Spatial Patterns of Exposure , Sensitivity and Adaptive Capacity for Santiago de Chile. *PLOS One*, 11(9), e0162464, doi.org/10.1371/journal.pone.0162464

Institut National de la Statistique (2023). Rapport «Agriculture et Conditions de vie des Ménages ».Retrieved from https://www.stat-niger.org/?publication_recente= rap port- agriculture-et-conditions-de-vie-des-menages, 11th July, 2024.

IPCC. (2001). Climate Change 2001: *Impacts, Adaptation, and Vulnerability Contribution of Working Group II to the Third Assessment Report of the Intergovernmental Panel on Climate Change*. In Cambridge University Press, Cambridge

IPCC. (2007). Climate Change 2007: *Impacts, Adaptation and Vulnerability. Contribution of Working Group II to the Fourth Assessment Report of the Intergovernmental Panel on Climate Change*. In Cambridge University Press, Cambridge, UK, 976pp. 37(6), doi.org/10.2134/JEQ2008.0015BR

IPCC. (2021). Sixth assessment report: Working Group II-Impacts, Adaptation and Vulnerability. Fact sheet-Human Settlements. Retrieved from https://www.ipcc.ch/report/ar6/wg2/, 28th September, 2024.

Ishtiaque, A., Estoque, R., Eakin, H., Parajuli, J., & Rabby, Y. W. (2022). IPCC's current conceptualization of 'vulnerability' needs more clarification for climate change vulnerability assessments. *Journal of Environmental Management*, 303, 14246, doi.org/10.1016/j.jenvman.2021.114246

Jagarnath, M., Thambiran, T., & Gebreslasie, M. (2020). Heat stress risk and vulnerability under climate change in Durban metropolitan, South Africa—identifying urban planning priorities for adaptation. *Climatic Change*, 163(2), 807–829, doi.org/10.1007/s10584-020-02908-x

Jaiye, D. (2020). Climate change and smart city development: The challenge of non-implementation of Abuja-Nigeria light rail project. *Journal of Geography and Regional Planning*, 13(1), 19–29, doi.org/10.5897/jgrp2020.0763

Jiang, J., Zhou, Y., Guo, X., & Qu, T. (2022). Calculation and Expression of the Urban Heat Island Indices Based on GeoSOT Grid. *Sustainability* ,14(5), 2588, doi.org/10.3390/SU14052588

Jiao, L., Mao, L., & Liu, Y. (2015). Multi-order Landscape Expansion Index: Characterizing urban expansion dynamics. *Landscape and Urban Planning*, *137*, 30–39. https://doi.org/10.1016/j.landurbplan.2014.10.023.

Kafy, A. A., Naim, M. N. H., Subramanyam, G., Faisal, A. Al, Ahmed, N. U., Rakib, A. Al, Kona, M. A., & Sattar, G. S. (2021). Cellular Automata approach in dynamic modelling of land cover changes using RapidEye images in Dhaka, Bangladesh. *Environmental Challenges*, 4, 100084, doi.org/10.1016/j.envc.2021.100084

Kamaraj, M., & Rangarajan, S. (2022). Predicting the future land use and land cover changes for Bhavani basin, Tamil Nadu, India, using QGIS MOLUSCE plugin. *Environmental Science and Pollution Research*, 29(57), 86337–86348, doi.org/10.1007/S11356-021-17904-6/METRICS

Kamer, L. (2022). Africa's fastest growing cities. Retrieved from https://www.statista.com/statistics/1234653/africa-s-fastest-growing-cities/, 27th June, 2022.

Kevin, M. (2018, August 29). NASA SVS | Earth System Diagram. NASA's Goddard Space Flight Center. Retrieved from https://svs.gsfc.nasa.gov/30988, 15th January, 2025.

Klotchkoff, J. C. (2012). *Samaria. Le Niger Aujourd'hui*. Retrived from https://nigerdiaspora.net/Archives-Nigerdiaspora-2003-2020/index.php/societe-archives/item/8509-samaria, 13th June, 2022.

Kunz-Plapp, T., Hackenbruch, J., & Schipper, J. W. (2016). Factors of subjective heat stress of urban citizens in contexts of everyday life. *Natural Hazards and Earth System Sciences*, 16(4), 977–994, doi.org/10.5194/nhess-16-977-2016

Lamine, K. (2023, June 1). *Niger, une augmentation exponentielle des cas de rougeole*. Retrieved from https://www.msf.fr/actualites/niger-augmentation-exponentielle-des-cas-de-rougeole, 23rd January, 2025.

Lazarus, R. S., & Folkman, S. (1987). Transactional theory and research on emotions and coping. *European Journal of personality*, *1*(3), 141-169. https://doi.org/10.1002/per.2410010304

Lee, K., & Lim, C. H. (2022). Analysis of the Surface Urban Heat Island Changes according to Urbanisation in Sejong City Using Landsat Imagery. *Korean Journal of Remote Sensing*, 38(3), 225–236, doi.org/10.7780/KJRS.2022.38.3.1

Leslie, R. C. C. (2015, February 17). *Zinder, point de chute des réfugiés face à Boko Haram.* Retrieved from https://www.lemonde.fr/afrique/video/2015/02/17/niger-zinder-point-de-chute-des-refugies-face-a-boko-haram_4578250_3212.html, 5th August, 2024.

Li, H., Zhou, Y., Jia, G., Zhao, K., & Dong, J. (2022). Quantifying the response of surface urban heat island to urbanisation using the annual temperature cycle model. *Geoscience Frontiers*, 13(1), 101141, doi.org/10.1016/J.GSF.2021.101141

Li, X., & Gong, P. (2016). Urban growth models: progress and perspective. *Science Bulletin*, 61(21), 1637–1650, doi.org/10.1007/s11434-016-1111-1

Li, X., Chen, G., Liu, X., Liang, X., Wang, S., Chen, Y., Pei, F., & Xu, X. (2017). A New Global Land-Use and Land-Cover Change Product at a 1-km Resolution for 2010 to 2100 Based on Human–Environment Interactions. *Annales of American Association of Geographers*. 107(5), 1040–1059, doi.org/10.1080/24694452.2017.1303357

Li, Z. L., Wu, H., Wang, N., Qiu, S., Sobrino, J. A., Wan, Z., Tang, B. H., & Yan, G. (2013). Land surface emissivity retrieval from satellite data. *International Journal of Remote Sensing*, 34(9–10), 3084–3127, doi.org/10.1080/01431161.2012.716540/ASSET/9FF76B7C-F13A-4CF3-A50DB705D21EE1A8/ASSETS/IMAGES/TRES_A_716540_O_F0005G.GIF

Liang, Z., Wu, S., Wang, Y., Wei, F., Huang, J., Shen, J., & Li, S. (2020). The relationship between urban form and heat island intensity along the urban development gradients. *Science of the Total Environme*nt, 708,135011, doi.org/10.1016/J.SCITOTENV.2019.135011

Lin, C., Wu, C. C., Tsogt, K., Ouyang, Y. C., & Chang, C. I. (2015). Effects of atmospheric correction and pansharpening on LULC classification accuracy using WorldView-2 imagery. *Information Processing in Agriculture*, 2(1), 25–36, doi.org/10.1016/j.inpa.2015.01.003

Lin, L., Gao, T., Luo, M., Ge, E., Yang, Y., Liu, Z., Zhao, Y., & Ning, G. (2020). Contribution of urbanisation to the changes in extreme climate events in urban agglomerations across China. *Science of the Total Environment*, 744, 140264, doi.org/10.1016/j.scitotenv.2020.140264

Liu, X., Li, X., Chen, Y., Tan, Z., Li, S., & Ai, B. (2010). A new landscape index for quantifying urban expansion using multi-temporal remotely sensed data. *Landscape Ecology*, 25(5), 671–682, doi.org/10.1007/s10980-010-9454-5

Lloyd, C. T., Sorichetta, A., & Tatem, A. J. (2017). High resolution global gridded data for use in population studies. *Scientific Data*, 4(1), 1–17, doi.org/10.1038/sdata.2017.1

López-Ballesteros, A., Beck, J., Bombelli, A., -, al, Elohor Oghenekaro, R., Kant -, S., Güneralp, B., Lwasa, S., Masundire, H., Parnell, S., & Seto, K. C. (2017). Urbanisation in Africa: challenges and opportunities for conservation. *Environmental Research Letters*, 13(1), 015002, doi.org/10.1088/1748-9326/AA94FE

Mahamane, L., & Mahamane, S. (2005). Biodiversity of ligneous species in semi-arid to arid zones of southwestern Niger according to anthropogenic and natural factors. Agriculture, *Ecosystems & Environment,* 105(1–2), 267–271, doi.org/10.1016/J.AGEE.2004.03.004

Malam, A. K. A., Mamadou, I., & Tanin, M. I. D. A. N. (2021). Risque d'innondation avant et après le programme de l'aménagement urbain « Zinder Saboua » dans les quartiers de Sabon Gari, Nassarawa Idi et Yadakondagué de la ville de Zinder au Niger. Rev. *Ivoir. Sci. Technol.*, 38, 253 – 280. Retrieved from researchgate.net

Malmquist, A., Hjerpe, M., Glaas, E., Karlsson, H., & Lassi, T. (2022). Elderly People's Perceptions of Heat Stress and Adaptation to Heat: An Interview Study. *International Journal of Environmental Research and Public Health*, 19(7), 3775, doi.org/10.3390/ijerph19073775

Mandich, M. J. (2019). Ancient City, Universal Growth? Exploring Urban Expansion and Economic Development on Rome's Eastern Periphery. *Frontiers in Digital Humanities*, 6 , 18, doi.org/10.3389/FDIGH.2019.00018

Manik, T., & Syaukat, S. (2017). Comparative Vulnerability Assessment of Urban Heat Islands in Two Tropical Cities in Indonesia. *British Journal of Environment and Climate Change*, *7*(2), 119–134, doi.org/10.9734/BJECC/2017/33529

Mansouri, S. T., & Zarghami, E. (2025). Investigating the effect of the physical layout of the architecture of high-rise buildings, residential complexes, and urban heat islands. *Energy and Built Environment,* 6(1), 1–17, doi.org/10.1016/J.ENBENV.2023.07.004

Manu, A., Twumasi, Y. A., Lu, K. S., & Coleman, T. L. (2015). Predicting urban growth of a developing country city using a statistical modelling approach. *International Journal of Geomatics and Geosciences*, 5(4), 603–613. Retrieved from https://www.researchgate.net/

Margaret, K., Simon, N., & Sabina, M. (2018). Sources of Occupational Stress and Coping Strategies among Teachers in Borstal Institutions in Kenya. Edelweiss: *Psychiatry Open Access,* 2(1), 18–21, doi.org/10.33805/2638-8073.111

MEDD. (2011). *Niger_Strategie nationale de developpement durable*. Retrieved from https://pnin-niger.org, 24th January, 2025

Mellos, K. (1988). *Theory of Eco-development. In Perspectives on Ecology: A Critical Essay* (pp. 59–74). Palgrave, Macmillan, UK, doi.org/10.1007/978-1-349-19598-5_4

Mineo, S., & Pappalardo, G. (2021). Rock Emissivity Measurement for Infrared Thermography Engineering Geological Applications. *Applied Sciences*, 11(9), 3773, doi.org/10.3390/APP11093773

Moussa, D. K. M., Lebailly, P., & Yamba, B. (2016). Land issue around the lands recoverd in the region of Tahoua Niger. *AGROFOR*, 1(1), 2016, doi.org/10.7251/agreng1601195k

Mushore, T. D., Mutanga, O., Odindi, J., & Dube, T. (2018). Determining extreme heat vulnerability of Harare Metropolitan City using multispectral remote sensing and socio-economic data. *Journal of Spatial Science* 63(1), 173–191, doi.org/10.1080/14498596.2017.1290558

Mwanzu, A., Nguyu, W., Nato, J., & Mwangi, J. (2023). Promoting Sustainable Environments through Urban Green Spaces: Insights from Kenya. *Sustainability*, 15(15), 11873, doi.org/10.3390/SU151511873

Nakul, C., Karma, T., Arun, S., & Eklabya, S. (2018). Ecological vulnerability to climate change in the mountains: a case study from the Eastern Himalayas. Google Scholar, 707-721.

Neteler, M. (2010). Estimating daily land surface temperatures in mountainous environments by reconstructed MODIS LST data. *Remote Sensing*, 2(1), 333–351, doi.org/10.3390/RS1020333

NOAA. (2003). National Centers for Environmental Information, Monthly Global Climate Report for Annual 2002. Retrieved from https://www.ncei.noaa.gov/access/monitoring/monthly-report/global/200213, 23rd January, 2025.

OECD. (2011). *Land Cover Monitoring*. Retrieved from http://oe.cd/land-cover. 9th November, 2022

Oh, K. Y., Lee, M. J., & Jeon, S. W. (2017). Development of the Korean Climate Change Vulnerability Assessment Tool (VESTAP)—Centered on Health Vulnerability to Heat Waves. *Sustainability*, 9(7), 1103, doi.org/10.3390/SU9071103

Oleson, K. W., Bonan, G. B., & Feddema, J. (2010). Effects of white roofs on urban temperature in a global climate model. Geophysical Research Letters, 37(3), 42194, doi.org/10.1029/2009GL042194

Oleson, K. W., Bonan, G. B., Feddema, J., & Jackson, T. (2011). An examination of urban heat island characteristics in a global climate model. *International Journal of Climatology*, 31(12), 1848–1865, doi.org/10.1002/JOC.2201

Oyugi, M. O. (2021). Urbanisation Footprints and the Distribution of Air Quality in Nairobi City, Kenya. *Journal of Environmental & Earth Sciences*, 3(2), 14–44, doi.org/10.30564/JEES.V3I2.3289

Park, R. E., Burgess, E. W., & McKenzie, R. D. (1925). The City Chicago. *Univ. Press, Chicago*. Retrivied from google scholar.

Parveen, S., Basheer, J., & Praveen, B. (2018). a Literature Review on Land Use Land Cover Changes. *International Journal of Advanced Research*, 6(7), 1–6, doi.org/10.21474/ijar01/7327

PDC. (2019). Plan de développement communeTahoua I. [Unpublished document], Tahoua, Niger.

Peštová, V. (2022). *Sustainable Urban Development: Case Study Copenhagen*. In *Proceedings from the EDAMBA 2021 conference*, 390, 399, 390-399, doi.org/10.53465/EDAMBA.2021.9788022549301.390-399

Pradhan, B., Al-sharif, A. A. A., & Abdullahi, S. (2017). Urban Sprawl Assessment. Spatial Modeling and Assessment of Urban Form: Analysis of Urban Growth: From Sprawl to Compact Using Geospatial Data. *Springer*, 1(4), 61–92, doi.org/10.1007/978-3-319-54217-1_4

Prasertsoong, N., & Puttanapong, N. (2025). Predicting Urban Land Expansion and Local Economic Growth by Integrating CLUE-S and Economic Model: An Application to Ban Chang District, Thailand. *Journal of Geovisualization and Spatial Analysis*, 9(1), 1–21. https://doi.org/10.1007/S41651-024-00204-1/FIGURES/16

Qiu, X., Wang, F., Zhang, Q., Tao, G., & Zhou, S. (2024). An improved Gaussian process for filling the missing data in GNSS position time series considering the influence of adjacent stations. *Scientific Reports*, 14(1), 1–13, doi.org/10.1038/s41598-024-70421-7

Ramachandra, T. V., Bharath, H. A., & Sowmyashree, M. V. (2014). Urban footprint of Mumbai - the commercial capital of India. *Journal of Urban and Regional Analysis*, 6(1), 71–94, doi.org/10.37043/jura.2020.6.1.5

Reid, C. E., O'Neill, M. S., Gronlund, C. J., Brines, S. J., Brown, D. G., Diez-Roux, A. V., & Schwartz, J. (2009). Mapping community determinants of heat vulnerability. *Environmental Health Perspectives*, 117(11), 1730–1736, doi.org/10.1289/EHP.0900683/ASSET/62CE8B2A-F901-4E02-893E-51B032189A06/ASSETS/GRAPHIC/EHP-117-1730F2.JPG

Reis, C., Lopes, A., & Nouri, A. S. (2022). Assessing urban heat island effects through local weather types in Lisbon's Metropolitan Area using big data from the Copernicus service. *Urban Climate*, 43, 101168, doi.org/10.1016/j.uclim.2022.101168

Rokni, & Komeil. (2023). Investigating the Impact of Pan Sharpening on the Accuracy of Land Cover Mapping in Landsat Oli Imagery. *GeCar*, 49(1), 12–18, doi.org/10.3846/GAC.2023.15308

Rossi, J.-P., & Dobigny, G. (2019). Urban Landscape Structure of a Fast-Growing African City: The Case of Niamey (Niger). *Urban Science*, 3(2), 63, doi.org/10.3390/urbansci3020063

Russo, S., Marchese, A. F., Sillmann, J., & Immé, G. (2016). When will unusual heat waves become normal in a warming Africa? *Environmental Research Letters*, 11(5), 054016, doi.org/10.1088/1748-9326/11/5/054016

Sapena, M., & Ruiz, L. A. (2015). Analysis of urban development by means of multi-temporal fragmentation metrics from LULC data. International Archives of the Photogrammetry, Remote Sensing and Spatial Information Sciences - *ISPRS Archives*, 40(7W3), 1411–1418, doi.org/10.5194/isprsarchives-XL-7-W3-1411-2015

Schwirian, K. (2007). Ecological Models of Urban Form: Concentric Zone Model, the Sector Model, and the Multiple Nuclei Model. *The Blackwell Encyclopedia of Sociology* doi.org/10.1002/9781405165518.WBEOSE004

Selod, H., & Shilpi, F. (2021). Rural-urban migration in developing countries: Lessons from the literature. *Regional Science and Urban Economics*, 91, 103713, doi.org/10.1016/j.regsciurbeco.2021.103713

Seydou, K. D., Morenikeji, W., Diouf, A., Dicko, K., Erdanaev, E., Loewner, R., & Okhimamhe, A. A. (2024). Dynamics of Zinder's Urban Landscape: Implications for Sustainable Land Use Management and Environmental Conservation. *Sustainability*, *16*(23), 1-18. https://doi.org/10.3390/su162310263

Shahfahad, Naikoo, M. W., Towfiqul Islam, A. R. M., Mallick, J., & Rahman, A. (2022). Land use/land cover change and its impact on surface urban heat island and urban thermal comfort in a metropolitan city. *Urban Climate*, 41, 101052, doi.org/10.1016/j.uclim.2021.101052

Shikary, C., & Rudra, S. (2020). Measuring Urban Land Use Change and Sprawl Using Geospatial Techniques: A Study on Purulia Municipality, West Bengal, India. *Journal of the Indian Society of Remote Sensing*, 49(2), 433–448, doi.org/10.1007/s12524-020-01212-6

Sina, A. K. S., Ali, N., Garba, A., & Minoungou, B. (2021). Vegetation Dynamics in the Northern Zones of Niger: Case of the Rural Commune of Tanout (Zinder) and Aderbissinat (Agadez). *European Journal of Environment and Earth Sciences*, 2(1), 30–36, doi.org/10.24018/ejgeo.2021.2.1.111

Siqi, J., & Yuhong, W. (2020). Effects of land use and land cover pattern on urban temperature variations: A case study in Hong Kong. *Urban Climate*, 34, 100693, doi.org/10.1016/j.uclim.2020.100693

Solecki, W. D., & Leichenko, R. M. (2006). Urbanisation and the metropolitan environment: Lessons from New York and Shanghai. *Environment*, 48(4), 8–23, doi.org/10.3200/ENVT.48.4.8-23/ASSET//CMS/ASSET/B71FD909-08F2-42BD-A232-625FAFF84241/ENVT.48.4.8-23.FP.PNG

Some, J. (2013). Les plans d'ajustement structurel : succès et échecs - Les Yeux du Monde. Les Yeux Du Monde. Retrieved from https://les-yeux-du-monde.fr, 13th June, 2022.

Stern, N. (2007). *Costs of Climate Change in Developed Countries. In N. Stern (Ed.), The Economics of Climate Change: The Stern Review* (pp. 138–160). Cambridge University Press doi.org/DOI: 10.1017/CBO9780511817434.011

Sun, Y., Zhang, X., Ren, G., Zwiers, F. W., & Hu, T. (2016). Contribution of urbanisation to warming in China. *Nature Climate Change*, 6(7), 706–709, doi.org/10.1038/nclimate2956

Tan, J., Zheng, Y., Tang, X., Guo, C., Li, L., Song, G., Zhen, X., Yuan, D., Kalkstein, A. J., Li, F., & Chen, H. (2010). The urban heat island and its impact on heat waves and human health in Shanghai. *International Journal of Biometeorology*, 54(1), 75–84, doi.org/10.1007/S00484-009-0256-X

Tomlinson, C. J., Chapman, L., Thornes, J. E., & Baker, C. J. (2011). Including the urban heat island in spatial heat health risk assessment strategies: A case study for Birmingham, UK. *International Journal of Health Geographics*, 10 , 10-42, doi.org/10.1186/1476-072X-10-42

Uejio, C. K., Wilhelmi, O. V., Golden, J. S., Mills, D. M., Gulino, S. P., & Samenow, J. P. (2011). Intra-urban societal vulnerability to extreme heat: The role of heat exposure and the built environment, socioeconomics, and neighborhood stability. *Health & Place*, 17(2), 498–507, doi.org/10.1016/J.HEALTHPLACE.2010.12.005

UNFCC. (2018). The Paris Agreement. Retrieved from https://unfccc.int/documents/184656, 22nd November, 2024.

UN-Habitat. (2020). Unpacking the Value of Sustainable Urbanisation doi.org/10.18356/c41ab67e-en

United Nations. (1973). United Nations Conference on the Human Environment. Stockholm, 5-16 June 1972. *Water Research*, 7(8), 1227–1233, doi.org/10.1016/0043-1354(73)90077-8

United Nations. (2012). United Nations Department of Economic and Social Affairs/Population Division. In World Urbanisation Prospects: The 2011 Revision 24(4) doi.org/10.2307/2808041

United Nations. (2018). World Urbanisation Prospects : The 2018 Revision Retrieved from https://population.un.org/wup/Publications/Files/WUP2018-KeyFacts.pdf, 25th Janvier, 2022.

Ustaoglu, E., & Aydinoglu, A. Ç. (2019). Theory, Data, and Methods (Issue October) doi.org/10.4018/978-1-5225-9238-9.ch009

Verdonck, M. L., Demuzere, M., Hooyberghs, H., Beck, C., Cyrys, J., Schneider, A., Dewulf, R., & Van Coillie, F. (2018). The potential of local climate zones maps as a heat stress assessment tool, supported by simulated air temperature data. *Landscape and Urban Planning*, 178, 183–197, doi.org/10.1016/J.LANDURBPLAN.2018.06.004

Vinayak, B., Lee, H. S., Gedam, S., & Latha, R. (2022). Impacts of future urbanisation on urban microclimate and thermal comfort over the Mumbai metropolitan region, India. *Sustainable Cities and Society,* 79, 103703, doi.org/10.1016/j.scs.2022.103703

Viskanta, R. (1963). Interaction of Heat Transfer by Conduction, Convection, and Radiation in a Radiating Fluid. *Journal of Heat Transfer*, 85(4), 318–328, doi.org/10.1115/1.3686120

Voelkel, J., Hellman, D., Sakuma, R., & Shandas, V. (2018). Assessing vulnerability to urban heat: A study of disproportionate heat exposure and access to refuge by socio-demographic status in Portland, Oregon. *International Journal of Environmental Research and Public Health*, 15(4), 640, doi.org/10.3390/IJERPH15040640

Vujovic, S., Haddad, B., Karaky, H., Sebaibi, N., & Boutouil, M. (2021). Urban Heat Island: Causes, Consequences, and Mitigation Measures with Emphasis on Reflective and Permeable Pavements. *CivilEng*, 2(2), 459–484, doi.org/10.3390/civileng2020026

Watson, K. E., Gardiner, K. M., & Singleton, J. A. (2020). The impact of extreme heat events on hospital admissions to the Royal Hobart Hospital. *Journal of Public Health*, 42(2), 333–339, doi.org/10.1093/pubmed/fdz033

Weber, H., & Sciubba, J. D. (2019). The Effect of Population Growth on the Environment: Evidence from European Regions. *European Journal of Population*, 35(2), 379–402, doi.org/10.1007/S10680-018-9486-0

Weber, T., Haensler, A., Rechid, D., Pfeifer, S., Eggert, B., & Jacob, D. (2018). Analyzing Regional Climate Change in Africa in a 1.5, 2, and 3°C Global Warming World. *Earth's Future*, 6(4), 643–655, doi.org/10.1002/2017EF000714

Wilhelmi, O. V., & Hayden, M. H. (2010). Connecting people and place: A new framework for reducing urban vulnerability to extreme heat. *Environmental Research Letters*, 5(1), 14021, doi.org/10.1088/1748-9326/5/1/014021

Williams, A. (2012). What is a city? Architectural Design, 82(1), 66–69, doi.org/10.1002/ad.1351

Wolf, T., & McGregor, G. (2013). The development of a heat wave vulnerability index for London, United Kingdom. *Weather and Climate Extremes*, 1, 59–68, doi.org/10.1016/j.wace.2013.07.004

World Bank. (2007). Think Hazard. Retrieved from https://www.thinkhazard.org/en/, 13th November, 2024.

World Bank. (2015) *East Asia's changing urban landscape. W. Bank, East Asia's Changing Urban Landscape: Measuring a Decade of Spatial Growth*. Retrieved from https://www.worldbank.org/en/topic/urbandevelopment/publication, 12th June, 2023.

World Population Review. (2024). Zinder Population 2024. World Population Review. Retrieved from ihttps://worldpopulationreview.com/world-cities/zinder-population, 31st July, 2024.

Wu, C., Li, C., Ouyang, L., Xiao, H., Wu, J., Zhuang, M., Bi, X., Li, J., Wang, C., Song, C., Qiu, T., Haase, D., Hahs, A., & Finka, M. (2022). Spatiotemporal evolution of urbanisation and its implications to urban planning of the megacity, Shanghai, China. *Landscape Ecology* 2022 38:4, 38(4), 1105–1124, doi.org/10.1007/S10980-022-01578-7

Wu, Y., Wu, H., Li, S., Wu, L., Guo, C., Zhang, Z., Fan, R., Yang, X., Zhou, G., Yang, J., Yuan, P., & Luo, G. (2024). Integrating urban development and ecological sustainability: a study on land surface temperature and urban heat island effect in a Karst River Basin. *Frontiers in Built Environment,* 10, 1457347, doi.org/10.3389/FBUIL.2024.1457347/BIBTEX

Xu, L. Y., Xie, X. D., & Li, S. (2013). Correlation analysis of the urban heat island effect and the spatial and temporal distribution of atmospheric particulates using TM images in Beijing. *Environmental Pollution*, 178, 102–114, doi.org/10.1016/j.envpol.2013.03.006

Xu, X., Wang, L., Sun, M., Fu, C., Bai, Y., Li, C., & Zhang, L. (2020). Climate change vulnerability assessment for smallholder farmers in China: An extended framework. *Journal of Environmental Management*, 276, 111315, doi.org/10.1016/j.jenvman.2020.111315

Yang, X., Ruby Leung, L., Zhao, N., Zhao, C., Qian, Y., Hu, K., Liu, X., & Chen, B. (2017). Contribution of urbanisation to the increase of extreme heat events in an urban agglomeration in east China. *Geophysical Research Letters*, 44(13), 6940–6950, doi.org/10.1002/2017GL074084

Zander, K. K., Mathew, S., & Carter, S. (2024). Behavioural (mal) adaptation to extreme heat in Australia: Implications for health and wellbeing. Urban Climate, 53, 101772, doi.org/10.1016/j.uclim.2023.101772

Zha, Y., Gao, J., & Ni, S. (2003). Use of normalized difference built-up index in automatically mapping urban areas from TM imagery. *International Journal of Remote Sensing*, 24(3), 583–594, doi.org/10.1080/01431160304987

Zhang, R., & Yan, W. (2024). The 50-year spatial transition of suburban industrial parks and impacts on sustainable urbanisation in the Tokyo metropolitan area. *Sustainable Cities and Society*, *113*, 105679, doi.org/10.1016/j.scs.2024.105679

Zhang, X., Alexander, L., Hegerl, G. C., Jones, P., Tank, A. K., Peterson, T. C., Trewin, B., & Zwiers, F. W. (2011). Indices for monitoring changes in extremes based on daily temperature and precipitation data. Wiley Interdisciplinary Reviews: *Climate Change*, 2(6), 851–870, doi.org/10.1002/WCC.147

Zhu, Q., Liu, T., Lin, H., Xiao, J., Luo, Y., Zeng, W., Zeng, S., Wei, Y., Chu, C., Baum, S., Du, Y., & Ma, W. (2014). The spatial distribution of health vulnerability to heat waves in guangdong province, China. *Global Health Action*, 7(1), doi.org/10.3402/GHA.V7.25051

APPENDICES

Appendix A: Questionnaire

URBAN HEAT SURVEY

Dear Sir/Ma,

Heat is an existing problem that affects many countries in Africa, and exposure to heat stress is projected to increase. Consequently, we need to work on adaptation strategies. This survey seeks to understand how people living in Zinder/Tahoua are sensitive and cope with increasing temperatures. It is part of a PhD research project on Climate Change and Human Habitat. Please answer the questions truthfully. Information supplied is anonymous and would be kept confidential. Should you have any questions or need further information, please contact:

Kadiza Doulay Seydou

+227 96355451; kadidjadoulaye@gmail.com

THANK YOU

SECTION I: IDENTIFICATION

1. Date ________________
2. Neighbourhood name ______________
3. GPS Coordinates _____________
4. Interviewer ____________

SECTION II: RESPONDENT'S PERSONAL INFORMATION

5. Gender: Male ☐ Female ☐
6. Age: 18-24 ☐ 25-34 ☐ 35-44 ☐ 45-60 ☐ Above 60 ☐
7. Marital status: Single ☐ Married ☐ Separated/Divorced ☐ Window ☐
8. Level of Formal Education: None ☐ Primary ☐ Secondary ☐ Tertiary ☐ Others ☐
9. Employment Status: Self-employed ☐ Employed ☐ Not employed at all ☐ Retired ☐ Others ☐
10. Number of years in the city _____________________
11. How do you feel about living in this city?

    Very good ☐ Good ☐ Neutral ☐ Bad ☐ Very bad ☐

SECTION III: HOUSING AND HOUSEHOLD CHARACTERISTICS

A. SENSITIVITY

12. Are you living alone? Yes ☐ No ☐
13. If not how many people are there in your household? _________
14. Number of people below 10 years in your household ____________
15. Number of people above 60 years in your household _____________

16. Number of people with chronic disease in your household ___________
17. Number of people with disability in your household __________
18. <u>Monthly Household</u> Income:

    less than 100,000CFA ☐ 100,001 to 200,000CFA ☐200,001 to 300,000CFA ☐

    300,001 to 400,000CFA ☐ 4000,001 to 500,000CFA ☐ over 500,000CFA ☐

B. ADAPTABILITY

19. Are there grasses and/or shrubs within approximately 5sqm immediately around the house, say, about 5 square metres? Yes ☐ No ☐
20. Is there water body near to the house? Yes ☐ No ☐
21. What is the source of water for your household?

Tape at home ☐ community tape ☐ well ☐ borehole ☐ ponds ☐ *Garouwa* ☐

Others ______________

22. Is there a change in the water supply during summer? Yes ☐ No ☐
23. If yes, rate the overall supply of water during summer

    Very dissatisfied ☐ Dissatisfied ☐ Neutral ☐ Satisfied ☐ Very Satisfied ☐
24. Do you have electricity? Yes ☐ No ☐
25. If yes rate the overall supply of electricity services during summer (cut-off, duration, frequency)

    Very dissatisfied ☐ Dissatisfied ☐ Neutral ☐ Satisfied ☐ Very Satisfied ☐
26. Do you use air conditioning during the heat?

    No ☐ Yes
27. How far is the nearest primary healthcare centre? Less than 1km ☐ 1km to 5km ☐

    More than 5km ☐
28. Do you wear different types of clothing during summer than during the regular time?

    No ☐ Yes

SECTION IV: RESPONDENTS' PERCEPTIONS OF EXTREME HEAT AND ITS IMPACTS

29. Do you think there is more heat (higher temperature) in Zinder over the years?

No ☐ Yes ☐ I don't know ☐

30. If yes, what do you think is the cause?

Climate change? ☐Urbanisation? ☐ Deforestation? ☐ Lack of rainfall ☐

Air pollution ☐ Others ____________

31. Do you think extreme heat has a negative impact on human health?

Yes ☐ No ☐ I don't know ☐

32. If yes, rate the level of impact

Low? ☐ Moderate? ☐ High? ☐

33. Which of these problems do you experience due to excessive heat?

a. Heat fatigue Yes ☐ No ☐
b. High blood pressure Yes ☐ No ☐
c. Skin rashes Yes ☐ No ☐
d. Dizziness Yes ☐ No ☐
e. Muscle cramps Yes ☐ No ☐
f. Nausea Yes ☐ No ☐
g. Headache Yes ☐ No ☐
h. Fainting Yes ☐ No ☐
i. Confusion/inability to concentrate Yes ☐ No ☐
j. Others ______________________

34. Does extreme heat affect your labour capacity?

Increase work ability ☐ Decrease capacity☐ No change ☐

35. Does extreme heat affect household income?

Increase income ☐ Decrease income ☐ No change ☐

36. Does extreme heat affect household expenses (e.g. costs for cooling the house)?

Increase expense ☐ Decrease expense ☐ No change ☐

SECTION V: COPING/ ADAPTATION STRATEGIES FOR HEAT

37. Which of these do you do to cope with excessive heat?

a.	Take a drink	Yes ☐ No ☐
b.	Take bath/shower	Yes ☐ No ☐
c.	Wear light or loose clothing	Yes ☐ No ☐
d.	Sleep outside the room	Yes ☐ No ☐
e.	Use air conditioning is	Yes ☐ No ☐
f.	Wet your clothe	Yes ☐ No ☐
g.	Use fan (ceiling, pedestal)	Yes ☐ No ☐
h.	Fan yourself by hand/manually	Yes ☐ No ☐
i.	Seek coping information online or in books	Yes ☐ No ☐
j.	Open doors/windows	Yes ☐ No ☐
k.	Wear a hat/cover head	Yes ☐ No ☐
l.	Wear sun glasses	
m.	Take a walk	Yes ☐ No ☐
n.	Go to swim	Yes ☐ No ☐
o.	Seek medical attention	Yes ☐ No ☐

38. List other things you do to cope with excessive heat?

____

____

____

39. Have you ever visited a doctor for heat related illness? Yes ☐ No ☐

40. What do you think can be done to reduce the impact of heat in urban areas?

a.	Plant vegetation inside the house	Yes ☐ No ☐
b.	Plant trees around the house/shade	Yes ☐ No ☐
c.	Increase window size	Yes ☐ No ☐
d.	Use low energy-efficient appliances	Yes ☐ No ☐
e.	Create more weather awareness services	Yes ☐ No ☐
f.	Create open spaces	Yes ☐ No ☐
g.	Reduce the use of cars and machines	Yes ☐ No ☐

Do you want to share any other relevant information?

____

____

Thank you very much for your time

Appendix B: Spatiotemporal variation of NDVI and NDBI in Tahoua and Zinder

(a)

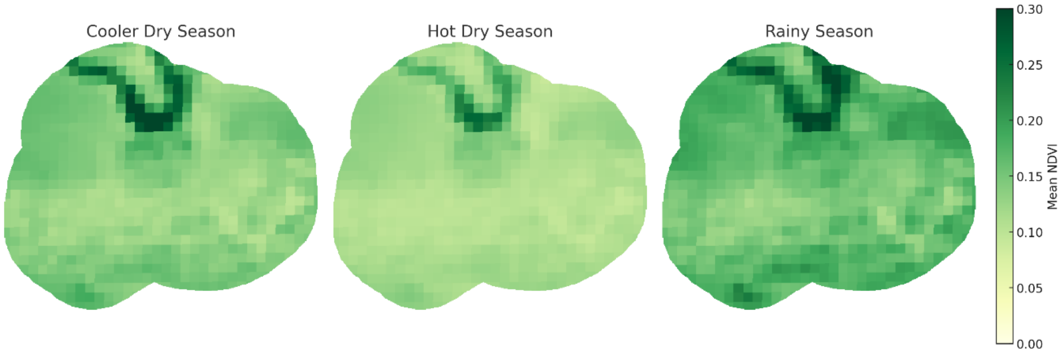

(b)

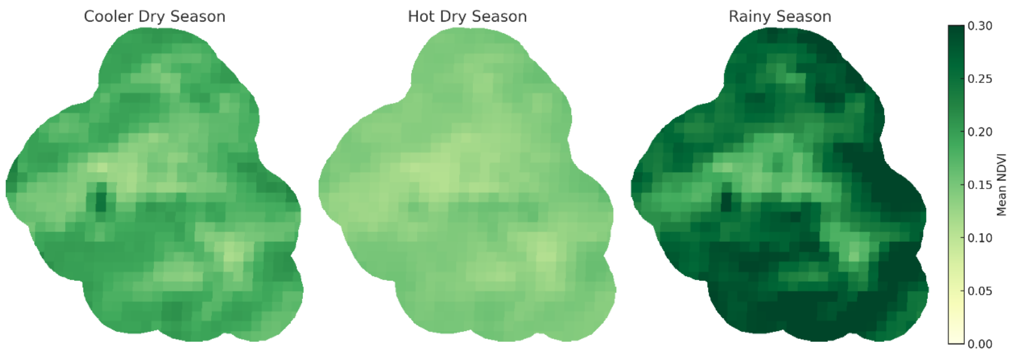

Figure 1: Mean seasonal NDVI from 2002 to 2022 in Tahoua (a) and Zinder (b)

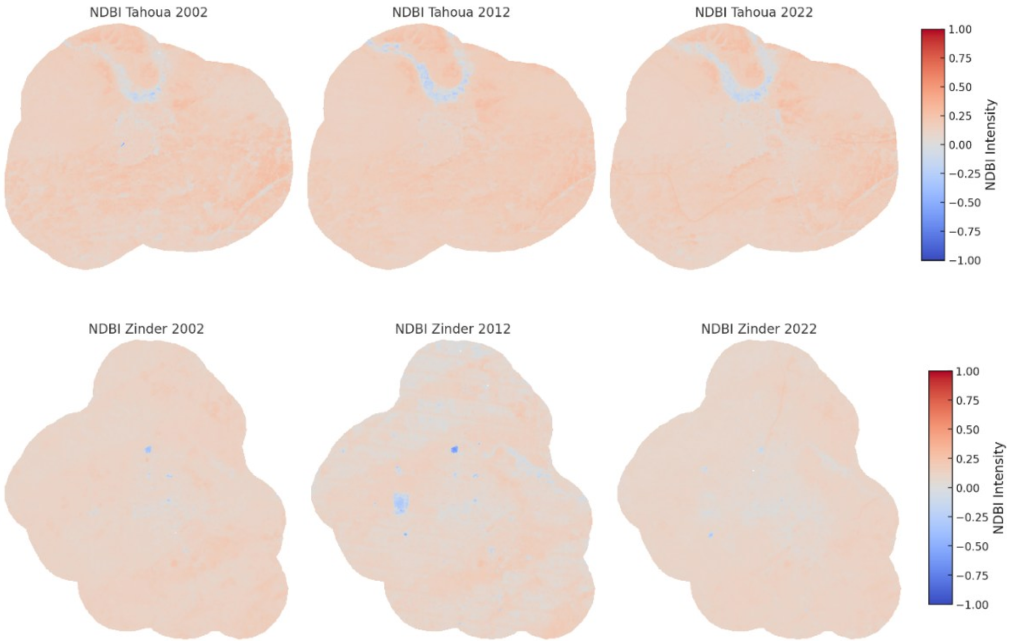

Figure 2: Mean seasonal NDBVI from 2002 to 2022 Tahoua (a) and Zinder (b)

Appendix C: auxiliary data for LULC prediction

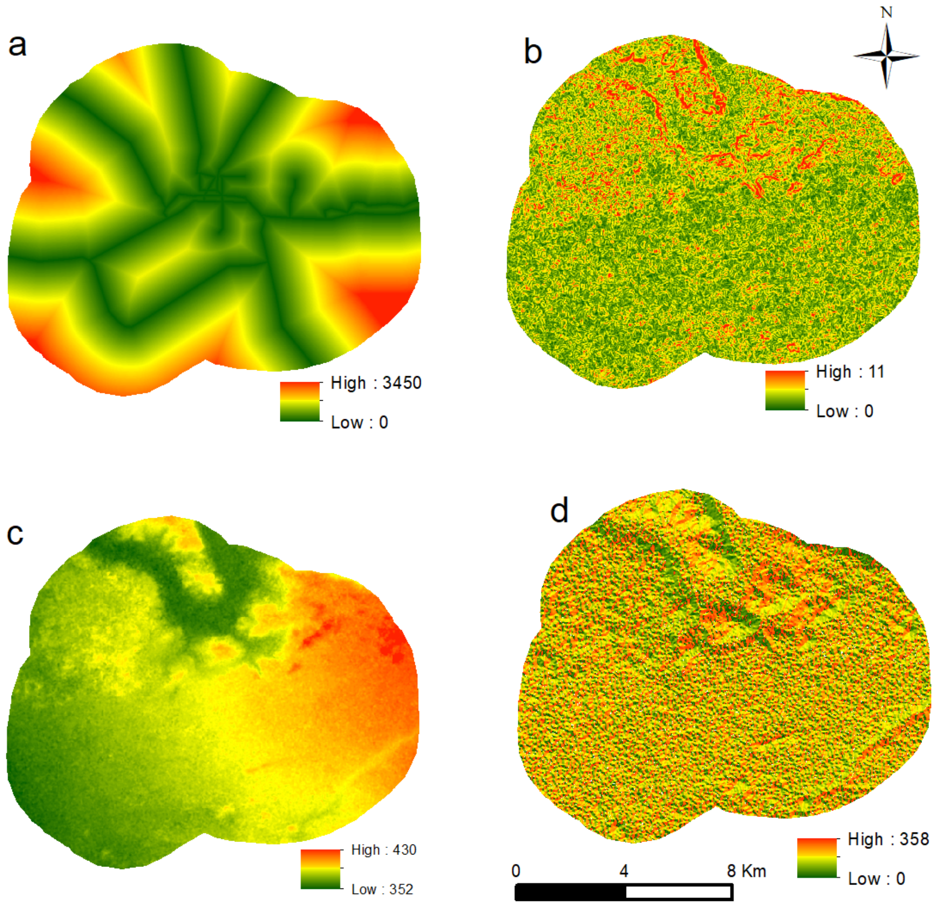

Figure 3: Tahoua (a) distance to major roads, (b) slope, (c) elevation, (d) aspect

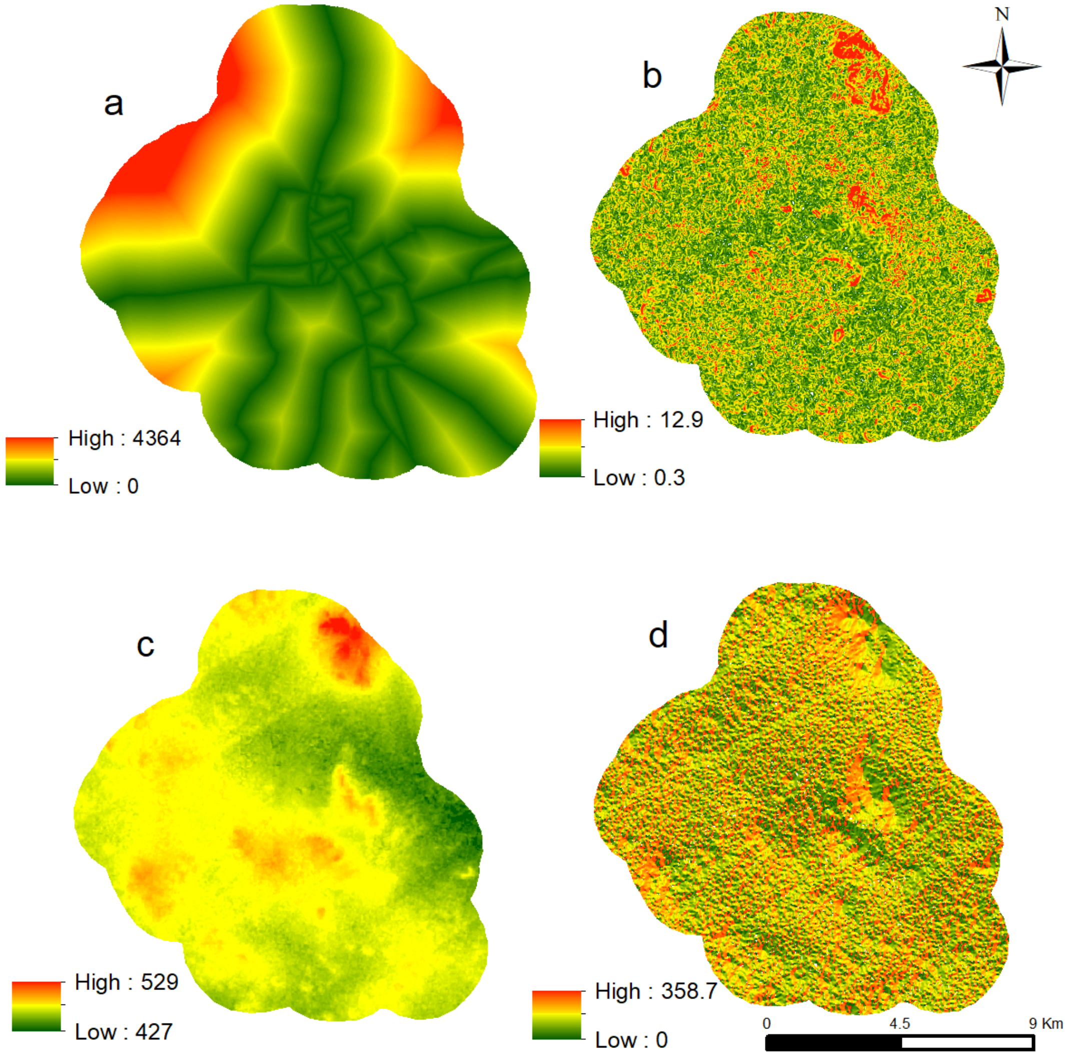

Figure 4: Zinder(a) distance to major roads, (b) slope, (c) elevation, (d) aspect

Appendix D: Background characteristics of respondents

Table 1: Background characteristics of respondents (Zinder n=82, Tahoua n=392)

Background characteristics	Zinder F	%	Tahoua F	%
Sex				
Female	129	33.6	143.0	36.0
Male	242	66.4	249.0	64.0
Age				
18-28 years	42	11.2	22.0	5.8
29-39 years	125	33.3	123.0	32.5
40-50 years	157	41.9	164.0	43.4
51-61years	33	8.8	51.0	13.5
More than 61 years	18	4.8	18.0	4.8
Marital status				
Single	54	14.4	31.0	8.2
Divorced	1	0.3	0.0	0.0
Married	319	85.1	343.0	90.7
Widow/widower	1	0.3	4.0	1.1
Job				
No job	39	10.4	49.0	13.0
Private worker	25	6.7	22.0	5.8
Public worker	71	18.9	63.0	16.7
Student	22	5.9	7.0	1.9
Retiered	6	1.6	13.0	3.4
Businessman/ woman	212	56.5	224.0	59.3
Level of education				
Coranic	89	23.7	79.0	20.9
None	23	6.1	50.0	13.2
Primary School	85	22.7	96	25.4
Secondary school	115	30.7	116	30.7
High School	63	16.8	37	9.8
Time spent in the city				
Less Than a year	14	1.1	19	1.1
1-3 years	24	3.7	39	5.0
4-7 years	9	6.4	26	10.3
8-11 years	4	2.4	4	6.9
More Than 11 years	324	1.1	290	1.1
Monthly income				
Less than 100 000 CFA	273.0	72.8	279.0	73.8
100 001 to 200 000 CFA	79.0	21.1	72.0	19.0
200 001 to 300 000 CFA	22.0	5.9	21.0	5.6
300 001 to 400 000 CFA	1.0	0.3	3.0	0.8
400 001 to 500 000 CFA	0.0	0.0	2.0	0.5
More than 500 000 CFA	0.0	0.0	1.0	0.3

Source: Field survey, 2023